The roles of ROS and p21 in apoptosis-inducing effect of cepharanthine in human colorectal cancer cells

Miss Rattana Saetung

A Thesis Submitted in Partial Fulfillment of the Requirements
for the Degree of Master of Science in Pharmacology
Inter-Department of Pharmacology
GRADUATE SCHOOL
Chulalongkorn University
Academic Year 2020

บทบาทของ ROS และ p21 ต่อการเหนี่ยวนำการตายแบบ apoptosis ของ cepharanthine ในเซลล์มะเร็งลำไส้ใหญ่และไส้ตรงของมนุษย์

น.ส.รัตนา แซ่ทึ่ง

วิทยานิพนธ์นี้เป็นส่วนหนึ่งของการศึกษาตามหลักสูตรปริญญาวิทยาศาสตรมหาบัณฑิต
สาขาวิชาเภสัชวิทยา สหสาขาวิชาเภสัชวิทยา
บัณฑิตวิทยาลัย จุฬาลงกรณ์มหาวิทยาลัย
ปีการศึกษา 2563

Thesis Title	The roles of ROS and p21 in apoptosis-inducing effect of cepharanthine in human colorectal cancer cells
By	Miss Rattana Saetung
Field of Study	Pharmacology
Thesis Advisor	Assistant Professor PIYANUCH WONGANAN, Ph.D.

Accepted by the GRADUATE SCHOOL, Chulalongkorn University in Partial Fulfillment of the Requirement for the Master of Science

..... Dean of the GRADUATE SCHOOL
(Associate Professor THUMNOON NHUJAK, Ph.D.)

THESIS COMMITTEE

..... Chairman
(Associate Professor SUREE JIANMONGKOL, Ph.D.)

..... Thesis Advisor
(Assistant Professor PIYANUCH WONGANAN, Ph.D.)

..... Examiner
(Associate Professor VARISA PONGRAKHANANON, Ph.D.)

..... External Examiner
(Associate Professor Pornpun Vivithanaporn, Ph.D.)

รัตนา แซ่ทึ่ง : บทบาทของ ROS และ p21 ต่อการเหนี่ยวนำการตายแบบ apoptosis ของ cepharanthine ในเซลล์มะเร็งลำไส้ใหญ่และไส้ตรงของมนุษย์. (The roles of ROS and p21 in apoptosis-inducing effect of cepharanthine in human colorectal cancer cells) อ.ที่ปรึกษาหลัก : ปิยนุช วงศ์อนันต์

Cepharanthine (CEP) เป็นสารธรรมชาติที่สกัดได้จากต้น *Stephania cepharantha* Hayata จากการศึกษาที่ผ่านมาพบว่า CEP มีฤทธิ์ต้านมะเร็งหลายชนิด รวมถึงมะเร็งลำไส้ใหญ่และไส้ตรง โดยพบว่าความเป็นพิษของ CEP ต่อเซลล์มะเร็งลำไส้ใหญ่และไส้ตรงมีความสัมพันธ์กับการสร้างอนุมูลอิสระ (reactive oxygen species, ROS) และการแสดงออกของ $p21^{Waf1/Cip1}$ อย่างไรก็ตามข้อมูลเกี่ยวกับกลไกการออกฤทธิ์ของ CEP ในการชักนำให้เซลล์มะเร็งเกิดการตายแบบอะพอพโทซิสยังมีอยู่อย่างจำกัด ดังนั้นงานวิจัยนี้จึงมีวัตถุประสงค์เพื่อศึกษาบทบาทของ ROS และ $p21^{Waf1/Cip1}$ ต่อการชักนำกระบวนการตายแบบอะพอพโทซิสของ CEP ในเซลล์มะเร็งลำไส้ใหญ่และไส้ตรง 2 ชนิดคือเซลล์ HCT116 ซึ่งเป็นเซลล์ที่มี p53 ปกติ และเซลล์ HT-29 ซึ่งเป็นเซลล์ที่มี p53 กลายพันธุ์ ผลการศึกษาครั้งนี้แสดงให้เห็นว่า CEP สามารถลดการอยู่รอดของเซลล์ HCT116 และเซลล์ HT-29 ได้อย่างมีนัยสำคัญทางสถิติ โดย CEP มีศักยภาพในการยับยั้งการเจริญเติบโตของเซลล์ HT-29 มากกว่ายาเคมีบำบัด L-OHP อีกทั้ง CEP ยังสามารถกระตุ้นให้เซลล์ทั้งสองชนิดเกิดการตายแบบ apoptosis โดย CEP มีผลเพิ่มการแสดงออกของ pro-apoptotic protein Bak ลดการแสดงออกของ anti-apoptotic protein Bcl-x_L และเหนี่ยวนำให้มีการตัดย่อยของ PARP นอกจากนี้ CEP ยังมีผลกระตุ้นการสร้างอนุมูลอิสระในเซลล์มะเร็งทั้งสองชนิด ทั้งนี้พบว่า N-acetyl cysteine (NAC) สามารถลดผลของ CEP ในการชักนำให้เซลล์เกิดการตายอะพอพโตซิส แสดงให้เห็นว่า CEP สามารถชักนำให้เซลล์เกิดการตายแบบอะพอพโทซิสผ่านการสร้าง ROS ภายในเซลล์ การศึกษาครั้งนี้ยังพบว่า CEP สามารถปรับเปลี่ยนวิถีการนำส่งสัญญาณของ ERK1 /2 โดยสามารถลดการแสดงออกของ p-ERK ในเซลล์ HT-29 และเพิ่มการแสดงออกของ p-ERK ในเซลล์ HCT116 และจากการศึกษาเพิ่มเติมพบว่า ROS มีความเกี่ยวข้องกับผลของ CEP ในการปรับเปลี่ยนวิถีการนำส่งสัญญาณของ ERK1 /2 อีกด้วย นอกจากนี้ยังพบว่า CEP สามารถเพิ่มการแสดงออกของ $p21^{Waf1/Cip1}$ ในเซลล์ HT-29 ในขณะที่ไม่มีผลต่อการเปลี่ยนแปลงระดับการแสดงออกของ $p21^{Waf1/Cip1}$ ในเซลล์ HCT116 และเมื่อยับยั้งการแสดงออกของ $p21^{Waf1/Cip1}$ ด้วยสาร UC2288 (a p21 inhibitor) ในเซลล์ HT-29 พบว่า UC2288 สามารถลดผลของ CEP ต่อการเหนี่ยวนำให้เซลล์ HT 29 เกิดการตายแบบอะพอพโตซิส แสดงให้เห็นว่า $p21^{Waf1/Cip1}$ มีบทบาทสำคัญต่อผลของ CEP ในการชักนำให้เซลล์ HT-29 ที่มี p53 กลายพันธุ์เกิดการตายแบบอะพอพโตซิส โดยสรุปผลการศึกษาครั้งนี้แสดงให้เห็นว่าการสร้างอนุมูลอิสระและการแสดงออกของ $p21^{Waf1/Cip1}$ มีบทบาทสำคัญต่อผลของ CEP ในการชักนำให้เซลล์มะเร็งลำไส้ใหญ่และไส้ตรงที่มีการกลายพันธุ์ของ p53 เกิดการตายแบบอะพอพโตซิส ซึ่งอาจนำมาใช้เป็นแนวทางในการรักษามะเร็งลำไส้ใหญ่และไส้ตรงชนิดที่มีการกลายพันธุ์ p53 ซึ่งเป็นสาเหตุที่สำคัญของการดื้อต่อยาเคมีบำบัดที่มีใช้อยู่ในปัจจุบัน

สาขาวิชา	เภสัชวิทยา	ลายมือชื่อนิสิต .....
ปีการศึกษา	2563	ลายมือชื่อ อ.ที่ปรึกษาหลัก .....

6087292020 : MAJOR PHARMACOLOGY
KEYWORD: CEPHARANTHINE, COLORECTAL CANCER, APOPTOSIS, P21, ROS

Rattana Saetung : The roles of ROS and p21 in apoptosis-inducing effect of cepharanthine in human colorectal cancer cells. Advisor: Asst. Prof. PIYANUCH WONGANAN, Ph.D.

Cepharanthine (CEP), a natural compound isolated from *Stephania cepharantha* Hayata, has been shown to possess anti-cancer activity against several cancers including colorectal cancer (CRC) cells. Previously, it was found that cytotoxicity of CEP was associated with ROS generation and $p21^{Waf1/Cip1}$ expression. However, information regarding to the molecular mechanisms underlying the apoptosis-inducing effects of CEP in CRC cells is still limited. Therefore, the present study aimed to evaluate the roles of ROS and $p21^{Waf1/Cip1}$ in the apoptosis-inducing effect of CEP in two human colorectal cancer cells lines, p53 wild-type HCT116 cells and p53 mutant HT-29 cells. The results demonstrated that CEP significantly inhibited the growth of both HT-29 and HCT116 cells. Remarkably, CEP was more effective than L-OHP in controlling the growth of HT-29 cells. Moreover, CEP induced apoptosis was mediated through upregulation of pro-apoptotic Bak, downregulation of anti-apoptosis Bcl-x_L, and induction of poly (ADP-ribose) polymerase (PARP) cleavage in both HT-29 cells and HCT116 cells. Additionally, CEP was found to induce ROS generation in HT-29 and HCT-116 cells. It should be noted that N-acetyl cysteine (NAC) could abolish the apoptosis-inducing effects of CEP in both HT-29 cells and HCT116 cells, suggesting that CEP-induced apoptosis is mediated through ROS generation. Furthermore, CEP could modulate ERK1/2 signaling pathway by inhibiting ERK1/2 phosphorylation in HT-29 cells while activating ERK1/2 phosphorylation in HCT116 cells, which was found to be associated with ROS generation. Notably, CEP markedly upregulated the expression of $p21^{Waf1/Cip1}$ in p53 mutant HT-29 cells but did not alter the expression of $p21^{Waf1/Cip1}$ in HCT116 cells. A p21 inhibitor, UC2288, could abolish apoptosis-inducing effect of CEP in HT-29 cells, suggesting that CEP-induced apoptosis is mediated via upregulation of $p21^{Waf1/Cip1}$ in p53 mutant HT-29 cells. Taken together, the results of this study demonstrated that generation of ROS and upregulation of $p21^{Waf1/Cip1}$ play a significant role in apoptosis-inducing effect of CEP in p53 mutant CRC cells. It may be useful for treatment of colorectal cancer carrying mutant p53 which often cause resistant to current chemotherapeutic agents.

Field of Study:	Pharmacology	Student's Signature .....
Academic Year:	2020	Advisor's Signature .....

ACKNOWLEDGEMENTS

This thesis work has been accomplished with the kindness and great help from many people, especially my advisor, Asst. Prof. Piyanuch Wonganan, at the Department of Pharmacology, Faculty of Medicine. I would like to express my sincere thank to Asst. Prof. Piyanuch Wonganan for her precious mentorship, patience, motivation, and knowledge. Her continuous support and guidance have helped me throughout the process of my graduate study. She always understood and encourage me when I felt hopeless. I could not have imagined having a better advisor and mentor for my study.

I would like to extend my sincere thanks to Assistant Professor Dr. Wacharee Limpanasithikul and Assistant Professor Dr. Wannarasmi Ketchart at the Department of Pharmacology, Faculty of Medicine. They have always encouraged and supported me. Thank you for giving me invaluable advice and suggestion.

I would also like to thank all staff members at the Department of Pharmacology, Faculty of Medicine for their advice and assistance. Also, thanks to my colleagues in the Cell Culture Laboratory for their friendships, encouragement and helpful suggestions about the laboratory techniques.

Finally, I really thank my family for their support and encouragement throughout my research and writing process. This work would not have been possible without them. Thank you.

Rattana Saetung

TABLE OF CONTENTS

LIST OF TABLES

Page

LIST OF FIGURES

Page

LIST OF ABBREVIATIONS

%	= Percentage
µg	= Microgram
µg /ml	= Microgram per milliliter
µl	= Microliter
µM	= Micromolar
5-FU	= 5-fluorouracil
AIF	= Apoptosis-inducing factor
AJCC	= American Joint Committee on Cancer
ANOVA	= Analysis of variance
Apaf-1	= Apoptosis protein-activating factor 1
APC	= Adenomatous polyposis coli
ATCC	= American Type Culture Collection
ATP	= Adenosine triphosphate
Bak	= Bcl-2 homologous antagonist killer
Bax	= Bcl-2 associated X protein
Bcl-2	= B-cell lymphoma-2
Bcl-xl	= B-cell lymphoma-extra large
BH domain	= Bcl-2 homology domain
Caspase	= Cysteine aspartic acid specific protease
CEP	= Cepharanthine
cDNA	= complementary Deoxyribonucleic acid
CO_2	= Carbon dioxide
cPARP	= Cleaved poly (ADP-ribose) polymerase
CRC	= Colorectal cancer
DCF	= 2',7'-dichlorofluorescein
DCFH-DA	= 2',7'-dichloro-dihydro-fluorescein diacetate
DISC	= Death-inducing signaling complex
DMEM	= Dulbecco's Modified Eagle Medium
DMSO	= Dimethyl sulfoxide

DNA = Deoxyribonucleic acid

DR = Death receptor

EDTA = Ethylene diamine tetraacetic acid

Endo G = Endonuclease G

ERK = Extracellular signal-regulated kinase

FAP = Familial adenomatous polyposis

FasR = Fibroblast associated antigen receptor

FBS = Fetal bovine serum

FdUMP = Fluorodeoxyuridine monophosphate

FdUTP = Fluorodeoxyuridine triphosphate

FITC = Fluorescein isothiocyanate

FUTP = Fluorouridine triphosphate

g/mol = Gram per mole

GAPDH = Glyceraldehyde 3-phosphate dehydrogenase

GDP = Guanosine diphosphate

GEF = Guanine nucleotide exchange factor

Grb2 = Growth factor receptor-bound protein 2

GTP = Guanosine-5'-triphosphate

h = Hour

H_2O_2 = Hydrogen peroxide

HBSS = Hank's buffered salt solution

HRP = Horseradish peroxidase

IARC = International Agency for Research on Cancer

IC_{50} = The half maximal inhibitory concentration

IR = irinotecan

JNK = c-Jun N-terminal kinase

KRAS = Kirsten rat sarcoma viral oncogene homolog

L-OHP = Oxaliplatin

LSD = Least square difference

MAPK = Mitogen-activated protein kinase

MEFs = mouse embryonic fibroblasts

MEK = Mitogen-activated protein kinase

MKP-1 = Mitogen-activated protein kinase (MAPK) phosphatase 1

ml = Milliliter

mM = Millimolar

MOMP = Mitochondria outer membrane permeabilization

mRNA = Messenger ribonucleic acid

mTOR = Mammalian target of rapamycin

MTT = 3-(4, 5-dimethylthiazol-2-yl)-2,5-diphenyltetrazolium bromide

MW = Molecular weight

NAC = *N*-acetyl cysteine

NaOH = Sodium hydroxide

NCI = National Cancer Institute

NFDM = Non-fat dry milk

Nrf2 = Nuclear factor erythroid 2-related factor 2

nm = Nanometer

O_2^- = Superoxide anion

$OH^\bullet$ = Hydroxyl radicals

p53 = Tumor suppressor protein 53

PAGE = Polyacrylamide gel electrophoresis

PARP = Poly (ADP-ribose) polymerase

PBS = Phosphate buffer saline

PCNA = proliferating cell nuclear antigen

p-ERK = Phosphorylated- extracellular signal-regulated kinases

PI = Propidium iodide

PS = Phosphatidylserine

PUMA = p53 upregulated modulator of apoptosis

PVDF = Polyvinylidene difluoride

RAF = Rapidly accelerated fibrosarcoma

RAS	= Rat sarcoma viral oncogene homolog
RIPA	= Radioimmunoprecipitation assay
ROS	= Reactive oxygen species
RPM	= Revolutions per minute
RPMI	= Roswell Park Memorial Institute
SAPKs	= Stress-activated protein kinases
SDS	= Sodium dodecyl sulfate
SEM	= Standard error of mean
Sos	= Son of sevenless
SPSS	= Statistical package for the social sciences
STAT3	= Signal transducer and activator of transcription 3
TEMED	= Tetramethylethylenedimine
TKIs	= Tyrosine kinase inhibitors
TRAILR	= TNF-related apoptosis-inducing ligand receptor
TrxR	= Thioredoxin reductase
TS	= Thymidylate synthase
UC2288	= p21 inhibitor
UV	= Ultraviolet irradiation
VEGF	= Vascular endothelial growth factor
VEGFR	= vascular endothelial growth

CHAPTER I

INTRODUCTION

1.1 Background and rationale

Colorectal cancer (CRC) is a major cause of cancer-related death worldwide. In 2019, The American Cancer Society reported that CRC was the third most common cancer in both men and women in the world (1). In Thailand, the National Cancer Institute (NCI) revealed that CRC has been the third most commonly diagnosed in men and women. Treatment options for CRC include surgery, radiotherapy, chemotherapy and targeted therapy (2). The chemotherapeutic agents commonly used in CRC are 5-fluorouracil (5-FU), oxaliplatin and irinotecan (2). Although currently marketed chemotherapeutic agents are commonly used, their application is still limited due to drug resistance and serious side effects such as myelosuppression, peripheral neuropathy and hypokalemia (3, 4). Therefore, new compounds with high anti-cancer and lower toxicity are extremely needed for CRC treatment.

Reactive oxygen species (ROS) such as superoxide anion ($O_2^{\bullet -}$), hydroxyl radical ($OH^{\bullet}$), and hydrogen peroxide (H_2O_2) play a crucial role in the regulation of several cellular processes such as cell proliferation and differentiation and cell death (5). Generally, the cancer cells have higher metabolic rates than normal cells, resulting in higher ROS levels (6). Excessive accumulation of ROS causes damage to nucleic acids, proteins, and lipids, leading to cell death (7, 8). Previous studies reported that many chemotherapeutic agents such as doxorubicin, cisplatin, carboplatin, and oxaliplatin increased ROS generation, leading to oxidative stress-induced apoptotic cell death (9, 10). Additionally, natural compound such as quercetin, capsaicin and p-coumaric acid was found to induce apoptosis through ROS production (11-13). Thus, ROS may be utilized as a strategy to induce cancer cell death for cancer therapy.

Accumulating evidence has shown that ROS induces cytotoxicity and apoptosis by activating or inhibiting ERK signaling pathway. For instance, Li et al also revealed that quercetin could induce apoptosis via ROS-mediated ERK activation in HL-60 leukemia cells (14). Moreover, sanguinarine induced apoptotic cell death via

activation of ERK phosphorylation, which was shown to be dependent on ROS generation in PC3 and DU145 prostate cancer cells (15). Conversely, apoptosis-inducing effect of zeaxanthin was associated with ROS-mediated inhibition of MAPK/ERK signaling pathway in human gastric cancer cells (16). Yuan et al revealed that koumine promotes ROS production which can inhibit the proliferation and promote apoptosis in Huh-7 and SNU-499 hepatocellular carcinoma cells via inhibition of ERK (17).

The cyclin-dependent kinase inhibitor p21 (known as $p21^{Waf1/Cip1}$) is a master downstream effector in the p53-dependent regulation of cell division and apoptosis (18). However, $p21^{Waf1/Cip1}$ has shown to be involved in p53-independent apoptosis. It was demonstrated that genistein induced $p21^{Waf1/Cip1}$ expression, which correlated with upregulation of pro-apoptotic protein, Bax, in the p53 mutant MDA-MB-231 breast cancer cells (19). Moreover, apoptosis-inducing effect of cisplatin was mediated through upregulation of $p21^{Waf1/Cip1}$ in the p53-deficient human ovarian carcinoma cell lines, SKOV3 and OVCAR3 (20). Thus, up-regulation of $p21^{Waf1/Cip1}$ may represent a novel therapeutic approach for cancer treatment.

Cepharanthine (CEP) is a biscoclaurine alkaloid isolated from the roots of *Stephania cepharantha* Hayata. It is also found in *Stephania suberusa* L.L forman and *Stephania erecta* Craib in Thailand. CEP has been widely used in Japan to treat a wide variety of acute and chronic diseases. It is also approved for the treatment of radiation-induced leukopenia, alopecia areata and alopecia pityrodes (21). Although CEP has been widely used, it serious side effects have never been reported (22). In addition, CEP has various pharmacological activities including anti-malarial, anti-oxidant, anti-inflammatory, anti-allergic effect, anti-platelet aggregation, anti-HIV, and anti-tumor (23, 24). Several studies revealed that CEP exhibited anticancer effect in many types of cancer including melanoma, leukemia, ovarian, breast, osteosarcoma, lymphoma, lung carcinoma, myeloma, cholangiocarcinoma, oral squamous carcinoma, colorectal cancer, and hepatocellular carcinoma (25-37). CEP was shown to inhibit cell growth in cancer cells through modulation of various signaling pathway, including NF-κB, Akt, ERK, JNK1/2, p38 MAPK and STAT3 pathways. Several studies

reported that apoptosis-inducing effect of CEP was mediated via ROS generation. For example, Biswas et al reported that CEP induced apoptotic cell death through production of ROS, activation of p38 and JNK1/2 signaling pathways and inhibition of AKT signaling pathway in hepatocellular carcinoma HUH-7 cells (35). Furthermore, CEP induced apoptosis in leukemia Jurkat and K562 cells through activation of caspase-3 and -9 and cleavage of PARP. CEP was also shown to induce apoptosis by activating p38 MAPK pathways in Jurkat cells and activating ERK and p38 MAPK pathways in K562 cells (26). Seubwai et al demonstrated that CEP inhibited NF-**κ**B activity and activated caspase-9 and -3, inducing apoptotic cell death in cholangiocarcinoma both *in vitro* and *in vivo* (32). Moreover, CEP was found to inhibit the growth of osteosarcoma SaOS2 cells by inhibiting STAT3 pathway both *in vitro* and *in vivo* (29).

Recently, Rattanawong et al reported that CEP inhibited proliferation of colorectal cancer through ROS generation and upregulation of $p21^{Waf1/Cip1}$ (34). Previous studies have reported that the production of reactive oxygen species (ROS) and the expression of $p21^{Waf1/Cip1}$ are associated with apoptosis (9, 10, 18). Therefore, the aim of this study was to investigate the roles of ROS and p21 in the apoptosis-inducing effect of CEP in two CRC cell lines, p53-wild-type HCT-116 cells and p53-mutant HT-29 cells.

1.2 Objectives

1. To investigate the roles of ROS and $p21^{Waf1/Cip1}$ in the apoptosis-inducing effect of CEP in colorectal cancer cells
2. To determine the effect of CEP on ERK signaling pathway in colorectal cancer cells

1.3 Hypothesis

1. CEP induces apoptosis through ROS generation and $p21^{Waf1/Cip1}$ upregulation in colorectal cancer cells.
2. CEP modulates ERK signaling pathway in colorectal cancer cells.

1.4 Conceptual framework

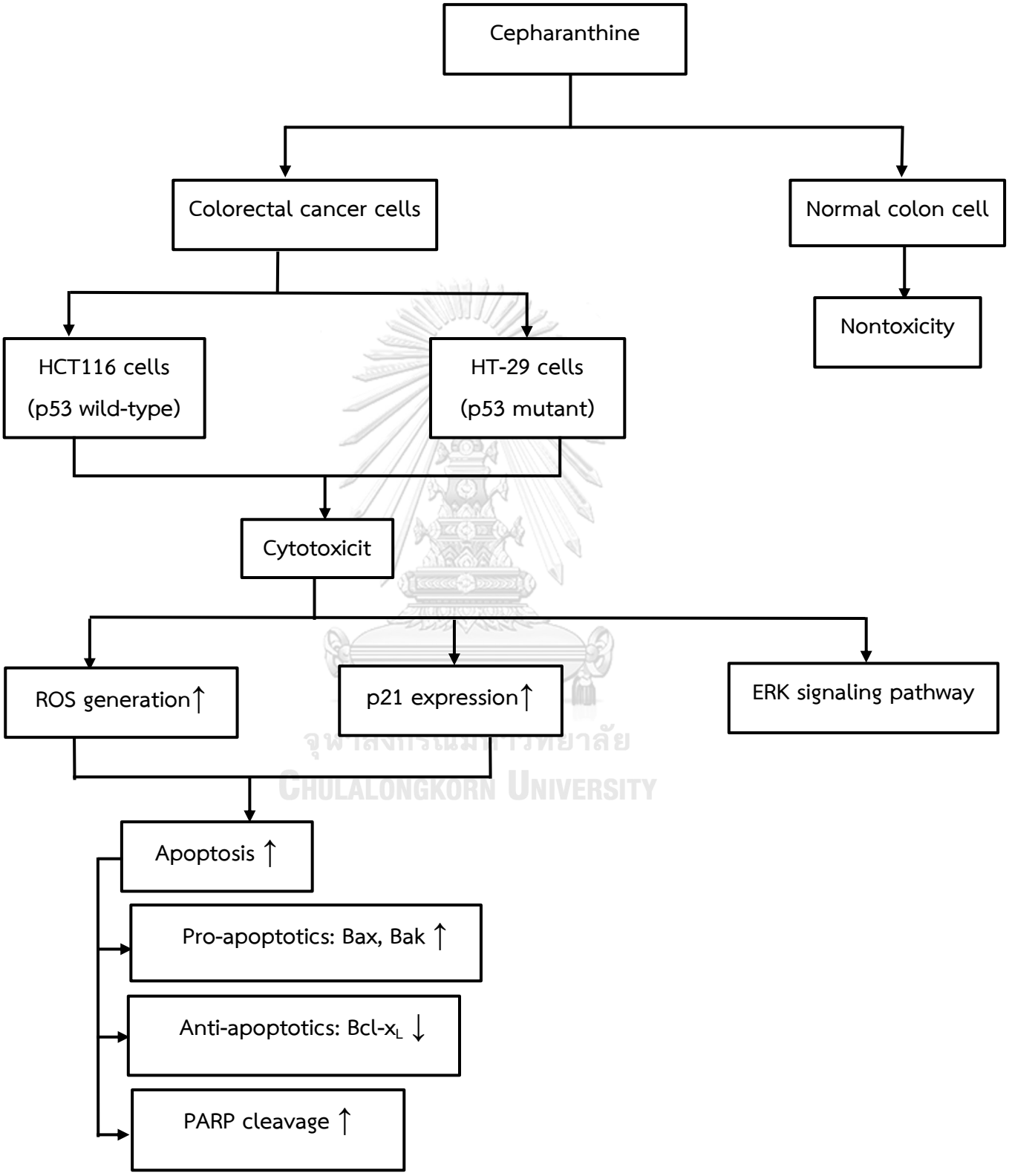

CHAPTER II

LITERATURE REVIEWS

2.1 Colorectal cancer

Colorectal cancer (CRC) accounts for 10–15% of all cancers and is the third leading cause of cancer-related death worldwide. In 2019, the American Cancer Society has revealed the greatest number of deaths are from cancers of the lung, prostate, and colorectum in men and the lung, breast, and colorectum in women (Figure 1) (1). In addition, the National Cancer Institute (NCI) reported in 2017 that the incidence of CRC was the third most commonly diagnosed cancer in both men and women in Thailand. The number of new cases of CRC was found to be the second in males and the third in females, accounting for 16.67% and 9.78%, respectively (38).

2.1.1 Type of CRC

Colorectal cancer results from the abnormalities in the division of the normal intestinal epithelium. CRC is divided into 3 groups (39), including

1. Sporadic CRC: it is the majority of CRC cases that found in approximately 70-85% of all CRC cases. It occurs in people without genetic predisposition or family history of CRC. Most patients with sporadic CRC are >50 years of age (39).

2. Familial CRC: patients have a family history of colon cancer that occurs approximately 20-25% of all CRC cases. The molecular mechanism underlying familial CRC are poorly understood. It probably occurs from combination of environmental and genetic alterations (40, 41).

3. Inherited CRC: inherited cancers account for about 5-10% of all CRC cases. It consists of familial adenomatous polyposis (FAP) and hereditary nonpolyposis colorectal cancer (HNPCC). These cancers are caused by inherited autosomal dominant manner (42).

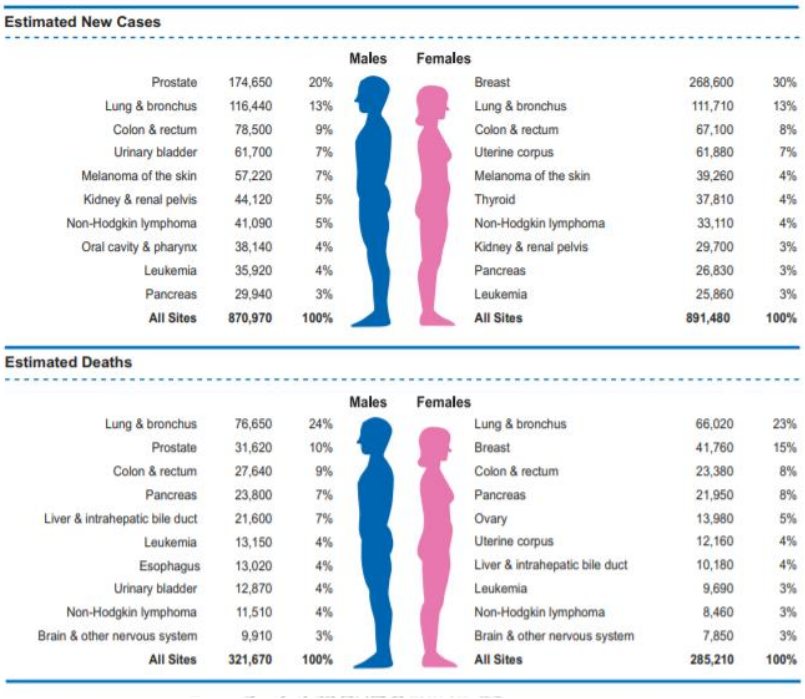

Estimated New Cases

Males			Females		
Prostate	174,650	20%	Breast	268,600	30%
Lung & bronchus	116,440	13%	Lung & bronchus	111,710	13%
Colon & rectum	78,500	9%	Colon & rectum	67,100	8%
Urinary bladder	61,700	7%	Uterine corpus	61,880	7%
Melanoma of the skin	57,220	7%	Melanoma of the skin	39,260	4%
Kidney & renal pelvis	44,120	5%	Thyroid	37,810	4%
Non-Hodgkin lymphoma	41,090	5%	Non-Hodgkin lymphoma	33,110	4%
Oral cavity & pharynx	38,140	4%	Kidney & renal pelvis	29,700	3%
Leukemia	35,920	4%	Pancreas	26,830	3%
Pancreas	29,940	3%	Leukemia	25,860	3%
All Sites	**870,970**	**100%**	**All Sites**	**891,480**	**100%**

Estimated Deaths

Males			Females		
Lung & bronchus	76,650	24%	Lung & bronchus	66,020	23%
Prostate	31,620	10%	Breast	41,760	15%
Colon & rectum	27,640	9%	Colon & rectum	23,380	8%
Pancreas	23,800	7%	Pancreas	21,950	8%
Liver & intrahepatic bile duct	21,600	7%	Ovary	13,980	5%
Leukemia	13,150	4%	Uterine corpus	12,160	4%
Esophagus	13,020	4%	Liver & intrahepatic bile duct	10,180	4%
Urinary bladder	12,870	4%	Leukemia	9,690	3%
Non-Hodgkin lymphoma	11,510	4%	Non-Hodgkin lymphoma	8,460	3%
Brain & other nervous system	9,910	3%	Brain & other nervous system	7,850	3%
All Sites	**321,670**	**100%**	**All Sites**	**285,210**	**100%**

Figure 1 Estimated new cancer cases and deaths by sex, 2019 (1).

2.1.2 Risk factors

Currently, there are several possible risk factors for developing of CRC including age, family history of cancer, genetic alteration such as adenomatous polyposis coli (*APC*), *TP53*, and Kirsten Rat Sarcoma (*KRAS*), personal history of inflammatory bowel diseases, smoking, heavy alcohol consumption, lack of exercise, foods (such as red meat, high fat and low fiber) (43, 44).

2.1.3 Stages of CRC

According to the American Joint Committee on Cancer (AJCC), the stages of CRC are classified into 4 stages including, stage 0, I, II, III and IV. (45)

Stage 0: Abnormal cells have grown in the innermost layer (mucosa) of the colon or rectum, which is called carcinoma *in situ*.

Stage I: Cancer has grown into the intestinal wall, through the mucosa (the inner lining), and into the submucosa and may have entered the muscle.

Stage II: Cancer has not yet spread to nearby lymph nodes or to distant sites. It is further divided into three categories:

Stage IIA: Cancer has spread through the muscle layer of the colon wall to the serosa (outermost layer) of the colon wall.

Stage IIB: Cancer has spread through the serosa of the colon wall to the tissue that lines the organs in the abdomen (visceral peritoneum).

Stage IIC: Cancer has grown through all the layers of the intestine and has grown into nearby organs or tissues.

Stage III: Cancer has spread to nearby lymph nodes but not to other parts of the body. It is further divided into three categories:

Stage IIIA: Cancer has grown into the intestine wall, through the mucosa into the submucosa and may have entered the muscle. It has spread to one to three nearby lymph nodes.

Stage IIIB: Cancer has spread through the muscle layer to the serosa layer of the colon wall or has spread through the serosa to the tissue that lines the organs in the visceral peritoneum. It has spread to one to three nearby lymp nodes.

Stage IIIC: Cancer has grown into or through the outermost layer of the colon or rectum and may have spread to four or more lymph nodes near the primary site. Cancer has also spread to nearby organs.

Stage IV: The cancer has spread through the blood and lymph nodes to other parts of the body. It is divided into stages IVA, IVB, and IVC.

Stage IVA: Cancer has spread to one area or organ such as the liver, lung, and ovary.

Stage IVB: Cancer has spread to more than one distant part of body.

Stage IVC: Cancer has spread to the abdomen and may have spread to other areas or organs.

2.1.4 Treatment of CRC

Colorectal cancer treatments are based largely on the stage of cancer. There are several treatment options for CRC, including surgery, radiotherapy, chemotherapy, and targeted therapy (2).

Surgery is the technique for removing cancer based on the anatomy of mass. It is commonly used for treating patients at an early stage or minimally invasive (46).

Radiation is the technique using powerful energy sources such as X-rays and protons to kill cancer cells and might be used to shrink large cancer before an operation so that it can be removed more easily (47).

Chemotherapy is used to synergist the effectiveness of the treatment and prevent a recurrence. Usually, two or more drugs are used to get the best results. Chemotherapeutic drugs used to treat colon cancer include 5-fluorouracil (5-FU), oxaliplatin (L-OHP) and irinotecan (IR) (48-50).

5-Fluorouracil (5-FU), an antimetabolite (pyrimidine analog), is converted into an active metabolite, fluorodeoxyuridine monophosphate (FdUMP), which inhibits the activity of thymidylate synthase (TS) that required in thymine nucleotide production process, resulting in DNA synthesis inhibition. In addition, 5 -FU is converted into two active metabolites, fluorodeoxyuridine triphosphate (FdUTP) and fluorouridine triphosphate (FUTP), which are inserted into the DNA and RNA, causing DNA and RNA damage (49).

Oxaliplatin (L-OHP) is a platinum derivative with a broad spectrum of anticancer activity. It forms DNA adducts by binding to the N7 site of the guanine residues, which interfere with DNA replication and transcription process (48).

Irinotecan (IR) is a prodrug that must be converted by enzymes carboxylesterase in the liver to SN-38, an active metabolite. SN-38 inhibits topoisomerase I, inducing lethal DNA strand breaks.

Since chemotherapy is most effective at killing rapidly dividing cells. Therefore, chemothereutic agents affects not only cancer cells but also fast-growing normal cells such as blood cells, hair follicles, stomach lining cells, resulting in many side effects such as low blood counts, hair loss, mouth sores, nausea, and diarrhea (48).

Targeted therapy is a treatment that uses drugs to specifically target cancer cells without affecting normal cells. Most targeted therapies are either small-molecule drugs or monoclonal antibodies. An example of a targeted drug used in the treatment of colon cancer is bevacizumab. The drug binds to the vascular endothelial growth factor (VEGF), making it impossible to bind the vascular endothelial growth receptor (VEGFR) on the surface of endothelial cells, which leads to inhibition of angiogenesis (51). Although, many targeted drugs have been approved, they are available only for certain types of cancer. The drugs are effective only in patients carrying target genes and many targeted drugs are very expensive.

2.2 Reactive oxygen species (ROS)

Reactive oxygen species (ROS) are small molecules that are short-lived and highly reactive with other molecules. ROS such as superoxide anion ($O_2^{\bullet -}$), and the hydroxyl radical ($OH^{\bullet}$) and non-radical molecules such as hydrogen peroxide (H_2O_2) are often found in the metabolism process (52). ROS plays a crucial role in the regulation of several cellular processes such as cell proliferation, differentiation and death. Therefore, the balance of ROS is very critical. The ROS levels are controlled by antioxidant mechanisms such as glutathione redox system, superoxide dismutase, and catalase enzyme (5). Excessive accumulation of ROS or oxidative stress can cause nucleic acids, proteins, lipids damage and might depolarizes the mitochondrial membrane, eventually resulting in cell death (53). Thus, overproduction of ROS may be used as a strategy to induce cancer cell death for cancer therapy (8).

Previous studies revealed that many currently available chemotherapeutic drugs such as doxorubicin, cisplatin, carboplatin, and oxaliplatin alter cellular ROS balance in cancer, leading to oxidative stress-triggered apoptotic cell death (9, 10). In addition, various natural compounds have shown to induce cancer cell apoptosis via ROS generation (8). For example, a previous study reported that quercetin inhibited thioredoxin reductase (TrxR), causing an increase in ROS level and subsequent apoptosis in A549 lung cancer cells (11). Similarly, apoptosis-inducing effect of capsaicin was demonstrated to be associated with an increase in ROS generation, a disruption of the mitochondrial transmembrane potential, and activation of caspase

3 in Colo320DM and LoVo colon cells (12). Furthermore, it was found that p-coumaric acid (p-CoA) triggered apoptosis by increasing ROS generation and mitochondrial depolarization, resulting in p53-mediated upregulation of Bax and downregulation of Bcl-2 in HCT-15 colon cancer cells (13). It has been reported that ROS could control the cellular functions such as cell proliferation, differentiation, apoptosis through modulation of mitogen-activated protein kinase (MAPK)/extracellular-signal-regulated kinase (ERK) (8, 54, 55). Accumulating evidence has shown that ROS induces cytotoxicity and apoptosis by activating or inhibiting ERK signaling pathway. For instance, Seok et al demonstrated that piperlongumine prevented cell proliferation by ROS-mediated activation of MAPK/ ERK pathway in A549 human lung cancer cells (56). Moreover, sanguinarine induced apoptotic cell death via activation of ERK1/2 phosphorylation, which was shown to be dependent on ROS generationin PC3 and DU145 prostate cancer cells (15). Li et al also revealed that quercetin could induce apoptosis via ROS-mediated ERK activation in HL-60 leukemia cells (14). Conversely, Yuan et al revealed that koumine promotes ROS production which can inhibit the proliferation and promote apoptosis in Huh-7 and SNU-499 hepatocellular carcinoma cells via inhibition of ERK (17). Isoliquiritigenin was also shown to increase the levels of ROS and subsequently decrease the expression of ERK phosphorylation, leading to apoptosis induction and cell cycle arrest in human hepatocellular carcinoma cells (57). Moreover, apoptosis-inducing effect of zeaxanthin was mediated via ROS-mediated inhibition of MAPK/ ERK signaling pathway in human gastric cancer cells (16).

2.3 Apoptosis

Apoptosis, or programmed cell death (PCD), is a homeostatic mechanism to maintain cell populations during development and aging in multiple organisms (58). It is characterized by a series of distinct morphological and biochemical alterations in the cells such as DNA fragmentation, chromatin condensation, cell shrinkage, and plasma membrane blebbing (Figure 2) (59). At the molecular level, apoptosis is mainly regulated by the activation of the aspartate-specific cysteine protease

(caspase) cascade. There are two main pathways of apoptosis, including the extrinsic (death receptor) and intrinsic (mitochondrial) pathways (Figure 3) (60).

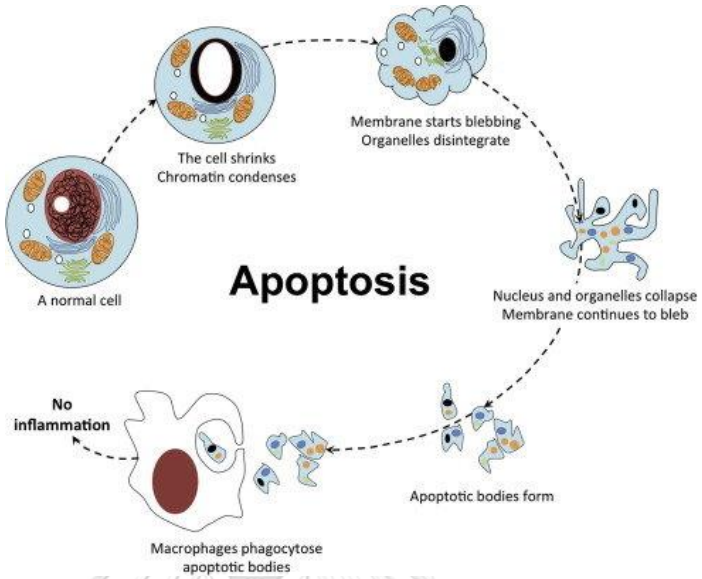

Figure 2 Morphological features of apoptotic cells (59).

2.3.1 Extrinsic pathway

The extrinsic apoptotic pathway is mediated by the activation of death receptors which are located on the cell surface that transmit apoptotic signals after binding with specific death ligands such as Fas ligand, tumor necrosis factor-α (TNF-α) and TNF-related apoptosis-inducing ligand (TRAIL also called Apo2L) (61). Binding of the death ligand to its death receptor creates a binding site for recruiting adaptor proteins such as TNFR-associated death domain (TRADD) and Fas-associated death domain (FADD), forming the death-inducing signaling complex (DISC).

Recruitment and accumulation of procaspase-8 or -10 at the DISC results in spontaneous activation of caspase-8 or -10 via autoproteolytic cleavage, and initiation of the apoptosis signal by cleaving other downstream or executioner caspases such as caspase-3, -6 or -7 (62).

2.3.2 Intrinsic pathway

The intrinsic apoptotic pathway is activated by vasious stimuli such as ultraviolet, irradiation, growth factor withdrawal, oxidative stress, and chemotherapeutic drugs. This non receptor-mediated pathway is regulated by Bcl-2 family proteins, which are classified into three sub-families based on the number of BH domains (63).

I. Anti-apoptotic Bcl-2 proteins such as Bcl-2 and Bcl-x_L consist of BH1, BH2, BH3, and BH4 domains.

II. Pro-apoptotic Bcl-2 effector proteins such as Bak and Bax consist of BH1, BH2, and BH3 domains.

III. BH3 only pro-apoptotic Bcl-2 proteins such as BAD, Bid, Bim, PUMA and NOXA consist of BH3 domains.

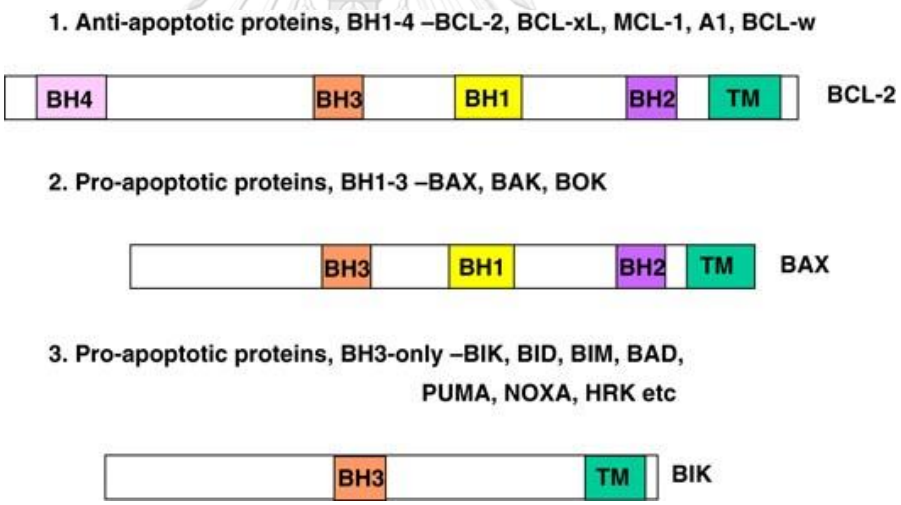

Figure 3 Bcl-2 family proteins (64).

Normally, anti-apoptotic Bcl-2 proteins form a complex with BH1-3 pro-apoptotic proteins to stabilize mitochondria outer membrane permeabilization (MOMP). When the cells obtained apoptotic stimuli, these can activate one or more of BH3 only pro-apoptotic Bcl-2 proteins to directly bind or neutralize anti-apoptotic Bcl-2 proteins, resulting in an opening of the mitochondrial permeability transition

(MPT) pore and release of apoptogenic factors such as cytochrome c from the mitochondrial intermembrane space (IMS) into the cytosol (63). Binding of cytochrome c to apoptotic protease activating factor 1 (Apaf-1) promote its oligomerization and binding to pro-caspase 9 to form a complex, termed the apoptosome, which results in autocatalytically cleavage of procaspase-9. Activated caspase-9 can further stimulates the execute caspases, such as caspase-3, eventually leading to apoptosis (65, 66).

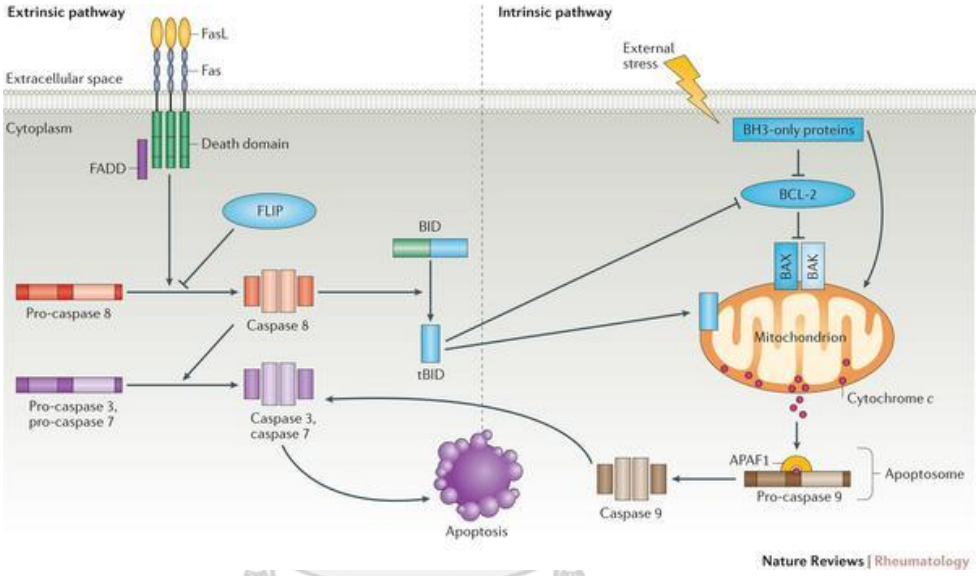

Figure 4 Extrinsic and intrinsic apoptotic signaling pathways (66).

2.4 p21$^{Waf1/Cip1}$

p21$^{Waf1/ Cip1}$ is tightly involved in balancing of cells. Generally, p21$^{Waf1/ Cip1}$ inhibits cell proliferation directly by binding to cyclin-dependent kinases (CDKs), proliferating cell nuclear antigen (PCNA) or several transcription factors and transcriptional coactivators such as c-myc, STAT3, and p300/CBP. Notably, under certain conditions, p21$^{Waf1/Cip1}$ plays a significant role in promoting apoptosis (18, 67). Li et al demonstrated that genistein induced p21$^{Waf1/ Cip1}$ expression, which was correlated with upregulation of pro-apoptotic protein, Bax, in the p53 mutant MDA-MB-231 breast cancer cells (19). Moreover, upregulation of p21$^{Waf1/Cip1}$ in response to

cisplatin treatment led to an increase in apoptosis in the p53-deficient human ovarian carcinoma cell lines, SKOV3 and OVCAR3 (20). Wu et al also reported that an increase in $p21^{Waf1/Cip1}$ expression could lead to DNA fragmentation, a morphological feature of apoptosis in p53 mutant human ovarian cancer cells (68). In addition, $p21^{Waf1/Cip1}$ was shown to promote ceramide-induced apoptosis cell death through downregulation of Bcl-2 and upregulation of Bax in p53-deficient Hep3B cells (69). Similarly, it was reported that high level of of $p21^{Waf1/Cip1}$ expression significantly increased the sensitivity of p53 mutant carcinoid (NCI-H727) cells to TNF-related apoptosis-inducing ligand (TRAIL)-induced apoptosis (70).

2.5 MAPK/ERK signaling pathway

Mitogen-activated protein kinases (MAPKs) are involved in the regulation of cell proliferation, differentiation, migration, and apoptosis (71). The MAP kinases can be grouped into three main families, including extracellular-signal-regulated kinases (ERKs), Jun amino-terminal kinases (JNKs), and stress-activated protein kinases (SAPKs/p38) (72). Previous studies reported that CRC usually has the mutations of KRAS and BRAF genes, which are approximately 45% and 10%, respectively, leading to hyperactivation of MEK/ERK signaling (73, 74). The activation of the ERK pathway is initiated by binding of ligands such as growth factors, cytokines, hormones to specific growth-factor receptor tyrosine kinases, resulting in receptor dimerization, and autophosphorylation of selected tyrosine residues on the receptor. Recruitment of the adaptor proteins growth-factor-receptor-bound protein 2 (GRB2) to specific phosphorylated residues on the receptors subsequently induce recruitment and activation of the son of sevenless (SOS). Then, SOS activates RAS by switching from diphosphate (GDP)-bound RAS (inactive) to guanosine triphosphate (GTP)-bound RAS (active), which causes the recruitment and activation of RAF. After that, activated RAF phosphorylates and actives MEK, which further phosphorylates and activates MAPK/extracellular signal-regulated kinase (ERK). Finally, active ERK translocates to the nucleus and then activates transcription factors that involve cellular processes (72, 75, 76).

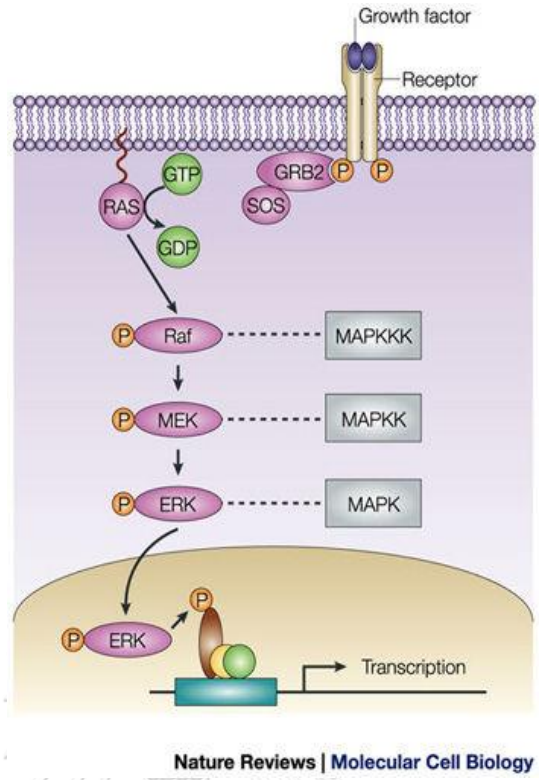

Figure 5 MAPK/ERK signaling pathway (73).

2.6 Cepharanthine

Cepharanthine (CEP) is a biscoclaurine alkaloid extracted from the roots of *Stephania cepharantha* Hayata (Figure 6). Additionally, it can be found in *Stephania suberusa* L.L forman and *Stephania erecta* Craib in Thailand. CEP has been used in Japan for more than 40 years to treat several acute and chronic diseases such as venomous snakebites, malaria and septic shock. Notably, CEP is approved by Japanese Ministry of Health for the treatment of radiation-induced leukopenia, alopecia areata and alopecia pityrodes (21). In addition, CEP has various pharmacological activities including anti-malarial, anti-oxidant, anti-inflammatory, anti-allergic effect, anti-platelet aggregation, anti-HIV, and anti-tumor (52, 53). Although CEP has been widely used, serious side effects have never been reported. Its side effects include anorexia, rash, diarrhea and headache. (22).

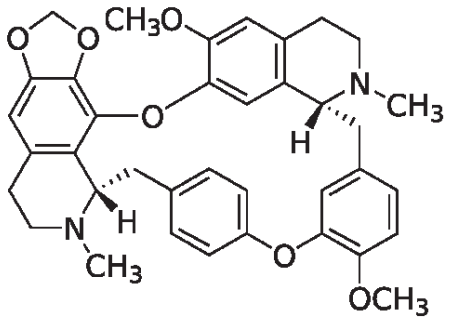

Figure 6 Chemical structure of cepharanthine (CEP) (21).

2.6.1 Anti-inflammatory effect

CEP has shown to possess anti-inflammatory activity by suppression of pro-inflammatory cytokines (77, 78). It was reported that CEP could inhibit the production of TNF-α in human monocyte and LPS-stimulated acute pulmonary vascular injury in rats (77). Moreover, in a mouse model of lipopolysaccharide (LPS)-induced mastitis, treatment with CEP decreased the level of pro-inflammatory cytokines, including TNF-α, IL-1β and IL-6, attenuated the infiltration of neutrophils, suppressed myeloperoxidase activity and inhibited NF-κB activation (78). Several mechanistic studies indicated that anti-inflammatory effect of CEP was mediated through modulation of various signaling pathways (79, 80). Previously, CEP was found to inhibit the activation of NF-κB, degradation of IκB-α, and phosphorylation of ERK, JNK and p38, preventing the release of proinflammatory cytokines such as TNF-α, IL-6, and IL-1β in LPS-stimulated RAW264.7 cells (79). Aota et al reported that CEP inhibited IFN-γ-induced CXCL10 (CXC chemokine) production by inhibiting the JAK2/STAT1 signaling pathway in human salivary gland ductal cells (80).

2.6.2 Anti-oxidant effect

Previous studies demonstrated that CEP serves as an effective free radical scavenger. CEP was shown to inhibit lipid peroxidation by 94.6% whereas three standard antioxidants, butylated hydroxyanisole, α-tocopherol and trolox inhibited

lipid peroxidation by 83.3% , 72.4% and 81.3% , respectively (81). Furthermore, CEP was able to reduce the level of intracellular free radicals and protecting DNA damage in lymphoblastoid TK6 cells (82). Similarly, Tsuyoshi et al reported that CEP could inhibit the active oxygen generation by suppressing PKC and NADPH oxidase activation in guinea-pig neutrophils (83).

2.6.3 Anti-maralia effect

It was demonstrated that intra-peritoneal injection and oral administration of CEP at a dose of 10 mg/ kg decreased malarial parasitemia by 47% and 50% , respectively in a mouse model (84).

2.6.4 Anti-virus effect

CEP was found to inhibit HIV-1 replication through suppression of NF-**κ**B activation in chronically infected monocytic (U1) cell lines (85).

2.6.5 Anti-cancer effect

Several studies revealed that CEP exhibited anticancer effect in many types of cancer including melanoma, leukemia, ovarian, breast, osteosarcoma, lymphoma, lung carcinoma, myeloma, cholangiocarcinoma, oral squamous carcinoma, colorectal cancer, and hepatocellular carcinoma (25-36, 86). Harada et al reported that CEP inhibited angiogenesis and the growth of oral squamous carcinoma by decreasing vascular endothelial growth factor (VEGF) and interleukin-8 (IL-8) via inhibition of NF-**κ**B activity in both *in vitro* and *in vivo* (33). Moreover, CEP induced apoptotic cell death through ROS production, which led to cytochrome c release, resulting in activation of caspases-3 and cleavage of PARP. Additionally, CEP was shown to induce apoptosis via activation of p38 and JNK1/ 2, and downregulation of AKT signaling pathway in hepatocellular carcinoma (HUH-7) cells (35). CEP induced ROS generation, which could disrupt mitochondria membrane potential and alter bcl-2 family proteins, inducing apoptotic cell death in non-small lung cancer (A549 and H1299) cells (31). Additionally, Seubwai et al have demonstrated that apoptosis-indicing effect of CEP was mediated through inhibition of NF-**κ**B activity and

activation of caspase-9 and -3 in cholangiocarcinoma both *in vitro* and *in vivo* (32). Similarly, CEP-inhibited the growth of lymphoma (PEL) cells and induced apoptosis via suppression of NF-**κ**B activity (30). Furthermore, CEP could induce apoptosis in leukemia (Jurkat and K562) cells through activation of ERK and p38 MAPK pathways (26). Kikukawa et al found that CEP blocked cell cycle progression via upregulation $p15^{INK4B}$ and $p21^{Waf/Cip1}$ and downregulation of cyclin D1 in myeloma cells (36). Moreover, CEP-induced apoptosis was associated with production of ROS, upregulation of Bax and activation of caspase-3 in myeloma cells (36). Moreover, in human adenosquamous cell carcinoma (TYS) cells, CEP was shown to induce apoptosis by activating caspase 3 and inducing cell cycle arrest at the G1 phase via the expression of $p21^{Waf1/Cip1}$ (86). Additionally, Zhu et al. found that CEP-triggered apoptosis was mediated via production of ROS, leading to activation of JNK, downregulation of Bcl-2 and upregulation of Bax in choroidal melanoma (MEL15-1) (25). Chen et al also revealed that CEP inhibited the growth of osteosarcoma (SaOS2) cells by inhibiting STAT3 pathway, resulting in downregulation of STAT3 transcriptional targets such as Bcl-x_L, cyclin D1, and c-Myc. Moreover, CEP was shown to decrease tumor volume and inhibit the expression of STAT3 *in vivo* study (29). In addition, it was reported that CEP induced sensitization of human cervical adenocarcinoma (HeLa) cells to radiation through inhibition of STAT3 signaling pathway and COX-2 expression both *in vitro* and *in vivo* (87). CEP was also shown to induce apoptosis by increasing Bax/Bcl-2 ratio and activating caspase cascade in breast (MCF-7 and MDA-MB-231) cancer cells (88). Furthermore, Payon et al. found that CEP induced apoptosis through downregulation of Bcl-2 and Bcl-x_L and upregulation of Bak expression (27). Notably, CEP could inhibit proliferation of colorectal cancer (HT-29 and COLO-205) cells by inducing cell cycle arrest through upregulation of $p21^{Waf1/Cip1}$ and downregulation of cyclin A (34). Recently, CEP has shown to synergize the apoptosis-inducing effect of 5-fluorouracil (5-FU) via upregulation of Bak and cleavage of PARP in p53-mutant colorectal cancer cells both *in vitro* and *in vivo* (89).

CHAPTER III

MATERIALS AND METHODS

3.1 Equipment

- Analytical balance 0.001 g (Mettler Toledo, Switzerland)
- Analytical balance 0.00001 g (Sartorius, Germany)
- Autoclave (Sanyo, Japan)
- Autopipette (Brand, Germany)
- Biohazard laminar flow hood (Labconco, USA)
- Flow cytometer (BD Bioscience, Heidelberg, Germany).
- Centrifuge (Hettich, Germany)
- CO_2 incubator (Thermo, USA)
- Controller pipette (Gilson, USA)
- Electrophoresis system (Bio-Rad, USA)
- Improm-II reverse transcription system (Promaga, USA)
- Light microscope (Nikon, Japan)
- Microplate reader (Thermo, Finland)
- NanoDrop One UV-Vis Spectrophotometer (Thermo, USA)
- pH meter (Mettler Toledo, Switzerland)
- StepOnePlus™ Real-Time PCR (Thermo Fisher Scientific, USA)
- Temperature control centrifuge (Eppendrof, Germany)
- Vortex mixer (Scientific Industries, USA)
- Water Bath (M-LAB, Thailand)

3.2 Materials

- 6 well plate (Corning Inc., USA)

- 96 well plate (Corning Inc., USA)

- 15 mL conical tube (Corning Inc., USA)

- 25 cm^2 rectangular cell culture flask (Corning Inc., USA)

- Polyvinylidene difluoride (PVDF) membrane (Merck, Germany)

3.3 Reagents

- 0.4% trypan blue dye (Sigma, USA)

- 40% acrylamide/Bis Solution (Bio-Rad, USA)

-1-(4-chloro-3-(trifluoromethyl) -phenyl) -3-((1r,4r) -4-(5-(trifluoromethyl) pyridin-2-yloxy)cyclohexyl) urea (UC2288) (Abcam, UK)

- 2,7-dichloro-dihydro-fluorescein diacetate (Sigma, USA)

- Ammonium persulfate (Sigma, USA)

- Annexin V, fluorescein conjugate (FITC) (ImmunoTools, Germany)

- Bromophenol blue (Sigma, USA)

- β-mercaptoethanol (Sigma, USA)

- Cepharanthine (Abcam, UK)

- Dimethyl sulfoxide (DMSO) [analytical grade] (Merck, Thailand)

- Dimethyl sulfoxide (DMSO) [molecular grade] (Sigma, USA)

- Dulbecco's Modified Eagle Medium (DMEM) (Gibco, USA)

- Fetal bovine serum (Gibco, USA)

- Glycerol (Sigma, USA)

- Glycine (Sigma, USA)

- Hank's buffered salt solution (HBSS) (Sigma, USA)

- *N,N,N,N*-tetramethyl ethylenediamine (TEMED) (Sigma, USA)

- *N*-acetylcysteine (NAC) (Sigma, USA)

- [SP-4-2-(1R-trans)]-(1,2-Cyclohexanediamine-N,N′)[ethanedioata(2--)-O,O'] platinum (Oxaliplatin) (Sigma, USA)

- Penicillin-streptomycin (Gibco, USA)

- Pyronin Y (Sigma, USA)

- Primary antibodies (Cell Signaling Technology, USA)

    - Bak rabbit monoclonal antibody (25 kDa)

    - Bax rabbit monoclonal antibody (20 kDa)

    - Bcl-xl rabbit monoclonal antibody (30 kDa)

    - GAPDH rabbit monoclonal antibody (37 kDa)

    - PARP rabbit monoclonal antibody (116, 89 kDa)

    - Phospho-p44/42 MAPK (Erk1/2) rabbit monoclonal antibody (44, 42 kDa)

    - p44/42 MAPK (Erk1/2) rabbit monoclonal antibody (44, 42 kDa)

    - p21 rabbit monoclonal antibody (21 kDa)

- Propidium iodide (ImmunoTools, Germany)

- Protease inhibitors (Sigma, USA)

- Protein assay kit (Bio-Rad, USA)

- RIPA lysis buffer (Thermo scientific, USA)

- Roswell Park Memorial Institute (RPMI)-1640 medium (Gibco, USA)

- Secondary antibody (Cell Signaling, USA)

    - Anti-IgG, horseradish peroxidase (HRP)-linked antibody

- Sodium dodecyl sulfate (SDS) (EM science, USA)

- SYBR-Green qPCR supermix universal (Life Technologies, USA)

- Thiazolyl blue tetrazolium bromide (MTT) (Sigma, USA)

- Tris base (Vivantis, USA)

- TRIzol Reagent (Invitrogen, USA)

- Trypsin/EDTA (Gibco, USA)

- Tween 20 (Sigma, USA)

- Western horseradish peroxidase substrate (Merck, Germany)

3.4 Methods

3.4.1 Preparation of oxaliplatin and cepharanthine stock solutions

Stock solutions of oxaliplatin (L-OHP; Sigma, USA) and cepharanthine (CEP; Abcam, UK) were prepared in dimethyl sulfoxide (DMSO) at 50 mM and stored at 4ºC until use. In the experiments, the stock solution was diluted in culture medium to give appropriate final concentrations. The 0.2% DMSO was used as a vehicle control.

3.4.2 Cell culture

Human colorectal cancer cell lines (HT-29 and HCT116) and human colon cells (CRL-1790) were obtained from American Type Culture Collection (ATCC, USA).

HT-29 cells were cultured in Dulbecco's modified Eagle's medium (DMEM; Gibco, USA) supplemented with 10% fetal bovine serum (FBS), 100 U/mL penicillin and 100 µg/mL streptomycin. HCT116 cells were cultured in Roswell Park Memorial Institute (RPMI-1640; Gibco, USA) medium supplemented with 10% FBS, 100 U/mL

penicillin and 100 µg/mL streptomycin. The DMEM with high glucose (4,500 mg/L) supplemented with 10% FBS, 100 U/mL penicillin, and 100 µg/mL streptomycin was used for culturing CRL-1790 cells. All cells were maintained at 37°C in a humidified 5% CO_2 atmosphere.

3.4.3 Determination of cytotoxicity using MTT assay

Cell viability was determined using methyl thiazolyl tetrazolium (MTT) colorimetric assay. Briefly, cells were seeded into 96-well plates at a density of $5x10^4$ cells/mL and incubated overnight at 37°C. Cells were then treated with CEP at the concentrations of 0.625, 1.25, 2.5, 5, 10 and 20 µM or L-OHP (positive control) at the concentrations of 0.1, 1, 10 and 100 µM for 48 h. Next, MTT solution (5 mg/mL) was added into each well and incubated for 3-4 h. After incubation, the MTT solution was replaced with DMSO to dissolve the purple formazan crystal. The absorbance of formazan solution was measured at 570 nm using a microplate reader (Thermo, Finland). Cell viability was calculated from the absorbance value and presented as percentage related to control. The half-maximal inhibitory concentration (IC_{50}) were calculated using GraphPad Prism 7 software.

3.4.4 Detection of apoptosis using Annexin-V/PI staining assay

HCT-116 and HT-29 cells were seeded at a density of $5x10^4$ cells/mL in 6-well plates. After overnight incubation, HCT116 cells were treated with 5, 10 and 20 µM of CEP or 5 µM of L-OHP, whereas HT-29 cells were treated with 1.25, 2.5 and 5 µM of CEP or 10 µM of L-OHP. After 24 h incubation, cells were collected, washed with phosphate buffer saline (PBS), and resuspended in 400 µL of 1× binding buffer. Subsequently, cells were stained with 3 µL of annexin V-FITC and 3 µL of propidium iodide (PI; ImmunoTools, Germany) in the dark at room temperature for 15 min. Apoptotic and necrotic cells were analyzed using flow cytometer (BD LSR II, Biosciences).

3.4.5 Detection of cellular ROS using DCFH-DA assay

2,7-Dichlorouorescein diacetate (DCFH-DA) is a fluorogenic dye used for detection of ROS within the cell. HCT-116 and HT-29 cells were seeded in 6-well plates at a density of $5x10^4$ cells/mL and incubated at 37°C overnight. Then, the

cells were wash with PBS and incubated with 1 mL of 10 μM DCFH-DA (Sigma, USA) in Hank's buffered salt solution (Sigma, USA) in the dark at room temperature for 30 min. After incubation, HCT-116 cells were treated with 5, 10 and 20 μM of CEP, 5 μM of L-OHP, 500 μM of H_2O_2 (positive control) or 0.2% DMSO for 1 h. HT-29 cells were treated with 1.25, 2.5 and 5 μM of CEP, 10 μM of L-OHP, 500 μM of H_2O_2 or 0.2% DMSO for 1 h. Then cells were collected by trypsinization and centrifuged at 1,500 rpm for 5 min. After that, the cells were washed and resuspended with 300 μL of cold PBS. The levels of ROS were measured by detecting DCF fluorescence intensity using flow cytometer (BD Bioscience, Heidelberg, Germany) . The fluorescence intensity in each group was presented as percentage related to control.

3.4.6 Determination of cytotoxicity through ROS production using MTT assay

HCT-116 and HT-29 cells were seeded into 96-well plates at a density of $5x10^4$ cells/mL and incubated overnight at 37°C. After pretreatment with 3 mM NAC for 2 h, HCT116 cells were treated with 5, 10 and 20 μM of CEP or 5 μM of L-OHP, whereas HT-29 cells were treated with 1.25, 2.5 and 5 μM of CEP or 10 μM of L-OHP. After 24 h incubation, cytotoxicity was evaluated using MTT assay as previously described.

3.4.7 Determination of apoptosis through ROS production using Annexin-V/PI staining assay

HCT-116 and HT-29 cells were seeded into 6-well plates at a density of $5x10^4$ cells/mL and incubated overnight at 37 °C. Cells were pretreated with 3mM NAC for 2 h. Then, HCT116 cells were treated with 5, 10 and 20 μM of CEP or 5 μM of L-OHP, whereas HT-29 cells were treated with 1.25, 2.5 and 5 μM of CEP and 10 μM of L-OHP. After 24 h incubation, apoptotic and necrotic cells were analyzed using annexin-V/PI staining assay as previously described.

3.4.8 Determination of protein expression using western blot analysis

HCT-116 and HT-29 cells were seeded into 6-well plates at a density of $5x10^4$ cells/mL. After overnight incubation, HCT116 cells were treated with 5, 10 and 20 μM

of CEP or 5 μM of L-OHP, whereas HT-29 cells were treated with 1.25, 2.5 and 5 μM of CEP or 10 μM of L-OHP. After incubation for 24 h, cells were washed with PBS and incubated with RIPA buffer for 1 h (Thermo scientific, USA). The cellular lysates were centrifuged at 14,000 rpm for 20 min at 4 ºC. After that, the supernatants were collected and total protein content was determined using the Bio-Rad DC protein assay reagents (Bio-Rad, USA). Equal amounts of the protein samples (20 μg) were loaded onto 8 % gels and electrophoresis was performed. The separated proteins were transferred to polyvinylidene difluoride (PVDF) membranes. The membranes were blocked with 5 % non-fat dry milk in 1X Tris-buffered saline (TBS) at room temperature for 1 h. Subsequently, membranes were washed with TBS containing 0.1% Tween 20 (TBST) and incubated with primary antibody, including Bak, Bax, Bcl-x_L, PARP, phospho-p44/42 MAPK (ERK1/2), p44/42 MAPK (ERK1/2), p21 $^{Waf1/Cip1}$ or GAPDH (Cell Signaling, USA) (dilution 1:1000) at 4ºC overnight. After incubation, the membranes were washed three times with TBST for 5 min each time. The membranes were further incubated with horseradish peroxidase (HRP)-conjugated secondary antibody (dilution 1: 2000) (Cell signaling, USA) for 1 h at room temperature. Finally, the signal form specific proteins were detected using a chemiluminescence substrate (Merck, Germany) and quantified using Image Studio software (LICOR, USA).

3.4.9 Determination of the of p21$^{Waf1/Cip1}$ mRNA level using quantitative real-time RT-PCR

HCT-116 and HT-29 cells were seeded into 6-well plates at a density of $5x10^4$ cells/mL. After overnight incubation, HCT116 cells were treated with 5, 10 and 20 μM of CEP or 5 μM of L-OHP, whereas HT-29 cells were treated with 1.25, 2.5 and 5 μM of CEP or 10 μM of L-OHP. After 24 h incubation. Total cellular RNA was extracted from cells with Trizol reagent (Invitrogen, USA). Then the amount of RNA was measured at 260 nm using NanoDrop Spectrophotometer. After that, the RNA was converted into cDNA using Improm-II^{TM} reverse transcription system (Promega, USA). The cDNA product of target gene was amplified using SYBR Green (Life Technologies, USA) with the specific primers (p21 primers: 5'-TGA GCC GCG ACT GTG ATG-3' (forward), 5'-GTC TCG GTG ACA AAG TCG AAG TT-3' (reverse)) and GAPDH was used as

an internal control. (GAPDH primers: 5 ’ -AAG GTC GGAGTCAAC GGATTT GGT-3 ’ (forward), 5’-ATG GCA TGG ACT GTG GTC ATG AGT-3’ (reverse)). Amplification was conducted under the following conditions: 50°C for 2 min, 95°C for 2 min, and 40 cycles of 95°C for 30s, 60°C for 30s, and 72°C for 30s using StepOnePlus™ Real-Time PCR (Thermo Fisher Scientific, USA). Calculating the fold change in mRNA level using the $2^{-\Delta\Delta CT}$ method.

3.4.10 Statistical analysis

All data were presented as mean ± standard error of mean (SEM) from three independent experiments performed in triplicate. One-way analysis of variance (ANOVA) followed by Fisher’s Least Significant Difference (LSD) post-hoc test was performed to determine the significance of differences between groups using SPSS programs (IBM Corporation, USA). Statistical significance was considered at $p < 0.05$.

CHAPTER IV

RESULTS

4.1 Effect of cepharanthine (CEP) and oxaliplatin (L-OHP) on the viability of human colorectal cancer cells and normal colon cells.

The cytotoxic effects CEP and L-OHP were initially evaluated on two human colorectal cancer cell lines, HCT116 carrying wild-type p53 and HT-29 carrying mutant p53, and normal colon CRL-1790 cells. The cells were incubated with CEP at the concentrations of 0.625, 1.25, 2.5, 5, 10 and 20 μM or L-OHP at the concentrations of 0.1, 1, 10 and 100 μM for 48 h. The cell viability was evaluated using MTT assays. As shown in Figures 7A-B, CEP and L-OHP significantly decreased the viability of HCT116 and HT-29 cells in a concentration-dependent manner ($p<0.05$). Similar to cancer cells, CEP and L-OHP at the concentrations of 0.625, 1.25, 2.5, 5, 10 and 20 μM significantly decreased the viability of normal colon CRL-1790 cells in a concentration dependent manner (Figures 8A-B, $p<0.001$). The values of half maximal inhibitory concentration (IC_{50}) of CEP and L-OHP were shown in Table 1. The results demonstrated that, when compared to L-OHP, CEP was more effective in controlling the growth of p53 mutant HT-29 cells. The IC_{50} values of CEP and L-OHP were 2.46±0.22 μM and 10.96±0.42 μM in p53 mutant HT-29 cells whereas they were 9.64±0.35 μM and 4.36±0.69 μM, respectively, in p53 wild-type HCT116 cells.

We further evaluated selectivity index (SI) values of CEP and L-OHP, which calculated from IC_{50} for normal cells/ IC_{50} for cancer cells for both CRC cell lines (Table 1). Remarkably, the SI values of CEP were approximately 4.22 and 1.08 while the SI values of L-OHP were approximately 0.27 and 0.68 in HT-29 and HCT116, respectively, suggesting that CEP was relatively safe to normal cells.

(A)

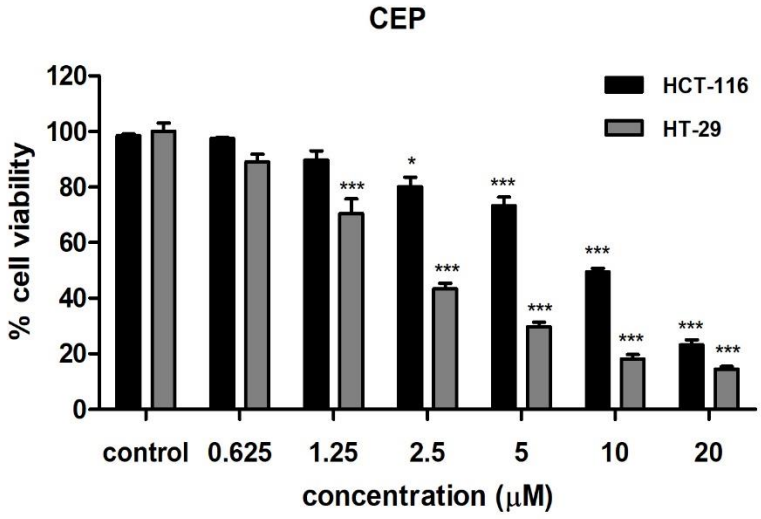

(B)

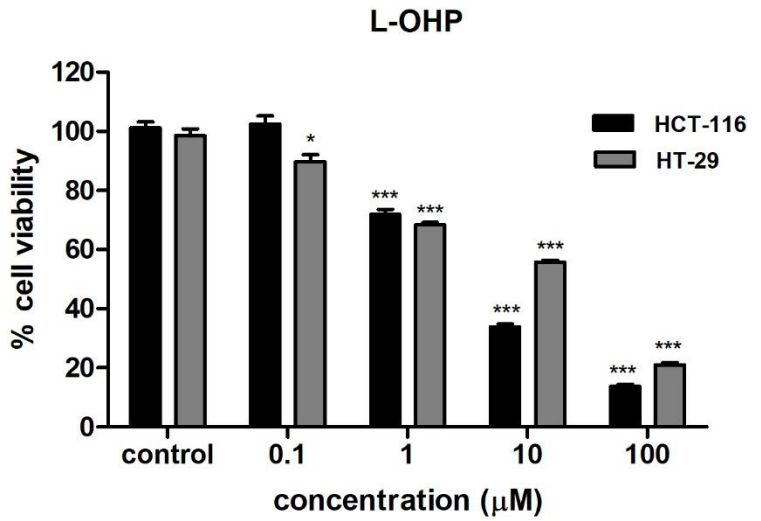

Figure 7 Effects of CEP and L-OHP on the viability of HCT116 and HT-29 cells. The cells were treated with CEP at 0.625, 1.25, 2.5, 5, 10 and 20 μM or L-OHP at 0.1, 1, 10 and 100 μM for 48 h. Cell viability was evaluated using MTT assays. Each value is expressed as the mean ± SEM (n=3). *p<0.05, **p<0.01, ***p<0.001 compared with vehicle control (0.2% DMSO).

(A) (B)

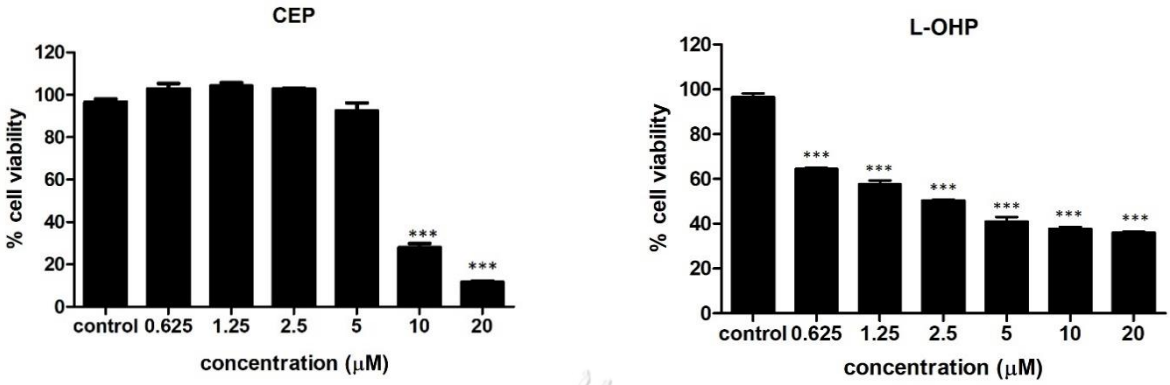

Figure 8 Effects of CEP and L-OHP on the viability of normal CRL-1790 cells. The cells were treated with CEP or L-OHP at 0.625, 1.25, 2.5, 5, 10 and 20 μM for 48 h. Cell viability was evaluated using MTT assays. Each value is expressed as the mean ± SEM (n= 3). *p<0.05, **p<0.01, ***p<0.001 compared with vehicle control (0.2% DMSO).

Table 1 IC_{50} at 48 h. and selectivity index values of CEP and L-OHP on HCT116, HT-29 and CRL-1790 cells.

Drugs	IC_{50} values (μM)			Selective index (SI)	
	HT-29	HCT116	CRL-1790	HT-29	HCT116
CEP	2.46±0.22	9.64±0.35	10.39±0.22	4.22	1.08
L-OHP	10.96±0.42	4.36±0.69	2.96±0.09	0.27	0.68

4.2 Effect of CEP on apoptosis induction in CRC cells

Previous studies have reported that CEP induced apoptosis in several cancer cells such as leukemia, lung, liver and breast cancer (26, 31, 35, 88). To determine whether apoptosis is involved in CEP-induced cytotoxicity in CRC cells, the cells were incubated with CEP or L-OHP for 24 h and apoptotic cells were determined using flow cytometry analysis after annexin V-FITC/PI staining. As shown in Figure 9A, CEP significantly triggered HT-29 cells to undergo apoptosis, which were approximately 27% higher than the vehicle control ($p<0.01$). In contrast to CEP, L-OHP did not induce apoptosis cell death in HT-29 cells. To further confirm the apoptosis-inducing effect of CEP in HT-29 cells, the expression of cleaved poly (ADP-ribose) polymerase (PARP), a marker of apoptosis, was determined using western blotting. As illustrated in Figure 9B, CEP at 5 μM significantly induced the cleavage of PARP. The expression level of cleaved PARP was approximately 5-fold above the vehicle control ($p<0.01$).

Similar to p53 mutant HT-29 cells, CEP at 20 μM significantly triggered p53 wild-type HCT116 cells to undergo apoptosis (Figure 10A, $p<0.01$) while L-OHP has no apoptosis-inducing effect in HCT-116 cells. Moreover, CEP and L-OHP significantly induced the cleavage of PARP in HCT116 cells. The expression levels of cleaved PARP were approximately 12 and 10 times higher than the vehicle control, after treatment with 20 μM of CEP and 5 μM of L-OHP, respectively (Figure 10B, $p<0.05$). Taken together, these results suggest that cytotoxic effect of CEP is partly mediated via apoptosis induction in both HT-29 and HCT116 cells.

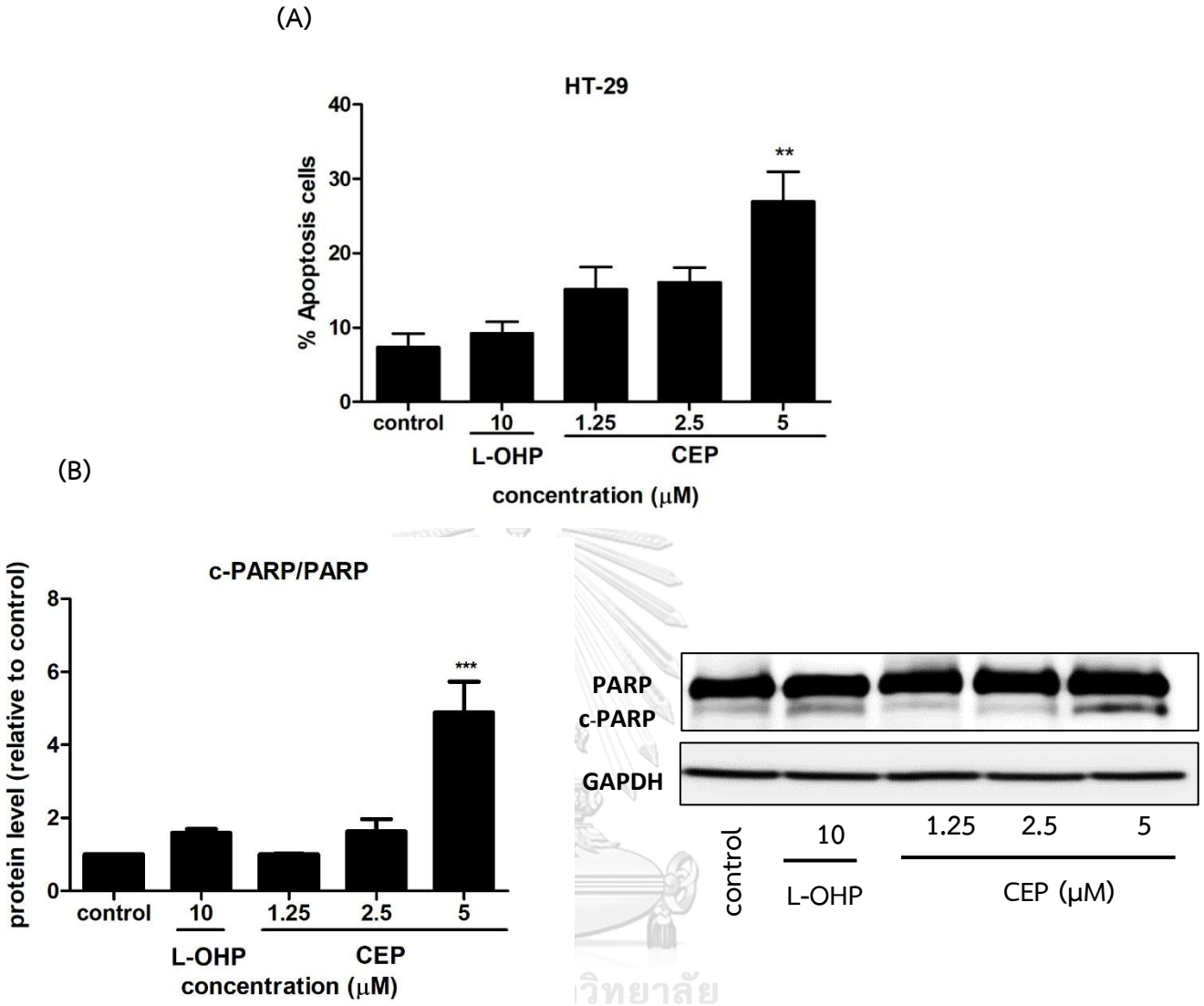

Figure 9 Effect of CEP on apoptosis in HT-29 cells. The cells were treated with CEP at 1.25, 2.5 and 5 μM or L-OHP at 10 μM for 24 h. (A) The apoptotic cells were analyzed by annexin V-FITC/PI staining followed by flow cytometry analysis. (B) The protein expression levels of cleaved PARP were determined by western blotting. Each value is expressed as the mean ± SEM (n= 3). *p<0.05, **p<0.01, ***p<0.001 compared with vehicle control (0.2% DMSO).

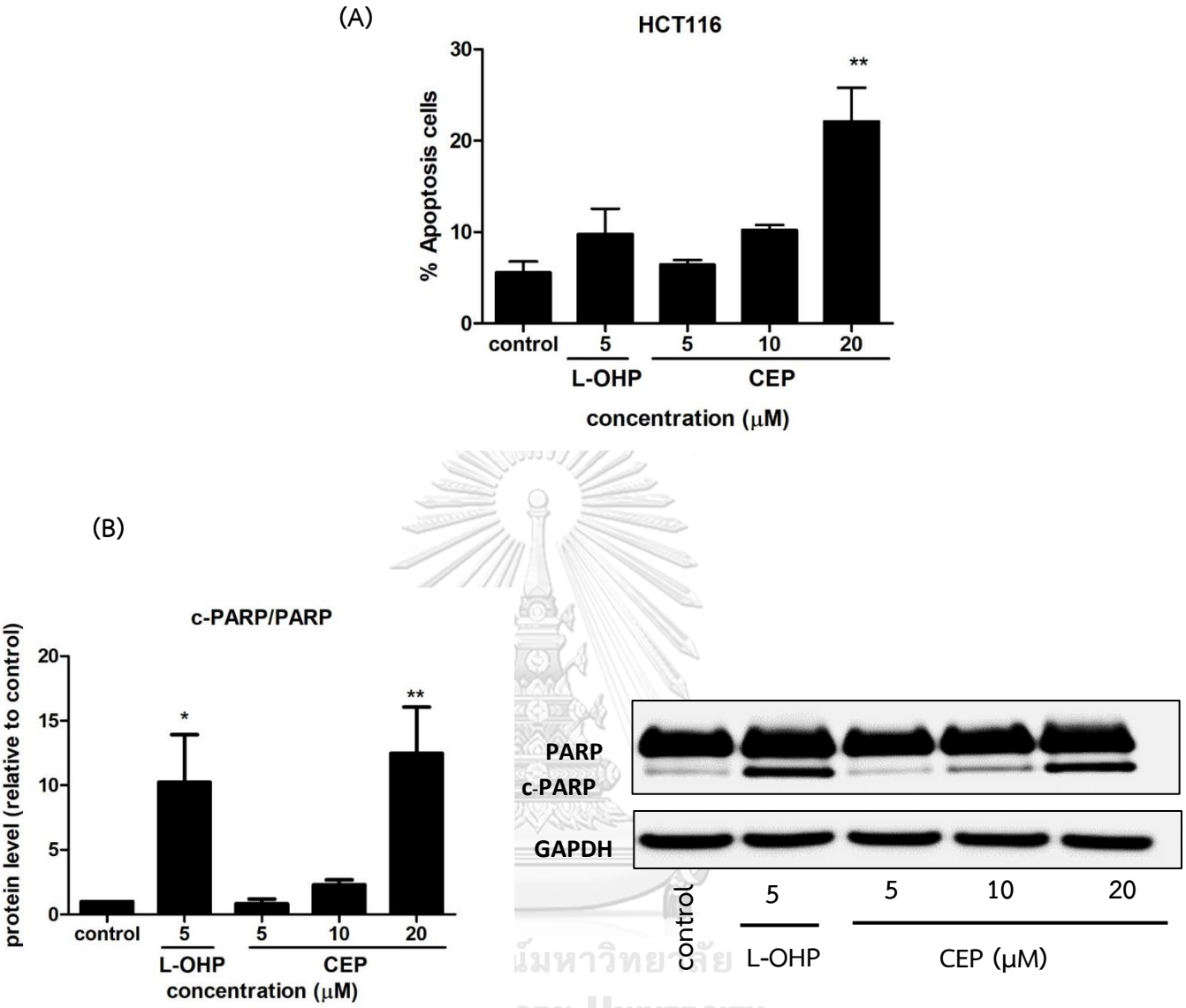

Figure 10 Effect of CEP on apoptosis in HCT116 cells. The cells were treated with CEP at 5, 10 and 20 μM or L-OHP at 5 μM for 24 h. (A) The apoptotic cells were analyzed by annexin V-FITC/PI staining followed by flow cytometry analysis. (B) The protein expression levels of cleaved PARP were determined by western blotting. Each value is expressed as the mean ± SEM (n=3). **p<0.05, **p<0.01, ***p<0.001 compared with vehicle control (0.2% DMSO).

4.3 Effect of CEP on the expression of Bcl-2 family proteins in CRC cells

The Bcl-2 family proteins are the key players in the intrinsic apoptotic pathway (90). Therefore, the expression levels of Bcl-2 family proteins, including pro-apoptotic proteins, Bax and Bak, and anti-apoptotic protein, Bcl-x_L, were determined using western blotting.

As shown in Figure 11A, CEP significantly upregulated the expression of Bak protein by approximately 2.6-fold above control ($p<0.05$) but it did not alter the expression of Bax protein (Figure 11B). Moreover, 2.5 and 5 μM of CEP significantly downregulated the expression of Bcl-x_L protein by approximately 20% and 40% of control, respectively (Figure 11C, $p<0.05$). In contrast to CEP, L-OHP at 10 μM did not alter the expression of Bcl-2 family proteins in HT-29 cells. These results suggest that CEP induced apoptosis through upregulation of Bak and downregulation of Bcl-x_L in HT-29 cells.

In a manner similar to HT-29 cells, CEP at 20 μM significantly upregulated the expression of Bak protein by approximately 1.4 -fold above control (Figure 12A, $p<0.05$) without affecting the expression of Bax protein in HCT116 cells (Figure 12B). Furthermore, CEP at 10 and 20 μM significantly downregulated the expression of Bcl-x_L by approximately 30% and 50% of control, respectively (Figure 12C, $p<0.05$). Similarly, L-OHP at 5 μM significantly upregulated the expression levels of Bak and Bax proteins by approximately 1.3 and 4.2-fold above control (Figure 12A-B, $p<0.05$). These results suggest that apoptosis-inducing effect of CEP is mediated via upregulation of Bak and downregulation of Bcl-x_L in HCT116 cells.

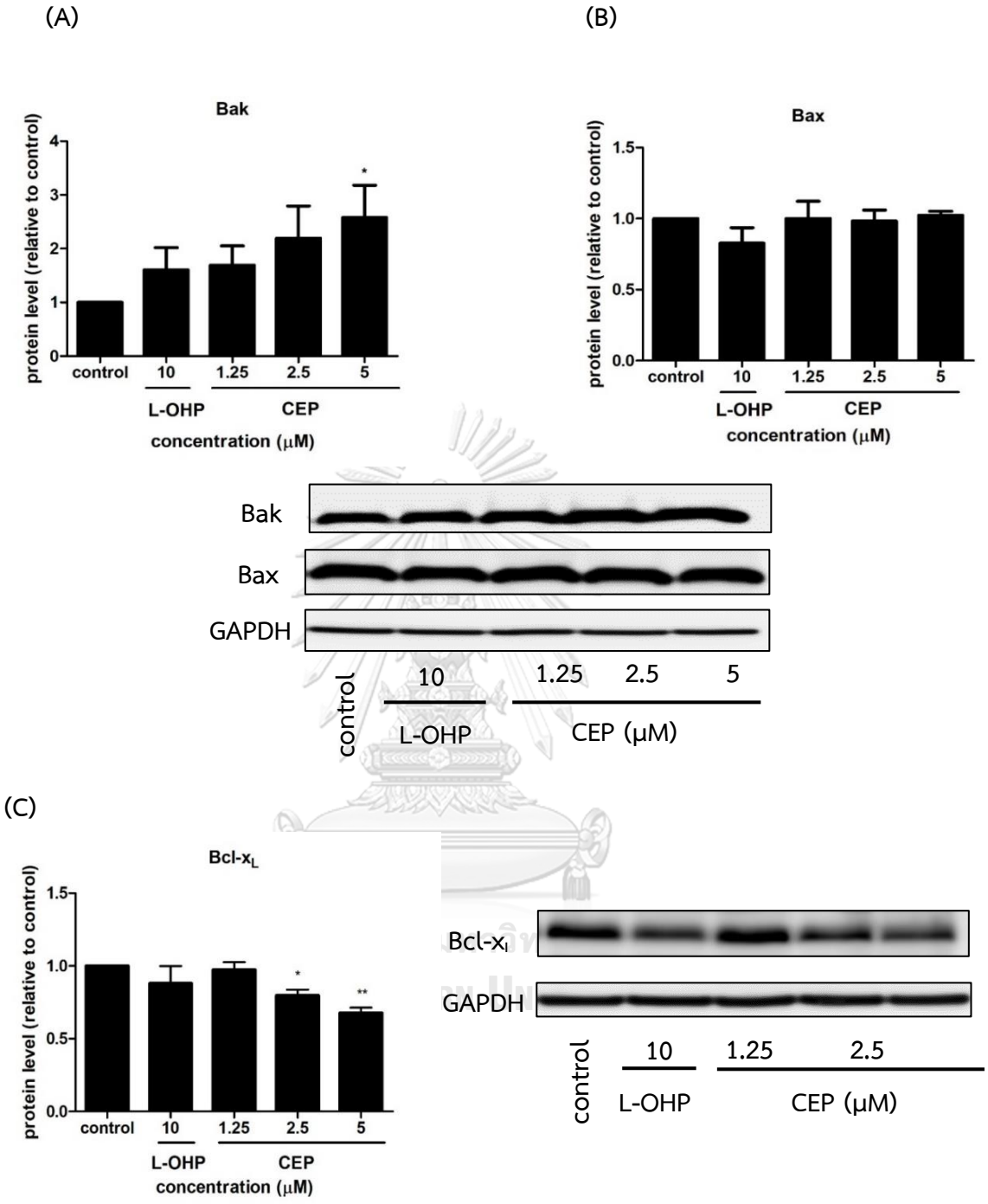

Figure 11 Effects of CEP on the expression of Bcl-2 family proteins in HT-29 cells. Cells were treated with CEP at 1.25, 2.5 and 5 μM or L-OHP at 10 μM for 24 h. The levels of pro-apoptotic proteins, including, (A) Bak and (B) Bax were determined by western blot analysis. The levels of an anti-apoptotic protein, (C) Bcl-x_L, were determined by western blot analysis. The values are shown as fold change relative

to the vehicle control. Each value is expressed as the mean ± SEM (n= 3). *p<0.05, **p<0.01, ***p<0.001 compared with vehicle control (0.2% DMSO).

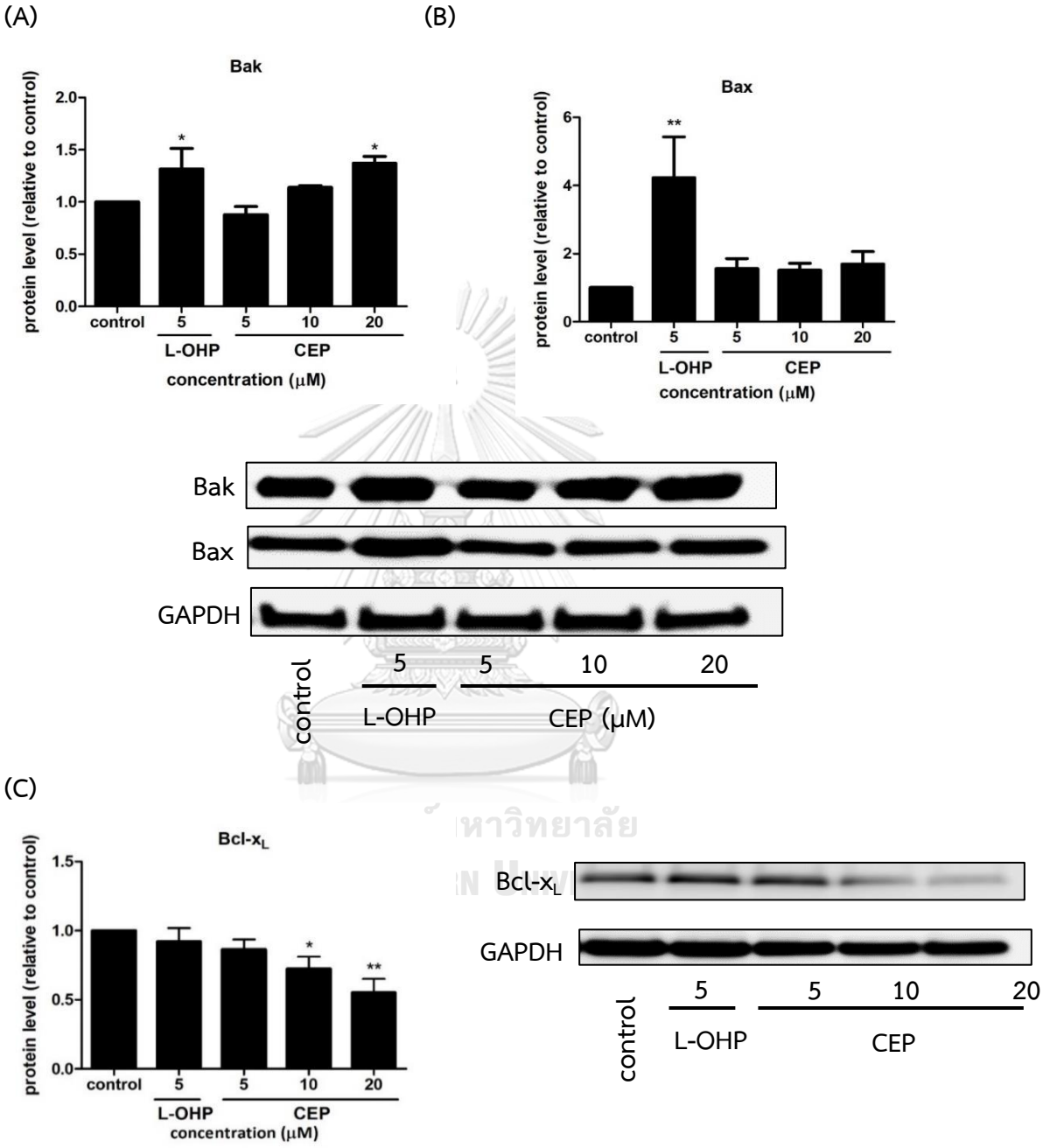

Figure 12 Effects of CEP on the expression of Bcl-2 family proteins in HCT116 cells. Cells were treated with CEP at 5, 10 and 20 μM or L-OHP at 5 μM for 24 h. The levels of pro-apoptotic proteins including, (A) Bak and (B) Bax were determined by western

blot analysis. The levels of an anti-apoptotic protein, (C) Bcl-x_L, were determined by western blot analysis. The values are shown as fold change relative to the vehicle control. Each value is expressed as the mean ± SEM (n= 3). *p<0.05, **p<0.01, ***p<0.001 compared with vehicle control (0.2% DMSO).

4.4 Effect of CEP on ROS generation in CRC cells

Previous studies reported that CEP induced reactive oxygen species (ROS) generation in several cancer cells (25, 31). Thus, the effect of CEP on ROS generation in CRC cells was evaluated.

HT-29 cells were treated with CEP at 1.25, 2.5 and 5 μM, L-OHP at 10 μM or H_2O_2 at 500 μM for 1 h and the levels of ROS were determined by measuring the DCF fluorescence intensity. As shown in Figure 13A, CEP at 5 μM and H_2O_2 at 500 μM significantly increased ROS levels approximately 2.8- and 3.4-fold above control, respectively, ($p<0.05$) whereas L-OHP has no effect on ROS generation in HT-29 cells.

In HCT116 cells, CEP at 10 and 20 μM and H_2O_2 at 500 μM significantly increased the ROS levels approximately 6, 30 and 3.6 times higher than control, respectively (Figure 13B, $p<0.05$). Conversely, L-OHP at 5 μM did not significantly alter the ROS levels in HCT116 cells.

It is commonly known that overproduction of ROS can lead to oxidative stress, causing cell death (91). Therefore, the present study determined whether ROS generation is involved in the cytotoxicity of CEP. HT-29 cells were treated with 3 mM of *N*-acetylcysteine (NAC), a ROS scavenger, for 2 h and then incubated with 1.25, 2.5 and 5 μM of CEP or 10 μM of L-OHP for 24 h. Cell viability was determined using MTT assay. The results indicated that pretreatment with NAC significantly increased the viability of HT-29 cells by 1.54, 1.57 and 2.02 fold when compared with the viability of the cells treated with CEP at 1.25, 2.5 and 5 μM alone, respectively. Similarly, pretreatment with NAC significantly prevented L-OHP-induced cytotoxicity in HT-29 cells (Figure 13C, $p<0.001$). In a manner similar to HT-29 cells, NAC significantly increased the viability of HCT116 cells by 1.15, 1.30 and 1.32, when compared with the viability of the cells treated with CEP alone at 5, 10 and 20 μM, respectively.

Also, pretreatment with NAC prevented L-OHP-induced cytotoxicity in HCT116 cells (Figure 13D, $p<0.001$). Together, these results suggest that cytotoxicity of CEP is partly mediated through ROS production in both HT-29 and HCT116 cells.

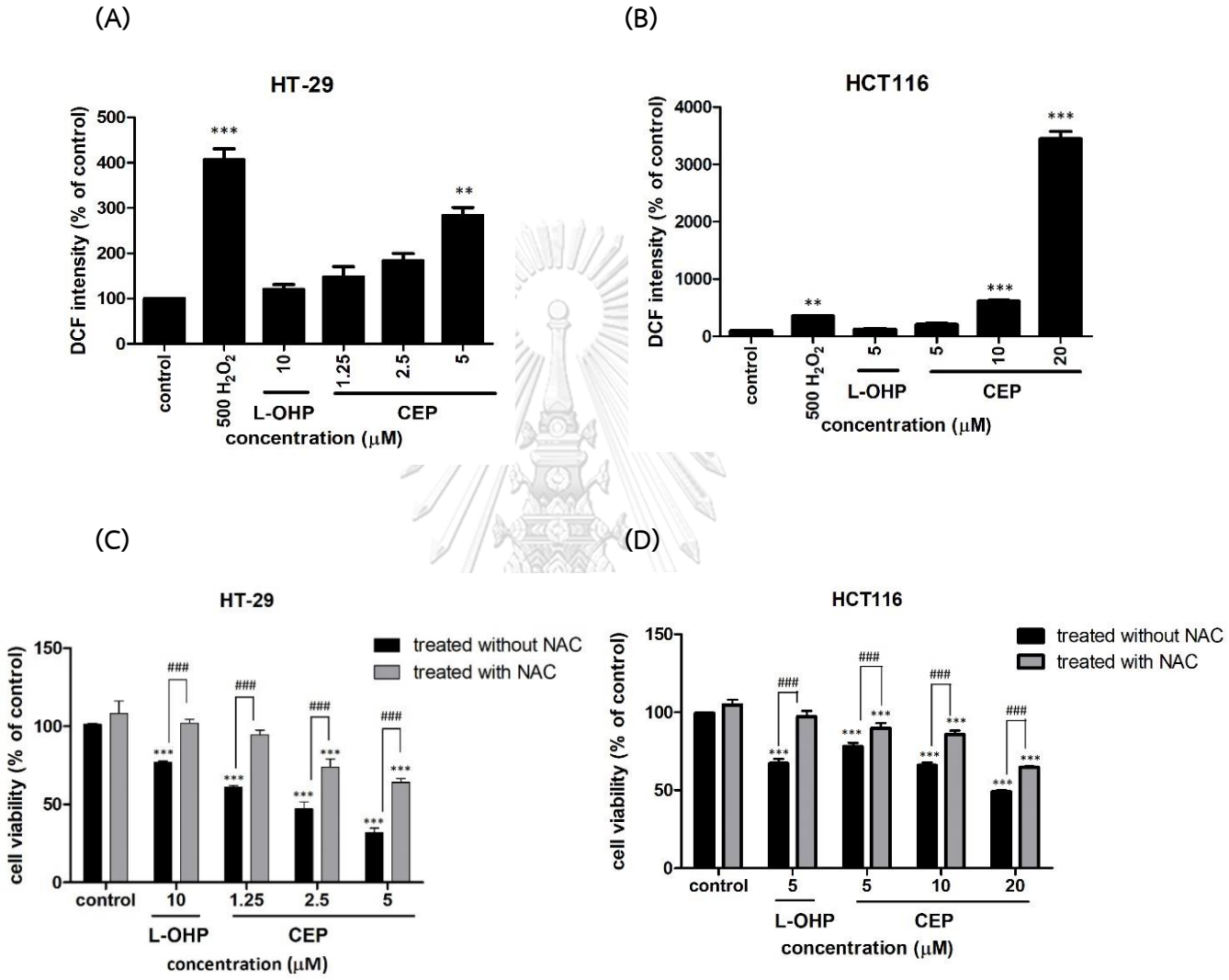

Figure 13 Effect of CEP on ROS generation in CRC cells. Cells were treated with CEP at 1.25, 2.5 and 5 μM or L-OHP at 10 μM for 1 h and the levels of ROS were then determined in (A) HT-29 and (B) HCT116 cells by measuring the DCF fluorescence intensity using a flow cytometer. H_2O_2 (500 μM) was used as a positive control. The viability of (C) HT-29 and (D) HCT116 cells treated with NAC, prior to CEP treatment, were determined using MTT assay. Each value is expressed as the mean ± SEM (n=3).

*p<0.05, **p<0.01, and ***p<0.001 vs. control. #p<0.05, ##p<0.01 and ###p<0.001 vs. group treated without NAC.

4.5 Role of ROS in apoptosis-inducing effect of CEP in CRC cells

High levels of reactive oxygen species (ROS) have been closely linked to activation of cell death processes such as apoptosis (5). Thus, we determined whether ROS is responsible for apoptosis-inducing effect of CEP in CRC cells. HT-29 cells were pretreated with NAC for 2 h, prior to treatment with CEP at 1.25, 2.5 and 5 μM or L-OHP at 10 μM for 24 h. Then, the cells were stained with annexin V-FITC/PI and analyzed by flow cytometry. As shown in Figure 14A, NAC significantly prevented CEP or L-OHP-induced apoptosis in HT-29 cells. The percentages of apoptotic cells were significantly decreased when the cells were pretreated with NAC by 1.42 and 1.5 folds, compared with the cells treated with 5 μM of CEP and 10 μM of L-OHP alone, respectively ($p<0.05$). To further confirm whether apoptosis-inducing effect of CEP is mediated through ROS, the present study determined the effect of pretreatment with NAC on CEP-induced PARP cleavage. The results showed that NAC significantly prevent the effect of CEP or L-OHP on PARP cleavage. The expression levels of cleaved PARP were decreased by 1.8 and 3.4 folds, respectively (Figure 14B, $p<0.01$), highlighting that ROS is partly responsible for apoptosis-inducing effect of CEP in HT-29 cells.

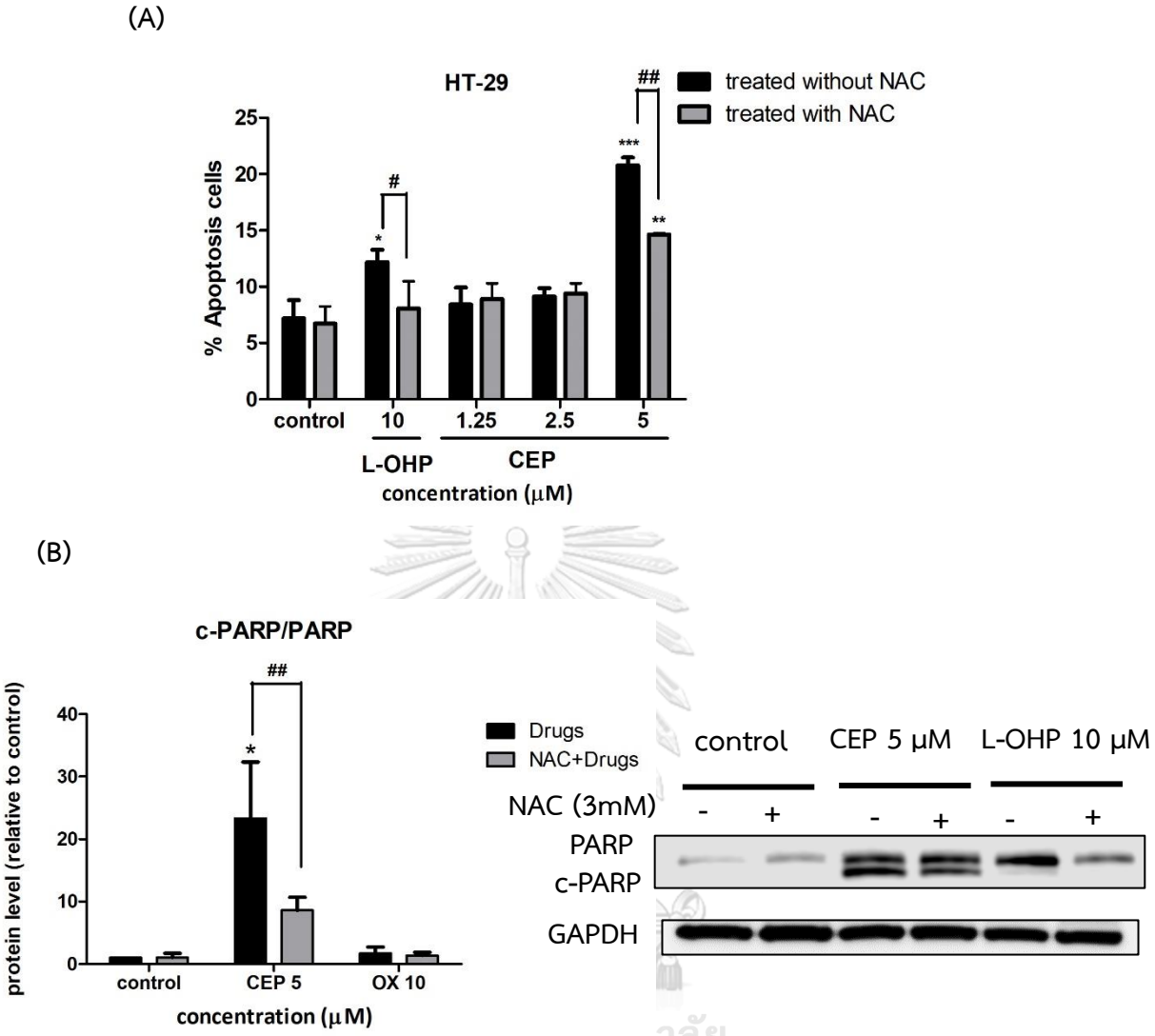

Figure 14 Roles of ROS in CEP-induced apoptosis in HT-29 cells. The cells were treated with 3 mM of NAC for 2 h, followed by CEP at 1.25, 2.5 and 5 μM or L-OHP at 10 μM for 24 h. (A) After staining cells with annexin V and PI, the percentages of apoptotic cells were evaluated using flow cytometry. (B) The expression levels of cleaved PARP were evaluated using western blot. The values are shown as fold change relative to the vehicle control. Each value is expressed as the mean ± SEM (n= 3). *p<0.05, **p<0.01, and ***p<0.001 vs. control. #p<0.05, ##p<0.01 and ###p<0.001 vs. group without NAC.

Similar to HT-29 cells, NAC significantly prevented CEP-induced apoptosis in HCT116 cells (Figure 15A). The percentages of apoptotic cells were significantly decreased when the cells were pretreated with NAC by 1.31 folds, compared with cells treated with 20 μM of CEP alone ($p<0.05$). Conversely, pretreatment with NAC had no significant effect on L-OHP-induced apoptosis. It however should be noted that NAC significantly prevented the effect of CEP or L-OHP on PARP cleavage. The expression levels of cleaved PARP were decreased by 1.59 and 5.93 folds, respectively (Figure 15B, $p<0.01$). These results suggest that CEP-induced apoptosis is partly mediated through ROS generation in HCT116 cells.

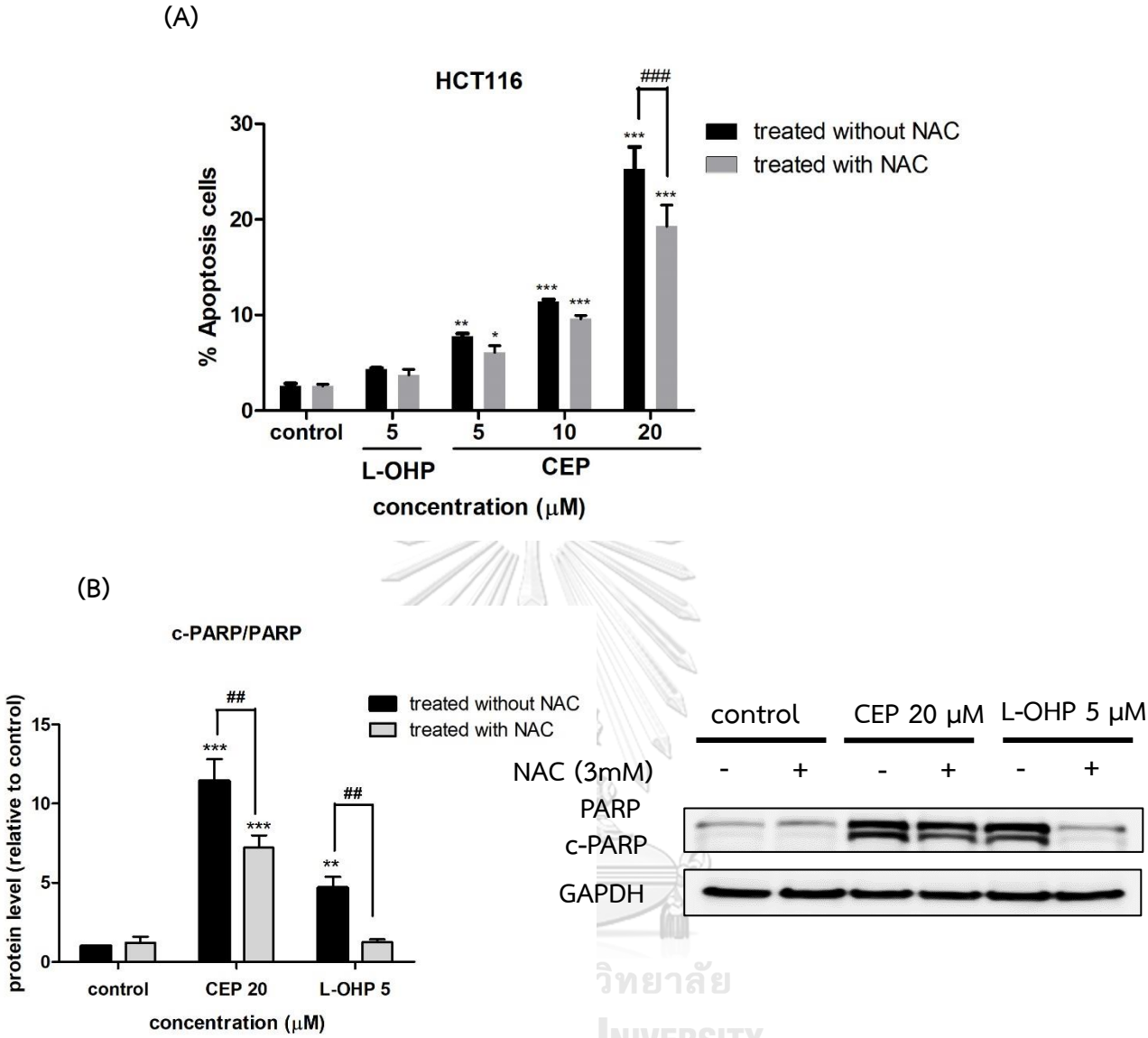

Figure 15 Roles of ROS in CEP-induced apoptosis in HCT116 cells. The cells were treated with 3 mM of NAC for 2 h, followed by CEP at 5, 10 and 20 μM or L-OHP at 5 μM for 24 h. (A) After staining cells with annexin V and PI, the percentages of apoptotic cells were evaluated using flow cytometry. (B) The expression levels of cleaved PARP were evaluated using western blot. The values are shown as fold change relative to the vehicle control. Each value is expressed as the mean ± SEM (n= 3). *p<0.05, **p<0.01, and ***p<0.001 vs. control. #p<0.05, ##p<0.01 and ###p<0.001 vs. group without NAC.

4.6 Effect of CEP on ERK signaling pathway in CRC cells

The MAPK/ERK signaling pathway is involved in regulation of various cellular biological functions such as cell proliferation, cell differentiation, cell cycle progression and cell apoptosis (92). Thus, the effects of CEP on the phosphorylation of ERK in CRC cells were determined using western blot analysis. As shown in Figure 16, treatment of HT-29 cells with CEP at 5 μM or L-OHP at 10 μM significantly inhibited the phosphorylation of ERK by approximately 44% and 45% , when compared with control (Figure 16A, $p<0.05$). Conversely, treatment of HCT116 cells with CEP at 20 μM or L-OHP at 5 μM dramatically induced the phosphorylation of ERK by approximately 2- and 1.7-fold above the control (Figure 16B, $p<0.05$). These results suggest cytotoxicity of CEP is likely mediated through modulation of the ERK signaling pathway in CRC cells.

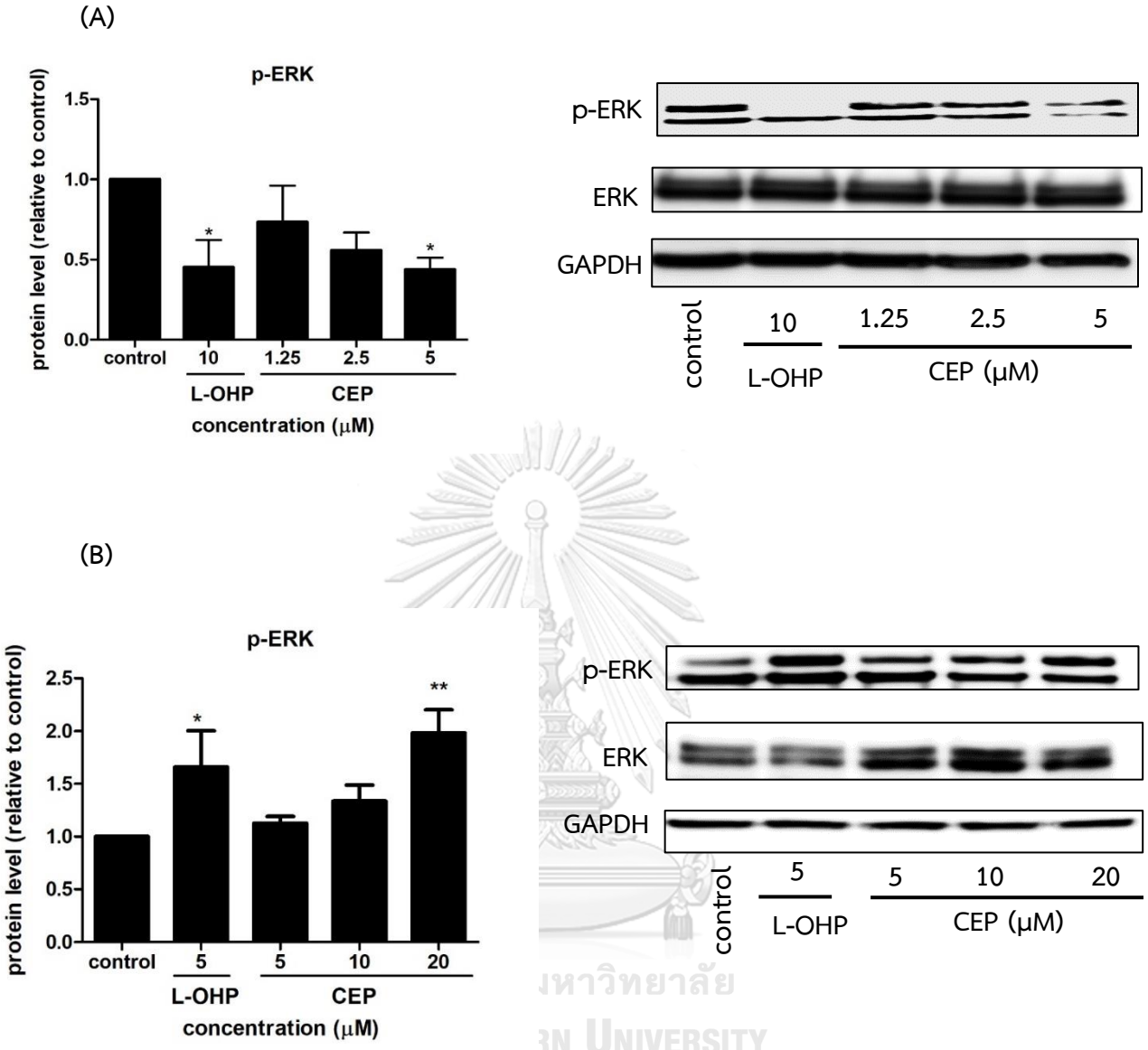

Figure 16 Effects of CEP on the phosphorylation of ERK in CRC cells.Cells were treated with CEP or L-OHP for 24 h and the expression levels of p-ERK and ERK proteins were evaluated using western blot. The expression ratios of p-ERK and ERK were quantified in (A) HT-29 and (B) HCT116 cells. The values are shown as fold change relative to the vehicle control. Each value is expressed as the mean ± SEM (n= 3). *p<0.05, p<0.01 and **p<0.001 compared with the vehicle control (0.2% DMSO).

4.7 Role of ROS in CEP-induced alteration of MAPK/ERK signaling pathway in CRC cells

Several studies have reported that ROS is involved in the effect of alkaloid compounds on the ERK signaling pathway (15, 17, 55). Since we found that CEP induced ROS generation and changes in ERK phosphorylation in both CRC cells, we determined whether ROS is associated with effect of CEP on MAPK/ ERK signaling pathway. As shown in Figure 17A, CEP at 5 μM and L-OHP at 10 μM significantly inhibited the phosphorylation of ERK. Remarkably, pretreatment with NAC significantly prevented CEP and L-OHP-mediated inhibition of ERK phosphorylation by 1.63 and 2.4 folds, respectively in HT-29 cells.

It should be noted that, in HCT116 cells, CEP at 20 μM and L-OHP at 5 μM significantly activated phosphorylation of ERK and pretreatment with NAC significantly prevented CEP-induced phosphorylation of ERK by approximately 3 fold. However, NAC did not significantly alter L-OHP-mediated ERK activation in HCT116 cells (Figure 17B).

These results suggest that ROS is partly associated with CEP-mediated alteration of MAPK/ERK signaling pathway in CRC cells.

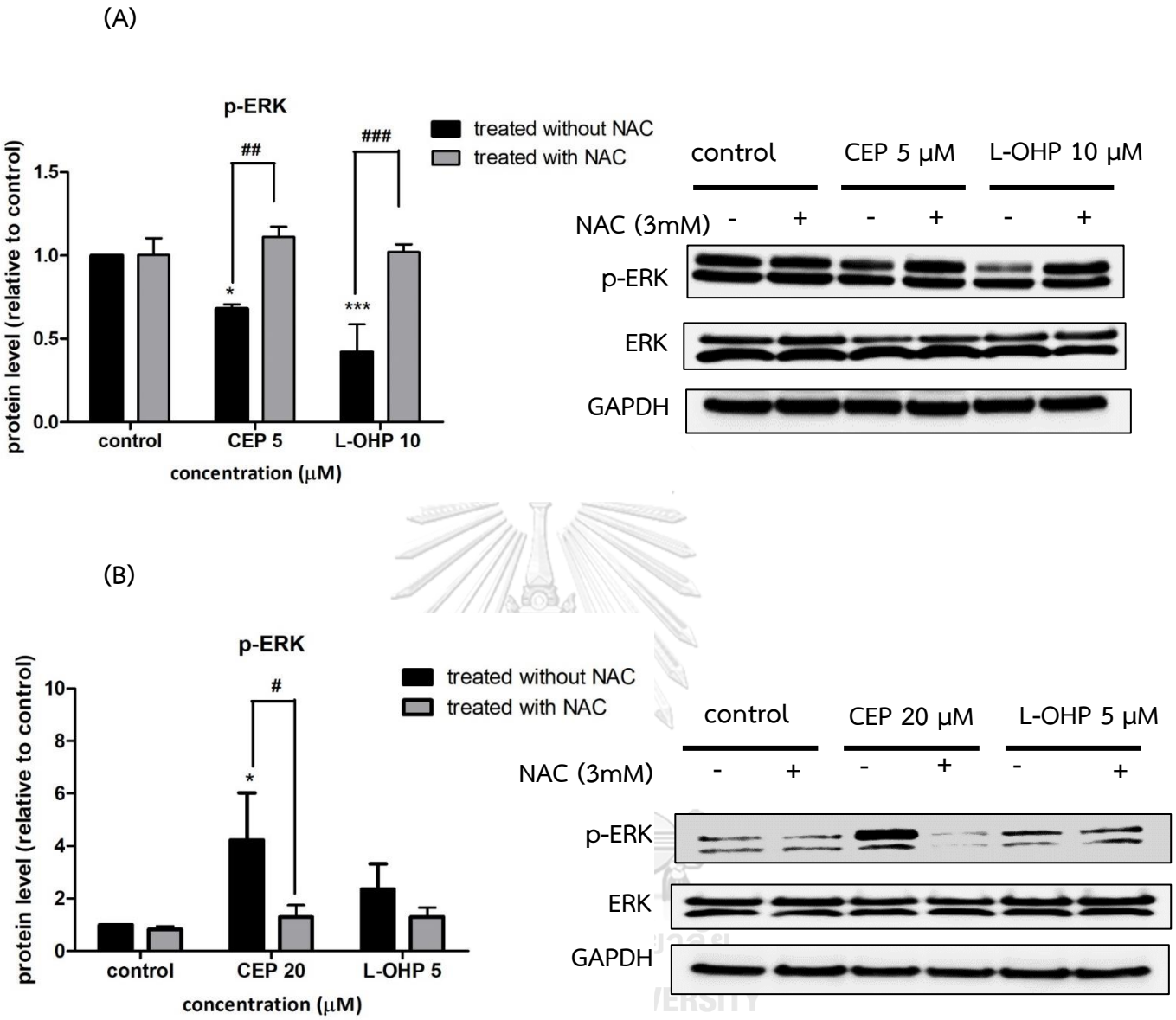

Figure 17 Roles of ROS in CEP-mediated alteration of MAPK/ERK signaling pathway in CRC cells. Cells were pretreated with NAC for 2 h and then treated with CEP at 5 μM or L-OHP 10 μM (for HT-29 cells) or treated with CEP at 20 μM or L-OHP 5 μM (for HCT116 cells) for 24 h. Western blot analysis for p-ERK and ERK was carried out. The ratio of phospho-ERK/ERK (p-ERK/ERK) in (A) HT-29 cells and (B) HCT116 cells. The values are shown as fold change relative to the vehicle control. Each value is expressed as the mean ± SEM (n=3). *p<0.05, **p<0.01, and ***p<0.001 vs. control. #p<0.05, ##p<0.01 and ###p<0.001 vs. group without NAC.

4.8 Effect of CEP on the expression levels of $p21^{Waf1/Cip1}$ mRNA and protein in CRC cells

$p21^{Waf1/Cip1}$ has a potential role in modulating apoptosis (93). Several previous studies reported that CEP increased mRNA and protein levels of $p21^{Waf1/Cip1}$ in several cancer cells such as adenosquamous cell carcinoma, ovarian, and colorectal cancer cells (27, 34, 37). Thus, the effect of CEP on $p21^{Waf1/Cip1}$ mRNA level was evaluated in CRC cells using RT-PCR. Notably, CEP at 5 μM significantly increased $p21^{Waf1/Cip1}$ mRNA levels approximately 30 times higher than control but L-OHP did not affect $p21^{Waf1/Cip1}$ mRNA levels in HT-29 cells (Figure 18A). To further confirm the real-time RT-PCR analysis results, the levels of $p21^{Waf1/Cip1}$ in CRC cells were measured by western blotting. As shown in Figure 18B, CEP at 2.5 and 5 μM significantly upregulated the expression levels of $p21^{Waf1/Cip1}$ protein by approximately 10 and 20 fold higher than control, respectively ($p<0.05$).

In contrast to HT-29 cells, CEP had no effect on $p21^{Waf1/Cip1}$ mRNA level whereas L-OHP significantly increased $p21^{Waf1/Cip1}$ mRNA level approximately 40 times above control in HCT116 cells (Figure 19A). Similarly, CEP did not affect the expression of $p21^{Waf1/Cip1}$ protein while L-OHP at 5 μM dramatically upregulated the expression of $p21^{Waf1/Cip1}$protein by approximately 6 fold above control (Figure 19B, $p<0.01$). These results indicated that CEP significantly upregulated the expression of $p21^{Waf1/Cip1}$ mRNA and protein in p53 mutant HT-29 cells.

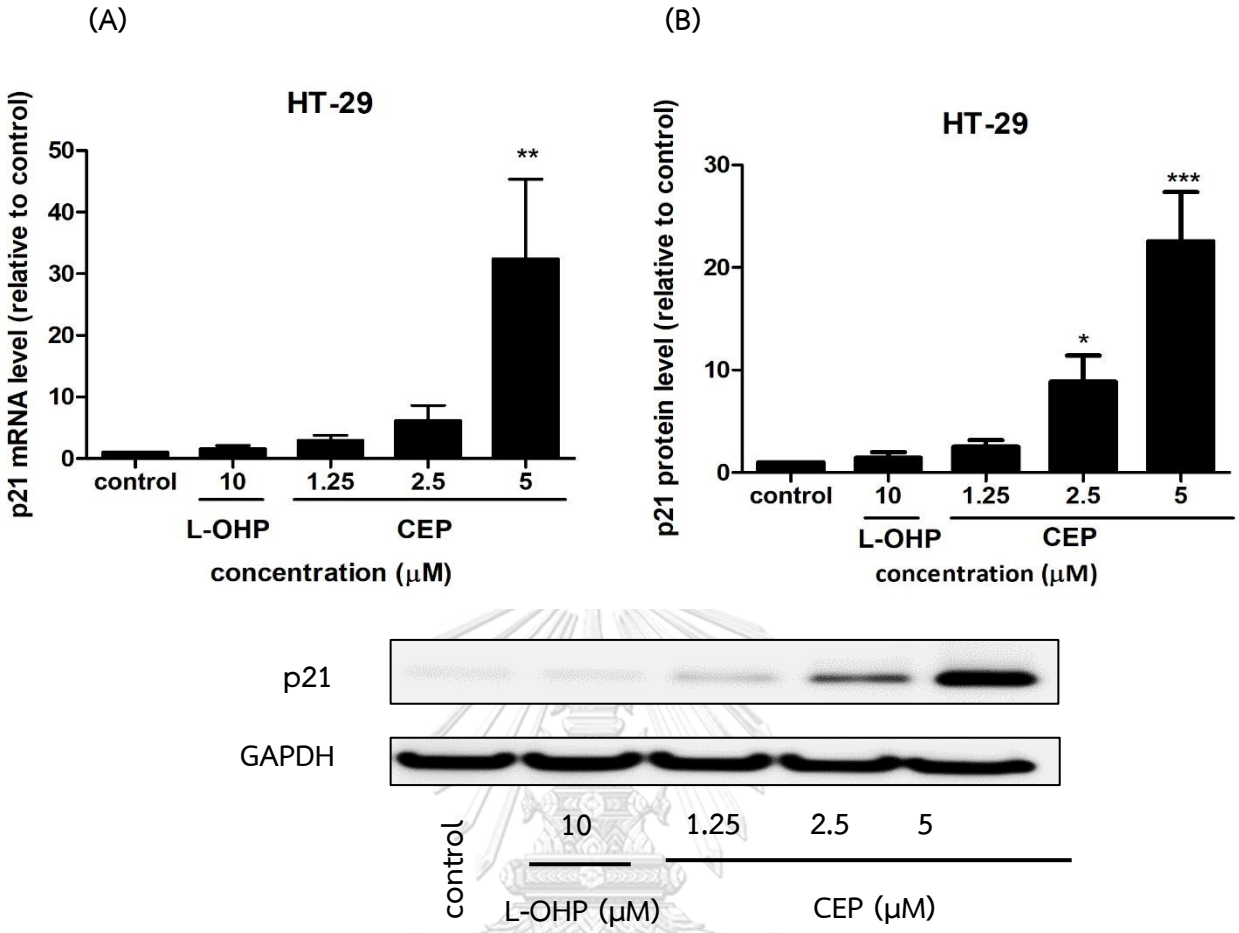

Figure 18 Effect of CEP on the expression levels of $p21^{Waf1/Cip1}$ in HT-29 cells. (A) mRNA and (B) protein. Cells were treated with CEP at 1.25, 2.5 and 5 μM or L-OHP at 10 μM. The mRNA and protein levels of $p21^{Waf1/Cip1}$ were detected using real-time RT-PCR and western blotting, respectively. *p<0.05, **p<0.01 and ***p<0.001 vs. control.

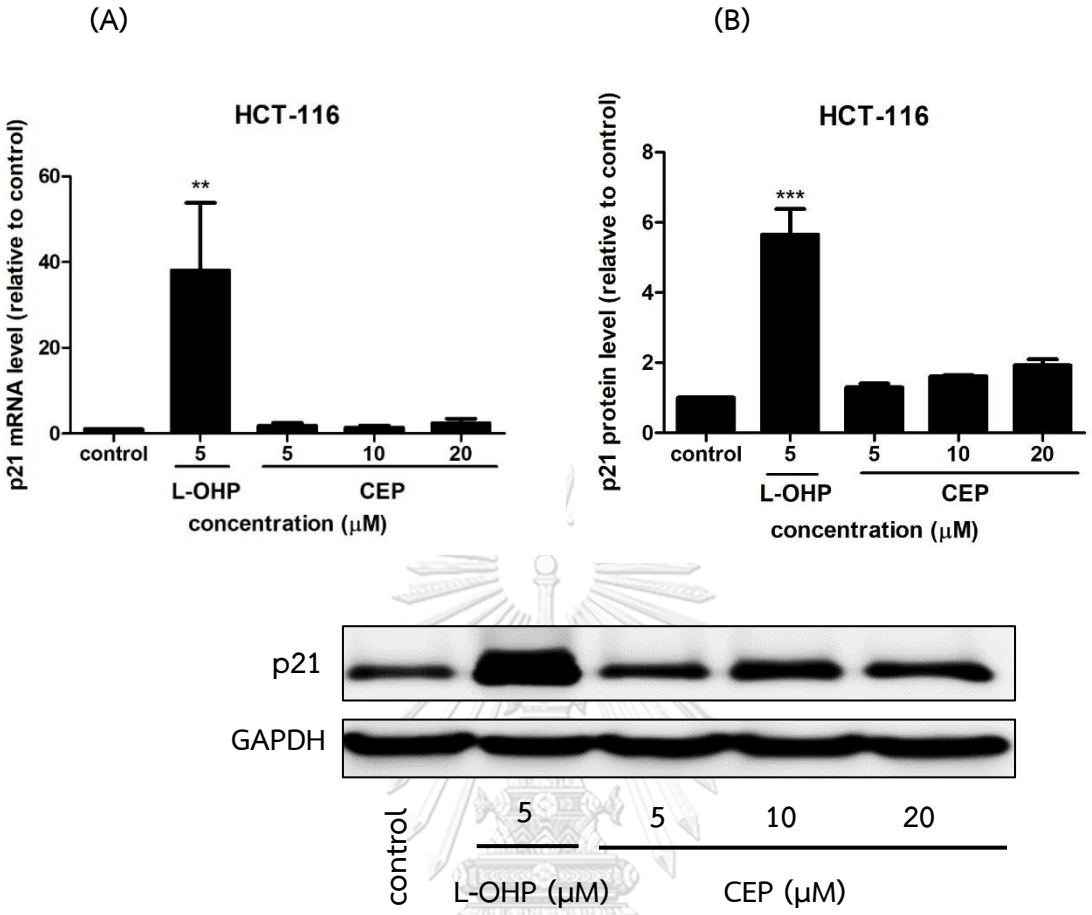

Figure 19 Effect of CEP on the expression levels of $p21^{Waf1/Cip1}$ in HCT116 cells. (A) mRNA and (B) protein. Cells were treated with CEP at 5, 10 and 20 μM or L-OHP at 5 μM. The mRNA and protein expression levels of $p21^{Waf1/Cip1}$ were detected using real-time RT-PCR and western blotting, respectively. **$p<0.01$ and ***$p<0.001$ vs. control.

4.9 The effect of UC2288 on p21$^{Waf1/Cip1}$ expression in HT-29 cells

Previous studies have reported that p21$^{Waf1/Cip1}$ promote apoptosis cell death in cells lacking p53 (19, 20). As CEP significantly upregulated p21$^{Waf1/Cip1}$ expression in p53 mutant HT-29 cells, we determine whether p21$^{Waf1/ Cip1}$ upregulation is responsible for the induction of apoptosis. Initially, HT-29 cells were pretreated with 10 and 50 nM of UC2288, a p21 $^{Waf1/Cip1}$ inhibitor, for 2 h prior to treatment with CEP for 24 h. As shown in Figure 20, UC2288 at 50 nM significantly decreased the expression of p21$^{Waf1/Cip1}$ by approximately 61% of control ($p<0.05$). Thus, UC2288 at a concentration of 50 nM was used for next experiments.

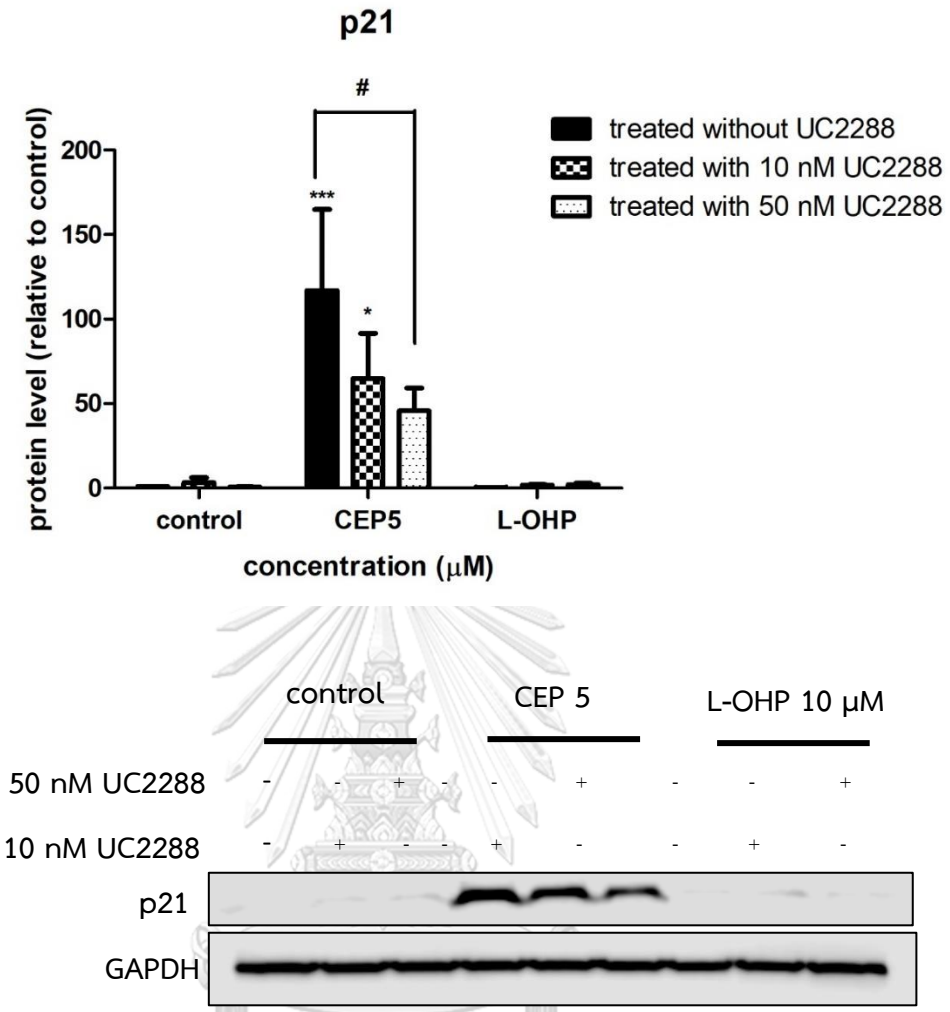

Figure 20 Effect of UC2288 on CEP-induced $p21^{Waf1/Cip1}$ upregulation in HT-29 cells. Cells were treated with CEP in the presence or absence of UC2288 for 24 h. The protein levels of p21Waf1/ Cip1 were evaluated using western blot. Each value is expressed as the mean ± SEM (n=3). *p<0.05, **p<0.01, and ***p<0.001 vs. control. #p<0.05 vs. group without UC2288.

4.10 Role of p21 $^{Waf1/Cip1}$ in CEP-induced ERK inhibition in HT-29 cells

A previous study has reported the links between p21$^{Waf1/Cip1}$ and p-ERK (94). This study therefore determined whether p21 $^{Waf1/Cip1}$ is involved in the effect of CEP on the phosphorylation of ERK in HT-29 cells. As illustrated in Figure 21, pretreatment with 50 nM UC2288 significantly prevented CEP-mediated inhibition of ERK phosphorylation in HT-29 cells ($p<0.05$) while UC2288 did not alter the inhibitory effect of L-OHP on ERK phosphorylation, suggesting that p21 $^{Waf1/Cip1}$ partly plays a role in CEP-mediated inhibition of ERK phosphorylation in HT-29 cells.

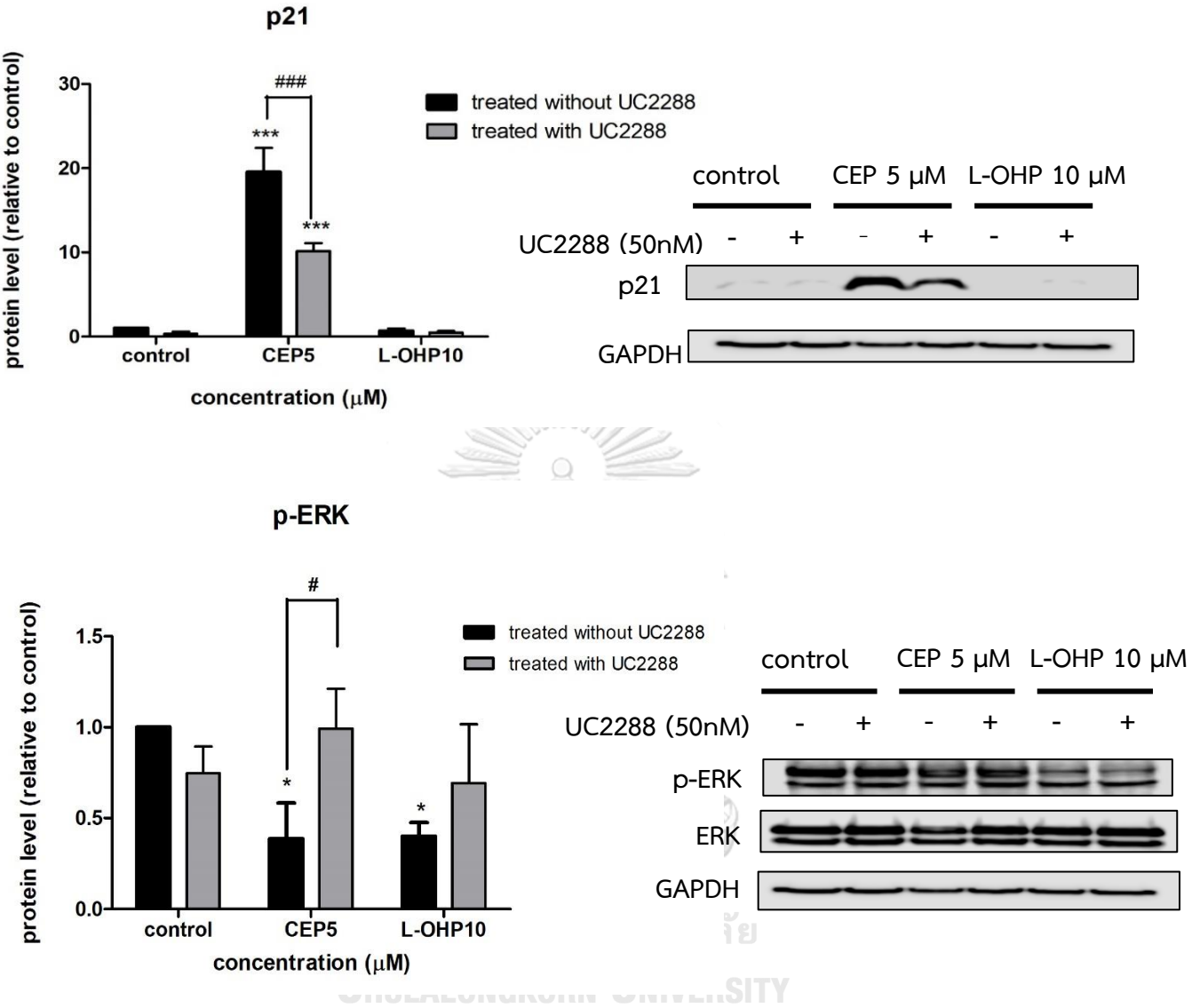

Figure 21 Role of $p21^{Waf1/Cip1}$ in CEP-mediated inhibition of ERK phosphorylation in HT-29 cells. Cells were treated with 50 nM of UC2288 for 2 h and then treated with CEP at 5 μM or L-OHP 10 μM for 24 h. The levels of protein were evaluated using western blot. The ratio of phospho-ERK/ERK (p-ERK/ERK) were quantified. Each value is expressed as the mean ± SEM (n=3). *p<0.05, **p<0.01, and ***p<0.001 vs. control. #p<0.05, ##p<0.01 and ###p<0.001 vs. group without UC2288.

4.11 Role of p21 $^{Waf1/Cip1}$ on CEP-induced PARP cleavage in HT-29 cells

To determine whether p21$^{Waf1/Cip1}$ is involved in CEP-induced apoptosis, HT-29 cells were pretreated with 50 nM of UC2288 for 2 h prior to treatment with CEP for 24 h. The expression levels of cleaved PARP proteins were determined using western blot analysis. The result showed that CEP at 5 μM or L-OHP at 10 μM significantly induced PARP cleavage by approximately 13 and 6 fold above the control, respectively ($p<0.001$). Notably, UC2288 significantly prevented CEP-induced PARP cleavage (Figure 22, $p<0.001$). In contrast to CEP, UC2288 has no effect on L-OHP-induced PARP cleavage. The expression levels of cleaved PARP between cells treated with L-OHP and UC288 were not different from that of cells trated with L-OHP alone. This result suggests the p21$^{Waf1/Cip1}$ expression is likely involved in apoptosis-inducing effect of CEP.

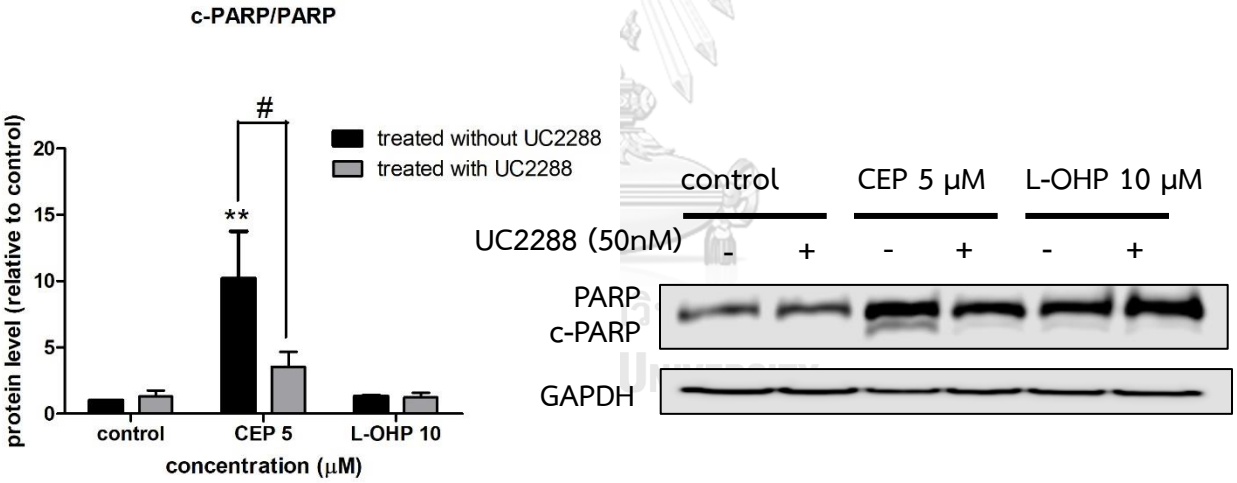

Figure 22 Role of p21$^{Waf1/Cip1}$ in CEP-induced PARP cleavage in HT-29 cells. Cells were treated with 50 nM of UC2288 for 2 h and then treated with CEP at 5 μM or L-OHP at 10 μM for 24 h. The protein levels were evaluated using western blot. The values are shown as fold change relative to the vehicle control. Each value is expressed as the mean ± SEM (n=3). **p<0.01, and ***p<0.001 vs. control. #p<0.05 vs. group without UC2288.

CHAPTER V

DISCUSSION AND CONCLUSION

Colorectal cancer is the third most common type of cancer and the leading cause of cancer-related mortality worldwide for both men and women (1). Although, chemotherapy has been one of the most effective and potent strategy to treat cancer but its use is still limited due to serious side effects and drug resistance (48-50). Thus, new compounds possess high anti-cancer efficacy and low toxicity are very needed for CRC treatment.

Cepharanthine (CEP) is a biscoclaurine alkaloid found in *Stephania suberusa* L.L forman and *Stephania erecta* Craib in Thailand. CEP has been widely used in Japan to treat a wide variety of acute and chronic diseases.It is also approved for the treatment of radiation-induced leukopenia, alopecia areata and alopecia pityrodes (21). Moreover, CEP exhibited anticancer effect against various cancer cell lines including melanoma, leukemia, ovarian, breast, osteosarcoma, lymphoma, lung carcinoma, myeloma, cholangiocarcinoma, oral squamous carcinoma, colorectal cancer, and hepatocellular carcinoma (23-35). Previously, we found the potent anticancer activity of CEP against p53 mutant colorectal cancer cells, which may be associated with upregulation of $p21^{Waf1/Cip1}$ and production of ROS. In the present study, we investigated the roles of ROS and $p21^{Waf1/Cip1}$ in the apoptosis-inducing effect of CEP in two CRC cell lines, p53-wild-type HCT-116 cells and p53-mutant HT-29 cells. The MTT results demonstrated that CEP significantly inhibited the growth of both HT-29 and HCT116 cells in a concentration-dependent manner with the IC_{50} of 2.46±0.22 μM and 9.64±0.35 μM in HT-29 and HCT-116 cells, respectively, indicating that CEP was more toxic to p53 mutant HT-29 cells than p53 wild-type HCT116 cells. This finding was consistent with the finding of Rattanawong et al that CEP was more effective in controlling the growth of the p53 mutant HT-29 cells than p53 wild-type COLO-205 cells (34). And the results of this study were in agreement with previous

studies that CRC cells expressing mutant p53 were more resistant to L-OHP than cells expressing wild-type p53 (95).

Several studies reported that anticancer activity of many natural compounds such as curcumin, piperine, sanguinarine and naringin were mediated through apoptosis induction (96-99). In the present study, the apoptosis-inducing effect of L-OHP, a commonly used chemotherapeutic agent, was only detected in HCT-116 cells. Studies in several cancer cell types such as hepatocellular carcinoma, gastric as well as colon cancer cells have demonstrated that L-OHP triggered apoptosis through alteration of Bcl-2 family proteins (28-30). Similar to preveious studies, this study found that L-OHP treatment could induce upregulation of Bak and Bax in HCT116 cells (Figure 1 2 A & B). Taken together, it is likely that L-OHP-induced apoptosis was mediate via modulation of Bcl-2 family proteins in p53 wild-type HCT116 cells. In agreement with our study, Therachiyil et al. reported that L-OHP induced apoptosis by increasing Bax/Bcl-2 ratio in HCT116 cells while it did not alter the Bax/Bcl-2 ratio in on p53 mutant HT-29 cells (100). It is known that p53 regulates apoptosis by regulating the transcription of proapoptotic members of the Bcl-2 family including Bax, Puma, Noxa, and Bid (32). Additionally, p53 can translocates from the nucleus to the mitochondria, after receiving apoptotic stimuli, to directly interact with Bcl-2 family proteins (101, 102). Since mutations in p53 have been shown to be associated with drug resistance in human cancer (33-35), it is likely that p53 may be responsible for the difference in L-OHP sensitivity between HCT-116 and HT-29 cells. It however should be noted that, in this study, CEP could induce apoptosis in both HT-29 and HCT116 cells. We also found that CEP upregulated the expression of Bak and downregulated the expression of Bcl-x_L in both HT-29 and HCT116 cells, suggesting that apoptosis-inducing effect of CEP is mediated via modulation of the Bcl-2 protein expression in both p53 wild-type and p53 mutant cancer cells (Figure 11 & 12). Similarly, a previous study revealed that CEP induced p53 wild-type A549 and p53 mutant H1299 NSCLC cells to undergo apoptosis by downregulating Bcl-2 expression and upregulating Bax expression (14). Zhu et al also reported that CEP induced apoptosis via a decreased in Bcl-2 and an increase in Bax in p53 wild-type

MEL15-1 melanoma cells (8) whereas apoptosis-inducing effect of CEP was shown to be associated with downregulation of Bcl-2 and Bcl-x_L and upregulation of Bak in mutant p53 OVCAR-3 cells (10).

A potent cyclin-dependent kinase inhibitor 1A, $p21^{Waf1/Cip1}$, represents a major target of p53 activity (103). The present study demonstrated that CEP upregulated the expression of $p21^{Waf1/Cip1}$ in p53 mutant HT-29 cells but it did not alter the expression of $p21^{Waf1/Cip1}$ expression in p53 wild-type in HCT116 cells. These results were consistent with our previous study showing that CEP dramatically increased $p21^{Waf1/Cip1}$ expression levels in HT-29 cells (17). In contrast to CEP, this study found that L-OHP treatment induced upregulation of $p21^{Waf1/Cip1}$ only in p53 wild type HCT116 cells (Figure 18 & 19). Our findings were in agreement with the findings of Hata et al that L-OHP caused a significant increase in $p21^{Waf1/Cip1}$ expression only in p53 wild type HCT116 but did not alter the expression of $p21^{Waf1/Cip1}$ in p53 mutant HT-29 CRC cells (61). These results suggest that L-OHP and CEP upregulated p21 in p53-dependent and in p53-independent manner, respectively. Accumulating evidence has reported that $p21^{Waf1/Cip1}$ play a significant role in apoptosis of cells lacking p53 (19, 70). Li et al demonstrated that genistein induced $p21^{Waf1/Cip1}$ expression, which correlated with upregulation of pro-apoptotic protein in p53 mutant MDA-MB-231 breast cancer cells (19). Moreover, pioglitazone promoted TNF-related apoptosis-inducing ligand (TRAIL)-induced apoptosis by upregulating the expression of $p21^{Waf1/Cip1}$ in p53 mutant carcinoid (NCI-H727) cells (70). In agreement with these observations, the present study found that UC2288, a $p21^{Waf1/Cip1}$ inhibitor, abolished CEP-induced PARP cleavage in HT-29 cells (Figure 22), suggesting that apoptosis-inducing effect of CEP was associated with upregulation of $p21^{Waf1/Cip1}$ in p53-mutant HT-29 cells.

A high level of ROS causes oxidative stress, resulting in DNA damage and subsequent apoptosis (9). Therefore, increased ROS production may be a novel strategy for cancer therapy (104). Several chemotherapeutic drugs such as doxorubicin, cisplatin and oxaliplatin as well as natural compounds such as quercetin, capsaicin, curcumin and koumine induced ROS generation, leading to

apoptosis in a large variety of cancer cells such as lung, colon cancer and hepatocellular carcinoma cells (11, 12, 17, 105). Moreover, many previous studies revealed that cytotoxic and apoptotic inducing effects of CEP were associated with ROS generation in many cancer cells such as lung, hepatocellular, myeloma (31, 35, 36). Similarly, the present study found that ROS generation was associated with CEP-induced cytotoxicity and apoptosis induction in both HT-29 and HCT-116 cells. It however should be noted that CEP treatment induced ROS production in HCT116 cells higher than HT-29 cells. It is known that nuclear factor erythroid 2-related factor 2 (Nrf2) is a transcription factor that regulate the expression of antioxidant proteins such as NAD(P)H quinone oxidoreductase 1 (NQO1), glutathione S-transferase 1 (GST-1) and cystine/ glutamate transporter (x-CT) (106). Since p53 can suppress Nrf2 activation (107), cells with p53 mutant have shown to have higher Nrf2 activity than cells with p53 wild-type (108). Thus, it is possible that upregulation of antioxidants, caused by Nrf2 actvation in p53 mutant cells may counteract with CEP-mediated production of ROS, leading to a lower level of ROS in HT-29 cells.

The MAPK/ ERK signaling pathways play important roles in promoting cell survival, differentiation, proliferation, migration, and apoptosis (71). It was reported that oxaliplatin inhibited the growth of CRC cells by targeting effector proteins in MAPK/ ERK signaling, including ERK (109, 110). Additionally, several studies demonstrated that several natural compounds such as kynurenic acid, piperlongumine, and baicalein inhibited the growth of CRC cells through modulation ERK signaling pathway (111-114). Peng et al showed that norcantharidin (NCTD) inhibited cell proliferation and induced apoptosis via inhibition of ERK phosphorylation in HT-29 cells (114). Also, kynurenic acid (KYNA) was found to inhibit proliferation of HT-29 cells by inhibiting ERK phosphorylation (112). Similar to these findings, the results of this study revealed that CEP and L-OHP inhibited ERK1/ 2 phosphorylation in HT-29 cells (Figure 16A). Conversely, we found that CEP and L-OHP activated ERK1/2 phosphorylation in HCT116 cells (Figure 16B). A recent study reported that baicalein induced apoptosis of HCT-116 cells via the activation ERK

(111). Moreover, apotosis-inducing effect of [10]-gingerol was shown to be mediated through activation of ERK (115). Accumulating evidence indicated that ROS could regulate ERK signaling pathway. Previously, Kim et al showed that downregulation of phospho-ERK by silibinin is dependent on ROS generation in MCF7 and MDA-MB-231 breast cancer cells (116) while Rahman et al. demonstrated that sanguinarine (SNG) induced ROS-dependent ERK1/ 2 phosphorylation, leading to apoptosis in prostate cancer cells (15). Additionally, Yuan et al reported that koumine exerted anti-tumor effects on hepatocellular carcinoma (HCC) cells through ROS-dependent ERK inhibition (117). Remarkably, the present findings showed that ROS was responsible for CEP-mediated inhibition and activation of ERK1/2 phosphorylation in HT-29 and in HCT116 cells, respectively (Figure 17A-B). Previously, Choi et al showed that oxidative stress could activate ERK-induced cell death through degradation of mitogen-activated protein kinase (MAPK) phosphatase 1 (MKP-1) (118). In contrast, Kim et al demonstrated that MKP-1-mediated dephosphorylation of ERK1/ 2 expression, leading to apoptosis in SH-SY5Y neuroblastoma cells (119). Notably, a recent study have reported that ROS was as inducers and as inhibitors, dependending on the concentrations, in the regulation of MKP-1 expression (54). Thus, it is possible that the levels of ROS, caused by CEP treatment, might be responsible for the opposite effect of CEP on ERK phophorylation in HCT-116 and HT-29 cells. The effect of CEP on MKP-1 expression in both cell lines require further investigation. In addition to ROS, $p21^{Waf1/Cip1}$ has shown to be involved in ERK signaling pathway. For example, Drosten et al demonstrated that inactivation of $p21^{Waf1/Cip1}$ resulted in activation of ERK signaling pathways, leading to sustained cell proliferation in mourse embryonic fibroblast (64). Of note, the present study found that UC2288 could abolish CEP-mediated inhibition of ERK phosphorylation in p53 mutant HT-29 cells (Figure 21), indicating that upregulation of $p21^{Waf1/Cip1}$ plays a role in CEP-mediated ERK inhibition in p53 mutant HT-29 cells. Previously, we demonstrated that ROS induced p21 upregulation in p53 mutant HT-29 cells (34). In the present study, we showed that both NAC and UC2288 could attenuate CEP-mediated inhibition of ERK phosphorylation. Thus, it is possible that, in p53 mutant HT-29 cells, CEP-induced ROS production, leading to ERK inhibition, dependently of p21. In contrast to

HT-29 cells, ROS was responsible for CEP-mediated activation of ERK in HCT-116 cells, which was independent on p21. It is commonly known that p53 is activated in response to elevated ROS in response to elevated ROS (56). A previous study demonstrated that apoptosis-inducing effect of quercetin was shown to be mediated activation of ERK in p53 wild type A549 lung carcinoma cells (120). Moreover, Singh et al reported that p53 regulated ERK activation in carboplatin induced apoptosis in p53 wild type cervical carcinoma (121). Taken together, it is possible that CEP-dependent p53-mediated production of ROS, cause ERK activation, in HCT116 cells. Further research is needed to understand the roles of p53 in CEP-induced modulation of ERK in HT-29 and HCT-116 cells.

Conclusion

The present study clearly demonstrated that CEP significantly inhibited the growth of two human colorectal cancer cell llines, p53 wild type HCT116 and p53-mutant HT-29 cells. CEP could induce apoptosis through generation of ROS, downregulation of Bcl-x_L, upregulation of Bak and induction of PARP cleavage in both HT-29 and HCT116 cells. Moreover, ROS was partly responsible for CEP-mediated inhibition of ERK phosphorylation in HT-29 cells and CEP-mediated activation of ERK phosphorylation in HCT116 cells. Remarkably, in p53 mutant HT-29 cells, CEP induced apoptosis and inhibited ERK phosphorylation were associated with upregulation of $p21^{Waf1/Cip1}$. Taken together, the results from this study suggest that apoptosis inducing effect of CEP was dependent on $p21^{Waf1/Cip1}$ upregulation and ROS production in CRC cells.

APPENDIX A

PREPARATION OF REAGENTS

1. Incomplete DMEM stock solution (1 L)

DMEM powder	10.4 g
$NaHCO_3$	3.7 g
ddH_2O	900 mL

Mix all of components until dissolve homogeneous mixture, the next step is to adjust pH to 7.2 using 1 N HCl or 1 N NaOH. Then adjust final volume to 1 L by ddH_2O. Finally, Incomplete DMEM was sterilized by filtering through a 0.2 sterile membrane filter and store at 4°C.

2. Incomplete RPMI 1640 stock solution (1 L)

RPMI powder	10.4 g
$NaHCO_3$	1.5 g
Glucose	4.5 g
Sodium pyruvate	0.11 g
HEPES (1M)	10 mL
ddH_2O	900 mL

Mix all of components until dissolve homogeneous mixture, the next step is to adjust pH to 7.2 using 1 N HCl or 1 N NaOH. Then adjust final volume to 1 L by ddH_2O. Finally, Incomplete RPMI was sterilized by filtering through a 0.2 sterile membrane filter and store at 4°C.

3. Incomplete DMEM high glucose stock solution (1 L)

DMEM powder	10.4 g

$NaHCO_3$	3.7 g
Glucose	4.5 g
ddH_2O	900 mL

Mix all of components until dissolve homogeneous mixture, the next step is to adjust pH to 7.2 using 1 N HCl or 1 N NaOH. Then adjust final volume to 1 L by ddH_2O. Finally, Incomplete DMEM high glucose was sterilized by filtering through a 0.2 sterile membrane filter and store at 4°C.

4. 1X Phosphate Buffer Saline (PBS) (1 L)

NaCl	8.065 g
KCl	0.2 g
KH_2PO_4	0.2 g
Na_2HPO_4	1.15 g
ddH_2O	900 mL

The mixture was adjusted pH to 7.4 with 1 N HCl or 1 N NaOH. Next, add ddH_2O to 1 L and sterilized by autoclaving. Then store at room temperature.

5. Hank's buffered salt solution (HBSS) (1 L)

Hank balance salt powder	9.8 g
$NaHCO_3$	0.35 g
ddH_2O	850 mL

The mixture was adjusted pH to 7.24 with 1 N HCl or 1 N NaOH. Next, add ddH_2O to 1 L and sterilized by filtering through a 0.2 sterile membrane filter. Then store at room temperature.

6. Separating buffer (500 mL)

Tris base	45.43 g
ddH_2O	350 mL

The mixture was adjusted pH to 8.8 with 1 N HCl or 1 N NaOH. Next, add ddH_2O to 500 mL and store at 4°C.

7. Stacking buffer (500 mL)

Tris base	15.14 g
ddH_2O	350 mL

The mixture was adjusted pH to 6.8 with 1 N HCl or 1 N NaOH. Next, add ddH_2O to 500 mL and store at 4°C.

8. Sample diluting buffer (SDB) (225 mL)

Stacking buffer	31.25 mL
10% Sodium dodecyl sulfate (SDS)	50 mL
Pyronin Y (0.5% stock)	5 mL
Bromophenol blue (0.5% stock)	5 mL
Glycerol	50 mL

Mix all of components until dissolve homogeneous mixture. Then, Add ddH_2O to 225 mL and store at room temperature.

9. 10X Laemli (Running) buffer (1L)

Tris base	30.25 g
Glycine	144 g
Sodium dodecyl sulfate (SDS)	10 g

ddH_2O	700 mL

Mix all of components until dissolve homogeneous mixture. Then, Add ddH_2O to mL and store at 4°C.

10. 1X Laemli (Running) buffer (1L)

10X Running buffer	100 mL
ddH_2O	900 mL

Store at 4°C

11. 10X Transfer buffer (1L)

Tris base	30 g
Glycine	144 g
ddH_2O	1 L

Store at 4°C

12. 1X Transfer buffer (1L)

10X Transfer buffer	100 mL
Methanol	200 mL
ddH_2O	700 mL

Store at 4°C

13. 10X Tris-Buffered Saline (TBS) (1L)

Tris base	12.1 g
NaCl	87.5 g
ddH_2O	800 mL

The mixture was adjusted pH to 7.4 with 1 N HCl or 1 N NaOH. Next, add ddH_2O to 1 L and store at 4°C.

14. 1X Tris-Buffered Saline (TBS) (1L)

10X Tris-Buffered Saline (TBS)	100 mL
ddH_2O	900 mL

Store at 4°C

15. 1X Tris-Buffered Saline (TBS)/Tween buffer (1L)

Tween 20	0.5 mL
1X Tris-Buffered Saline (TBS)	999.5 mL

Store at 4°C

APPENDIX B

RESULTS

Appendix B-1: Representative cytograms of cell apoptosis analysis of HCT116 cells (p53 wild type) after treatment with 5, 10 and 20 μM of CEP and 5 μM of L-OHP for 24 h.

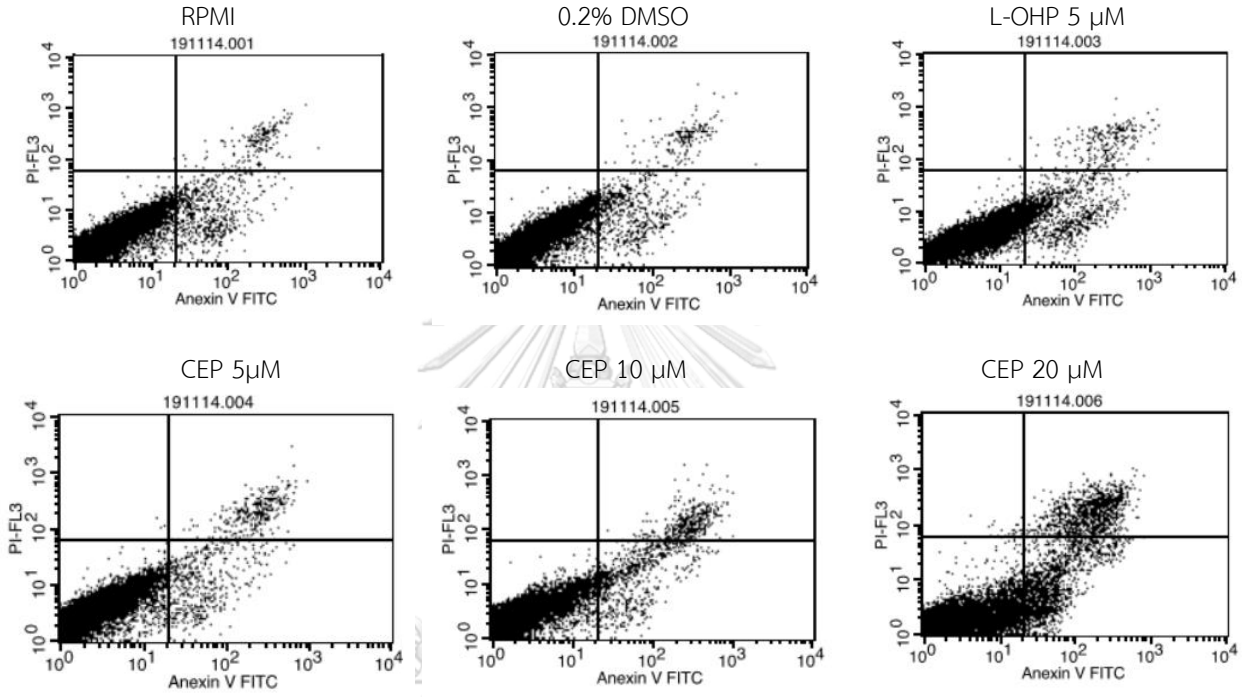

Appendix B-2: The percentages of apoptotic and necrotic cells of HCT-116 cells after treatment with 5, 10 and 20 μM of CEP and 5 μM of L-OHP for 24 h

Treatment	Cell population (%)		
	Alive	Apoptosis	Necrosis
RPMI	95.48±1.81	4.43±1.84	0.08±0.04
0.2%DMSO	94.31±1.15	5.60±1.20	0.09±0.05
L-OHP 5 μM	90.15±2.77	9.79±2.78	0.07±0.02
CEP 5 μM	93.40±0.48	6.43±0.52	0.17±0.09
CEP 10 μM	89.51±0.42	10.23±0.56	0.26±0.14
CEP 20 μM	77.09±3.65	22.14±3.67	0.77±0.45

Data represent mean±SEM from three independent experiments.

Appendix B-3: Representative cytograms of cell apoptosis analysis of HT-29 cells (p53 mutant) after treatment with 1.25, 2.5 and 5 μM of CEP and 10 μM of L-OHP for 24 h.

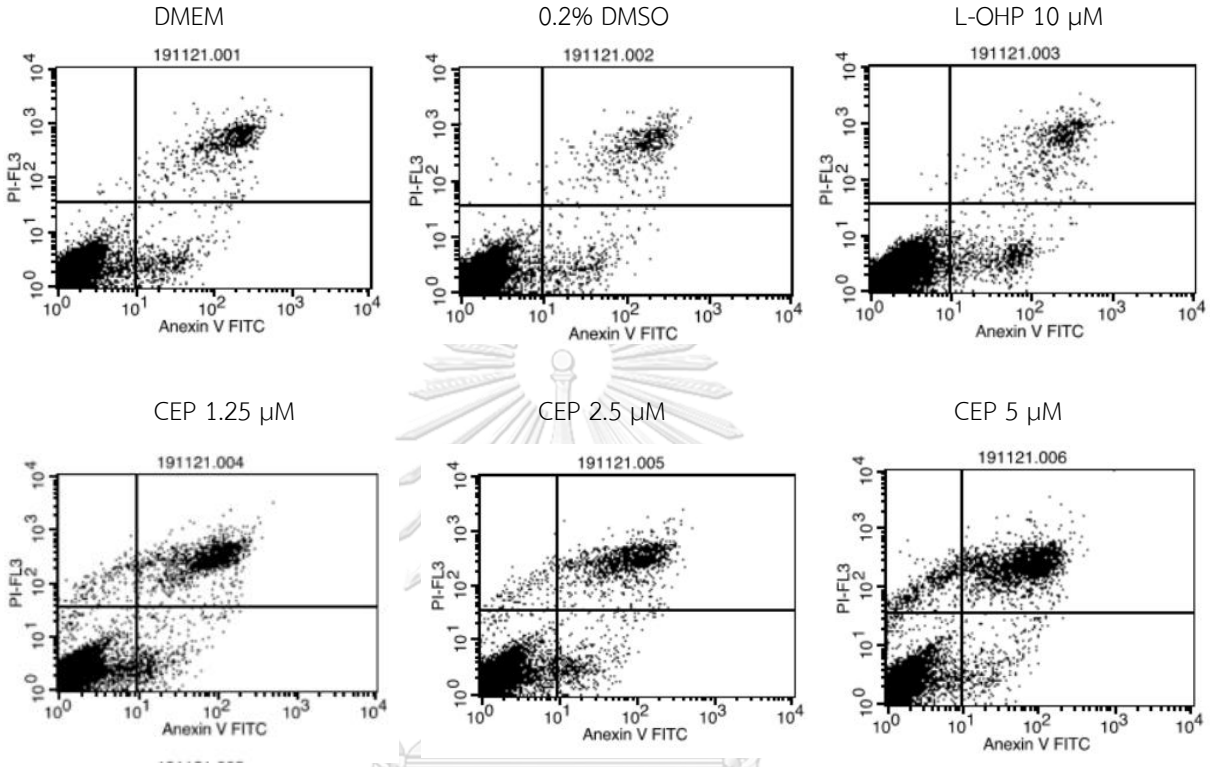

Appendix B-4: The percentages of apoptotic and necrotic cells of HT-29 cells after treatment with 1.25, 2.5 and 5 μM of CEP and 10 μM of OX for 24 h.

Treatment	Cell population (%)		
	Alive	Apoptosis	Necrosis
DMEM	92.08±2.33	7.79±2.34	0.13±0.02
0.2%DMSO	92.53±1.80	7.35±1.82	0.13±0.02
OX 10 μM	90.60±1.49	9.21±1.55	0.2±0.08
CEP 1.25 μM	83.50±2.90	15.13±2.99	1.38±0.22
CEP 2.5 μM	82.09±1.61	16.06±2.00	1.86±0.42
CEP 5 μM	67.29±3.04	26.94±3.97	5.77±1.29

Data represent mean±SEM from three independent experiments.

Appendix B-5: Representative cytograms of cell apoptosis analysis of HCT116 cells after treatment with or without 3 mM of NAC for 2 h and then treated with 5, 10 and 20 μM of CEP and 5 μM of L-OHP for 24 h.

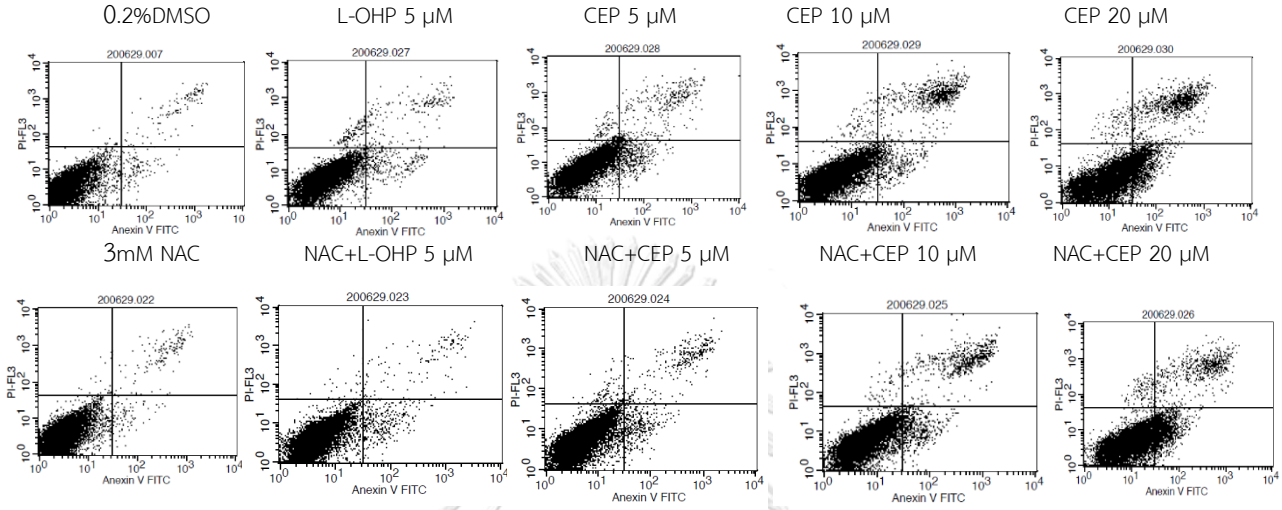

Appendix B-6: The percentage of apoptotic cells of HCT116 cells after treatment with or without 3 mM of NAC for 2 h and then treated with 5, 10 and 20 μM of CEP and 5 μM of L-OHP for 24 h

Treatment	Cell apoptosis (%)	
	3 mM NAC	
	+	-
0.2%DMSO	2.60±0.17	2.61±0.23
L-OHP 5 μM	3.73±0.58	4.32±0.15
CEP 5 μM	6.10±0.70	7.77±0.29
CEP 10 μM	9.61±0.36	11.42±0.22
CEP 20 μM	19.28±2.24	25.29±2.29

Data represent mean±SEM from three independent experiments.

Appendix B-7: Representative cytograms of cell apoptosis analysis of HT-29 cells after treatment with or without 3 mM of NAC for 2 h and then treated with 1.25, 2.5 and 5 μM of CEP and 10 μM of L-OHP for 24 h.

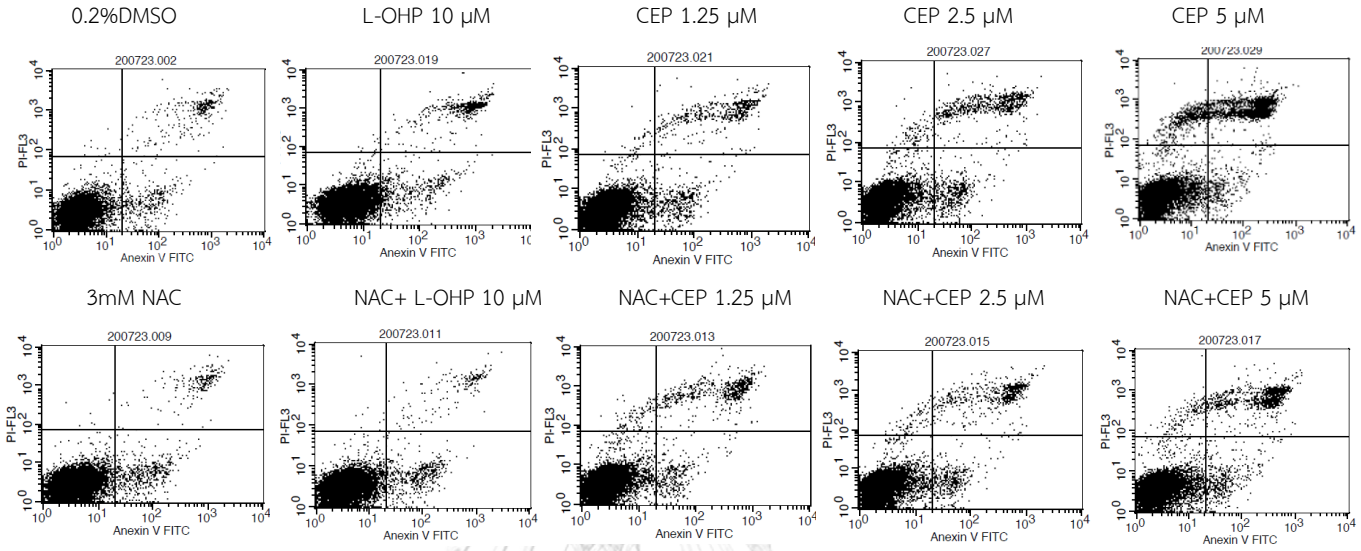

Appendix B-8: The percentage of apoptotic cells of HT-29 cells after treatment with or without 3 mM of NAC for 2 h and then treated with 1.25, 2.5 and 5 μM of CEP and 10 μM of L-OHP for 24 h.

Treatment	Cell apoptosis (%)	
	3 mM NAC	
	+	-
0.2%DMSO	6.73±1.53	7.21±1.59
L-OHP 10 μM	8.08±2.42	12.18±1.09
CEP 1.25 μM	8.91±1.41	8.42±1.50
CEP 2.5 μM	9.41±0.89	10.13±1.06
CEP 5 μM	14.64±0.11	20.78±0.68

Data represent mean±SEM from three independent experiments.

Appendix B-9: Representative cytograms of ROS production in HCT116 after treatment with 5, 10 and 20 μM of CEP and 5 μM of L-OHP for 1 h.

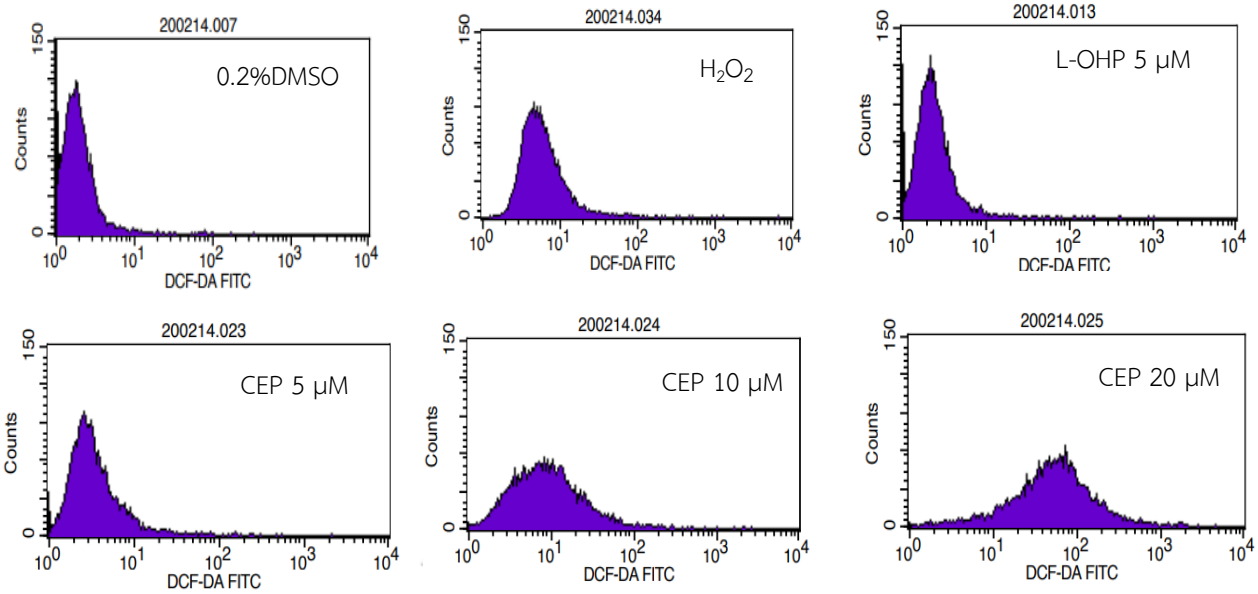

Appendix B-10: The percentage of ROS production in HCT116 after treatment with 5, 10 and 20 μM of CEP and 5 μM of L-OHP for 1 h.

Treatment	DCF-DA intensity	ROS production (% of control)
0.2%DMSO	2.28±0.06	100±0.00
H_2O_2 500 μM	8.09±0.04	355.80±8.71
L-OHP 5 μM	2.91±0.09	128.08±6.15
CEP 5 μM	4.77±0.39	209.89±17.96
CEP 10 μM	14.01±0.06	616.25±13.82
CEP 20 μM	78.39±1.58	3448.67±126.73

Data represent mean±SEM from three independent experiments.

Appendix B-11: Representative cytograms of ROS production in HT-29 after treatment with 1.25, 2.5 and 5 μM of CEP and 10 μM of L-OHP for 1 h.

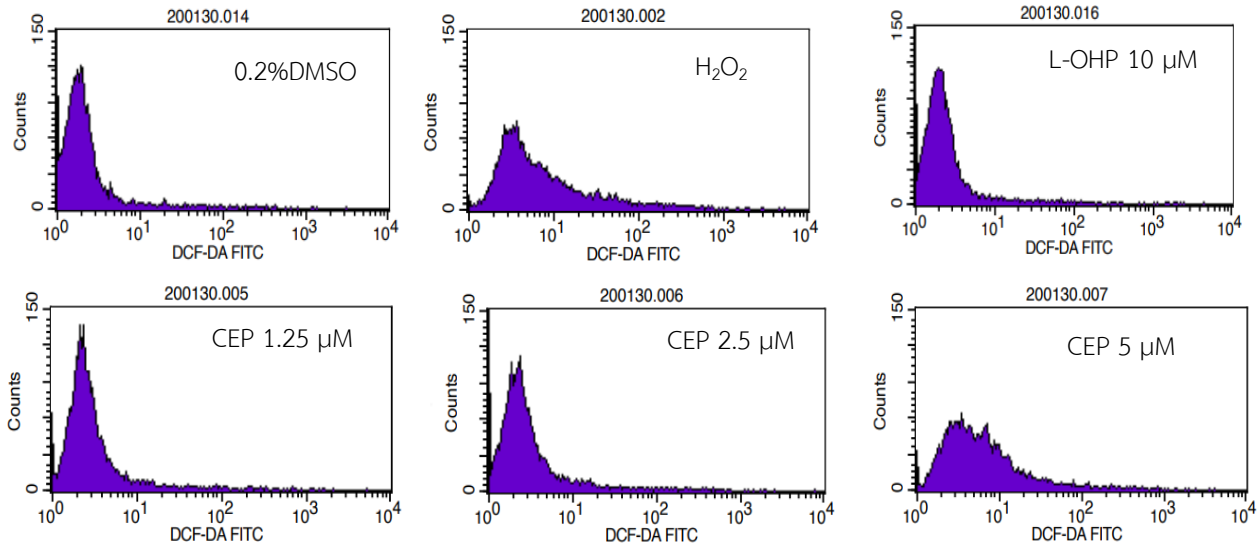

Appendix B-12: The percentage of ROS production HT-29 after treatment with 1.25, 2.5 and 5 μM of CEP and 10 μM of L-OHP for 1 h.

Treatment	DCF-DA intensity	ROS production (% of control)
0.2%DMSO	5.30±0.52	100±0.00
H_2O_2 500 μM	21.31±0.92	406.80±23.65
L-OHP 10 μM	6.32±0.67	120.11±10.80
CEP 1.25 μM	7.59±0.70	147.59±23.17
CEP 2.5 μM	9.74±1.29	184.04±15.59
CEP 5 μM	14.84±0.65	283.42±17.45

Data represent mean±SEM from three independent experiments.

REFERENCES

1. Siegel RL, Miller KD, Jemal A. Cancer statistics, 2019. CA Cancer J Clin. 2019;69(1):7-34.
2. Topçul M, Çetin İ. Treatment Of Colon Cancer. 2015. p. 1-15.
3. Macdonald JS. Toxicity of 5-fluorouracil. Oncology (Williston Park). 1999;13(7 Suppl 3):33-4.
4. Giampieri R, Maccaroni E, Sotte V, Baleani MG, Meletani T, Giglio E, et al. Acute Peripheral Motor Neuropathy Induced by Oxaliplatin-Correlated Hypokalaemia. Oncology and Therapy. 2020;8(1):161-9.
5. Redza-Dutordoir M, Averill-Bates DA. Activation of apoptosis signalling pathways by reactive oxygen species. Biochim Biophys Acta. 2016;1863(12):2977-92.
6. Perillo B, Di Donato M, Pezone A, Di Zazzo E, Giovannelli P, Galasso G, et al. ROS in cancer therapy: the bright side of the moon. Experimental & Molecular Medicine. 2020;52(2):192-203.
7. Schieber M, Chandel NS. ROS function in redox signaling and oxidative stress. Curr Biol. 2014;24(10):R453-R62.
8. NavaneethaKrishnan S, Rosales JL, Lee KY. ROS-Mediated Cancer Cell Killing through Dietary Phytochemicals. Oxid Med Cell Longev. 2019;2019:9051542.
9. Kim SJ, Kim HS, Seo YR. Understanding of ROS-Inducing Strategy in Anticancer Therapy. Oxid Med Cell Longev. 2019;2019:5381692.
10. Conklin KA. Chemotherapy-associated oxidative stress: impact on chemotherapeutic effectiveness. Integr Cancer Ther. 2004;3(4):294-300.
11. Lu J, Papp LV, Fang J, Rodriguez-Nieto S, Zhivotovsky B, Holmgren A. Inhibition of Mammalian thioredoxin reductase by some flavonoids: implications for myricetin and quercetin anticancer activity. Cancer Res. 2006;66(8):4410-8.
12. Yang KM, Pyo JO, Kim GY, Yu R, Han IS, Ju SA, et al. Capsaicin induces apoptosis by generating reactive oxygen species and disrupting mitochondrial transmembrane potential in human colon cancer cell lines. Cell Mol Biol Lett. 2009;14(3):497-510.
13. Jaganathan SK, Supriyanto E, Mandal M. Events associated with apoptotic effect

of p-Coumaric acid in HCT-15 colon cancer cells. World J Gastroenterol. 2013;19(43):7726-34.

14. Lee W-J, Hsiao M, Chang J-L, Yang S-F, Tseng T-H, Cheng C-W, et al. Quercetin induces mitochondrial-derived apoptosis via reactive oxygen species-mediated ERK activation in HL-60 leukemia cells and xenograft. Archives of Toxicology. 2015;89(7):1103-17.

15. Rahman A, Pallichankandy S, Thayyullathil F, Galadari S. Critical role of H2O2 in mediating sanguinarine-induced apoptosis in prostate cancer cells via facilitating ceramide generation, ERK1/2 phosphorylation, and Par-4 cleavage. Free Radical Biology and Medicine. 2019;134:527-44.

16. Sheng Y-N, Luo Y-H, Liu S-B, Xu W-T, Zhang Y, Zhang T, et al. Zeaxanthin Induces Apoptosis via ROS-Regulated MAPK and AKT Signaling Pathway in Human Gastric Cancer Cells. Onco Targets Ther. 2020;13:10995-1006.

17. Yuan Z, Liang Z, Yi J, Chen X, Li R, Wu J, et al. Koumine Promotes ROS Production to Suppress Hepatocellular Carcinoma Cell Proliferation Via NF-kappaB and ERK/p38 MAPK Signaling. Biomolecules. 2019;9(10).

18. Kreis NN, Louwen F, Yuan J. The Multifaceted p21 (Cip1/Waf1/CDKN1A) in Cell Differentiation, Migration and Cancer Therapy. Cancers (Basel). 2019;11(9).

19. Li Y, Upadhyay S, Bhuiyan M, Sarkar FH. Induction of apoptosis in breast cancer cells MDA-MB-231 by genistein. Oncogene. 1999;18(20):3166-72.

20. Lincet H, Poulain L, Remy JS, Deslandes E, Duigou F, Gauduchon P, et al. The p21(cip1/waf1) cyclin-dependent kinase inhibitor enhances the cytotoxic effect of cisplatin in human ovarian carcinoma cells. Cancer Lett. 2000;161(1):17-26.

21. Rogosnitzky M, Danks R. Therapeutic potential of the biscoclaurine alkaloid, cepharanthine, for a range of clinical conditions. Pharmacol Rep. 2011;63(2):337-47.

22. Sato T, Tsuyoshi Ohnishi S. In vitro anti-sickling effect of cepharanthine. European Journal of Pharmacology. 1982;83(1):91-5.

23. Furusawa S, Wu J. The effects of biscoclaurine alkaloid cepharanthine on mammalian cells: Implications for cancer, shock, and inflammatory diseases. Life Sciences. 2007;80(12):1073-9.

24. Bailly C. Cepharanthine: An update of its mode of action, pharmacological

properties and medical applications. Phytomedicine. 2019;62:152956.

25. Zhu Q, Guo B, Chen L, Ji Q, Liang H, Wen N, et al. Cepharanthine exerts antitumor activity on choroidal melanoma by reactive oxygen species production and c-Jun N-terminal kinase activation. Oncol Lett. 2017;13(5):3760-6.

26. Wu J, Suzuki H, Zhou YW, Liu W, Yoshihara M, Kato M, et al. Cepharanthine activates caspases and induces apoptosis in Jurkat and K562 human leukemia cell lines. J Cell Biochem. 2001;82(2):200-14.

27. Payon V, Kongsaden C, Ketchart W, Mutirangura A, Wonganan P. Mechanism of Cepharanthine Cytotoxicity in Human Ovarian Cancer Cells. Planta Med. 2019;85(1):41-7.

28. Gao S, Li X, Ding X, Qi W, Yang Q. Cepharanthine Induces Autophagy, Apoptosis and Cell Cycle Arrest in Breast Cancer Cells. Cellular Physiology and Biochemistry. 2017;41(4):1633-48.

29. Chen Z, Huang C, Yang YL, Ding Y, Ou-Yang HQ, Zhang YY, et al. Inhibition of the STAT3 signaling pathway is involved in the antitumor activity of cepharanthine in SaOS2 cells. Acta Pharmacol Sin. 2012;33(1):101-8.

30. Takahashi-Makise N, Suzu S, Hiyoshi M, Ohsugi T, Katano H, Umezawa K, et al. Biscoclaurine alkaloid cepharanthine inhibits the growth of primary effusion lymphoma in vitro and in vivo and induces apoptosis via suppression of the NF-kappaB pathway. Int J Cancer. 2009;125(6):1464-72.

31. Hua P, Sun M, Zhang G, Zhang Y, Tian X, Li X, et al. Cepharanthine induces apoptosis through reactive oxygen species and mitochondrial dysfunction in human non-small-cell lung cancer cells. Biochem Biophys Res Commun. 2015;460(2):136-42.

32. Seubwai W, Vaeteewoottacharn K, Hiyoshi M, Suzu S, Puapairoj A, Wongkham C, et al. Cepharanthine exerts antitumor activity on cholangiocarcinoma by inhibiting NF-kappaB. Cancer Sci. 2010;101(7):1590-5.

33. Harada K, Ferdous T, Itashiki Y, Takii M, Mano T, Mori Y, et al. Cepharanthine inhibits angiogenesis and tumorigenicity of human oral squamous cell carcinoma cells by suppressing expression of vascular endothelial growth factor and interleukin-8. International journal of oncology. 2009;35:1025-35.

34. Rattanawong A, Payon V, Limpanasittikul W, Boonkrai C, Mutirangura A, Wonganan P. Cepharanthine exhibits a potent anticancer activity in p53-mutated

colorectal cancer cells through upregulation of p21Waf1/Cip1. Oncol Rep. 2018;39(1):227-38.

35. Biswas KK, Tancharoen S, Sarker KP, Kawahara K, Hashiguchi T, Maruyama I. Cepharanthine triggers apoptosis in a human hepatocellular carcinoma cell line (HuH-7) through the activation of JNK1/2 and the downregulation of Akt. FEBS Lett. 2006;580(2):703-10.

36. Kikukawa Y, Okuno Y, Tatetsu H, Nakamura M, Harada N, Ueno S, et al. Induction of cell cycle arrest and apoptosis in myeloma cells by cepharanthine, a biscoclaurine alkaloid. International journal of oncology. 2008;33:807-14.

37. Harada K, Bando T, Yoshida H, Sato M. Characteristics of antitumour activity of cepharanthin against a human adenosquamous cell carcinoma cell line. Oral Oncol. 2001;37(8):643-51.

38. Imsamran W CA, Wiangnon S, Pongnikorn D. Hospital-Based Cancer Registry NCI2 2016. National cancer Institute. 2017;32:1-94.

39. Mármol I, Sánchez-de-Diego C, Pradilla Dieste A, Cerrada E, Rodriguez Yoldi MJ. Colorectal Carcinoma: A General Overview and Future Perspectives in Colorectal Cancer. Int J Mol Sci. 2017;18(1):197.

40. Armelao F, de Pretis G. Familial colorectal cancer: a review. World J Gastroenterol. 2014;20(28):9292-8.

41. Yamagishi H, Kuroda H, Imai Y, Hiraishi H. Molecular pathogenesis of sporadic colorectal cancers. Chin J Cancer. 2016;35:4-.

42. Kastrinos F, Syngal S. Inherited colorectal cancer syndromes. Cancer J. 2011;17(6):405-15.

43. Amersi F, Agustin M, Ko CY. Colorectal cancer: epidemiology, risk factors, and health services. Clin Colon Rectal Surg. 2005;18(3):133-40.

44. Simon K. Colorectal cancer development and advances in screening. Clin Interv Aging. 2016;11:967-76.

45. Burlefinger R, Ottenjann R. [Colorectal cancer--diagnosis, early detection and staging]. Internist (Berl). 1991;32(6):321-9.

46. Brown C, Raval M. Advances in minimally invasive surgery in the treatment of colorectal cancer. Expert review of anticancer therapy. 2008;8:111-23.

47. Kye B-H, Cho H-M. Overview of radiation therapy for treating rectal cancer. Ann Coloproctol. 2014;30(4):165-74.

48. Grivicich I, Mans DR, Peters GJ, Schwartsmann G. Irinotecan and oxaliplatin: an overview of the novel chemotherapeutic options for the treatment of advanced colorectal cancer. Braz J Med Biol Res. 2001;34(9):1087-103.

49. Longley DB, Harkin DP, Johnston PG. 5-fluorouracil: mechanisms of action and clinical strategies. Nat Rev Cancer. 2003;3(5):330-8.

50. Hammond WA, Swaika A, Mody K. Pharmacologic resistance in colorectal cancer: a review. Ther Adv Med Oncol. 2016;8(1):57-84.

51. Ellis LM. Mechanisms of action of bevacizumab as a component of therapy for metastatic colorectal cancer. Semin Oncol. 2006;33(5 Suppl 10):S1-7.

52. Ray PD, Huang BW, Tsuji Y. Reactive oxygen species (ROS) homeostasis and redox regulation in cellular signaling. Cell Signal. 2012;24(5):981-90.

53. Sharma P, Jha AB, Dubey RS, Pessarakli M. Reactive Oxygen Species, Oxidative Damage, and Antioxidative Defense Mechanism in Plants under Stressful Conditions. Journal of Botany. 2012;2012:217037.

54. Son Y, Cheong Y-K, Kim N-H, Chung H-T, Kang DG, Pae H-O. Mitogen-Activated Protein Kinases and Reactive Oxygen Species: How Can ROS Activate MAPK Pathways? Journal of Signal Transduction. 2011;2011:792639.

55. Zhang J, Wang X, Vikash V, Ye Q, Wu D, Liu Y, et al. ROS and ROS-Mediated Cellular Signaling. Oxid Med Cell Longev. 2016;2016:4350965.

56. Seok JS, Jeong CH, Petriello MC, Seo HG, Yoo H, Hong K, et al. Piperlongumine decreases cell proliferation and the expression of cell cycle-associated proteins by inhibiting Akt pathway in human lung cancer cells. Food and Chemical Toxicology. 2018;111:9-18.

57. Wang JR, Luo YH, Piao XJ, Zhang Y, Feng YC, Li JQ, et al. Mechanisms underlying isoliquiritigenin-induced apoptosis and cell cycle arrest via ROS-mediated MAPK/STAT3/NF-**K**B pathways in human hepatocellular carcinoma cells. Drug Dev Res. 2019;80(4):461-70.

58. Elmore S. Apoptosis: a review of programmed cell death. Toxicol Pathol.

2007;35(4):495-516.

59. Abou-Ghali M, Stiban J. Regulation of Ceramide Channel Formation and Disassembly: Insights on the Initiation of Apoptosis. Saudi Journal of Biological Sciences. 2015;274.

60. Reed JC. Mechanisms of apoptosis. Am J Pathol. 2000;157(5):1415-30.

61. Kalimuthu S, Se-Kwon K. Cell survival and apoptosis signaling as therapeutic target for cancer: marine bioactive compounds. Int J Mol Sci. 2013;14(2):2334-54.

62. Ashkenazi A, Dixit VM. Death receptors: signaling and modulation. Science. 1998;281(5381):1305-8.

63. Lomonosova E, Chinnadurai G. BH3-only proteins in apoptosis and beyond: an overview. Oncogene. 2008;27 Suppl 1:S2-19.

64. Lomonosova E, Chinnadurai G. BH3-only proteins in apoptosis and beyond: an overview. Oncogene. 2008;27(1):S2-S19.

65. Campbell KJ, Tait SWG. Targeting BCL-2 regulated apoptosis in cancer. Open Biol. 2018;8(5).

66. Cuda CM, Pope RM, Perlman H. The inflammatory role of phagocyte apoptotic pathways in rheumatic diseases. Nat Rev Rheumatol. 2016;12(9):543-58.

67. Al Bitar S, Gali-Muhtasib H. The Role of the Cyclin Dependent Kinase Inhibitor p21(cip1/waf1) in Targeting Cancer: Molecular Mechanisms and Novel Therapeutics. Cancers. 2019;11(10):1475.

68. Wu Q, Kirschmeier P, Hockenberry T, Yang TY, Brassard DL, Wang L, et al. Transcriptional regulation during p21WAF1/CIP1-induced apoptosis in human ovarian cancer cells. J Biol Chem. 2002;277(39):36329-37.

69. Kang KH, Kim WH, Choi KH. p21 Promotes Ceramide-Induced Apoptosis and Antagonizes the Antideath Effect of Bcl-2 in Human Hepatocarcinoma Cells. Experimental Cell Research. 1999;253(2):403-12.

70. Göke R, Göke A, Göke B, El-Deiry WS, Chen Y. Pioglitazone inhibits growth of carcinoid cells and promotes TRAIL-induced apoptosis by induction of p21waf1/cip1. Digestion. 2001;64(2):75-80.

71. Munshi A, Ramesh R. Mitogen-activated protein kinases and their role in radiation response. Genes Cancer. 2013;4(9-10):401-8.

72. Morrison DK. MAP kinase pathways. Cold Spring Harb Perspect Biol. 2012;4(11):a011254.

73. Guo YJ, Pan WW, Liu SB, Shen ZF, Xu Y, Hu LL. ERK/MAPK signalling pathway and tumorigenesis (Review). Exp Ther Med. 2020;19(3):1997-2007.

74. Ye Q, Cai W, Zheng Y, Evers BM, She QB. ERK and AKT signaling cooperate to translationally regulate survivin expression for metastatic progression of colorectal cancer. Oncogene. 2014;33(14):1828-39.

75. Sebolt-Leopold JS, Herrera R. Targeting the mitogen-activated protein kinase cascade to treat cancer. Nature Reviews Cancer. 2004;4(12):937-47.

76. McKay MM, Morrison DK. Integrating signals from RTKs to ERK/MAPK. Oncogene. 2007;26(22):3113-21.

77. Murakami K, Okajima K, Uchiba M. The prevention of lipopolysaccharide-induced pulmonary vascular injury by pretreatment with cepharanthine in rats. Am J Respir Crit Care Med. 2000;161(1):57-63.

78. Ershun Z, Yunhe F, Zhengkai W, Yongguo C, Naisheng Z, Zhengtao Y. Cepharanthine attenuates lipopolysaccharide-induced mice mastitis by suppressing the NF-**K**B signaling pathway. Inflammation. 2014;37(2):331-7.

79. Huang H, Hu G, Wang C, Xu H, Chen X, Qian A. Cepharanthine, an Alkaloid from Stephania cepharantha Hayata, Inhibits the Inflammatory Response in the RAW264.7 Cell and Mouse Models. Inflammation. 2014;37(1):235-46.

80. Aota K, Yamanoi T, Kani K, Azuma M. Cepharanthine Inhibits IFN-γ-Induced CXCL10 by Suppressing the JAK2/STAT1 Signal Pathway in Human Salivary Gland Ductal Cells. Inflammation. 2018;41(1):50-8.

81. Gülçin I, Elias R, Gepdiremen A, Chea A, Topal F. Antioxidant activity of bisbenzylisoquinoline alkaloids from Stephania rotunda: cepharanthine and fangchinoline. J Enzyme Inhib Med Chem. 2010;25(1):44-53.

82. Halicka D, Ita M, Tanaka T, Kurose A, Darzynkiewicz Z. Biscoclaurine alkaloid cepharanthine protects DNA in TK6 lymphoblastoid cells from constitutive oxidative damage. Pharmacological reports : PR. 2008;60(1):93-100.

83. Tsuyoshi M, Kunzoorita O, Keisuke E, Hirotsugu K, Eisuke F S, Bunji I, et al.

Inhibition of active oxygen generation in guinea-pig neutrophils by biscoclaurine alkaloids. Biochemical Pharmacology. 1990;39(7):1255-9.

84. Chea A, Hout S, Bun S-S, Tabatadze N, Gasquet M, Azas N, et al. Antimalarial activity of alkaloids isolated from Stephania rotunda. Journal of Ethnopharmacology. 2007;112(1):132-7.

85. Okamoto M, Ono M, Baba M. Potent Inhibition of HIV Type 1 Replication by an Antiinflammatory Alkaloid, Cepharanthine, in Chronically Infected Monocytic Cells. AIDS Research and Human Retroviruses. 1998;14(14):1239-45.

86. Harada K, Bando T, Yoshida H, Sato M. Characteristics of antitumour activity of cepharanthin against a human adenosquamous cell carcinoma cell line. Oral Oncology. 2001;37(8):643-51.

87. Fang ZH, Li YJ, Chen Z, Wang JJ, Zhu LH. Inhibition of signal transducer and activator of transcription 3 and cyclooxygenase-2 is involved in radiosensitization of cepharanthine in HeLa cells. Int J Gynecol Cancer. 2013;23(4):608-14.

88. Gao S, Li X, Ding X, Qi W, Yang Q. Cepharanthine Induces Autophagy, Apoptosis and Cell Cycle Arrest in Breast Cancer Cells. Cell Physiol Biochem. 2017;41(4):1633-48.

89. Unson S, Kongsaden C, Wonganan P. Cepharanthine combined with 5-fluorouracil inhibits the growth of p53-mutant human colorectal cancer cells. Journal of Asian Natural Products Research. 2019;22:1-16.

90. Pistritto G, Trisciuoglio D, Ceci C, Garufi A, D'Orazi G. Apoptosis as anticancer mechanism: function and dysfunction of its modulators and targeted therapeutic strategies. Aging (Albany NY). 2016;8(4):603-19.

91. Liou GY, Storz P. Reactive oxygen species in cancer. Free Radic Res. 2010;44(5):479-96.

92. Guo YJ, Pan WW, Liu SB, Shen ZF, Xu Y, Hu LL. ERK/MAPK signalling pathway and tumorigenesis. Exp Ther Med. 2020;19(3):1997-2007.

93. Al Bitar S, Gali-Muhtasib H. The Role of the Cyclin Dependent Kinase Inhibitor p21(cip1/waf1) in Targeting Cancer: Molecular Mechanisms and Novel Therapeutics. Cancers (Basel). 2019;11(10).

94. Drosten M, Sum EYM, Lechuga CG, Simon-Carrasco L, Jacob HKC, Garcia-Medina R, et al. Loss of p53 induces cell proliferation via Ras-independent activation of the

Raf/Mek/Erk signaling pathway. P Natl Acad Sci USA. 2014;111(42):15155-60.

95. Hata T, Yamamoto H, Ngan CY, Koi M, Takagi A, Damdinsuren B, et al. Role of p21waf1/cip1 in effects of oxaliplatin in colorectal cancer cells. Mol Cancer Ther. 2005;4(10):1585-94.

96. Wang J-b, Qi L-l, Zheng S-d, Wu T-x. Curcumin induces apoptosis through the mitochondria-mediated apoptotic pathway in HT-29 cells. J Zhejiang Univ Sci B. 2009;10(2):93-102.

97. Yaffe PB, Power Coombs MR, Doucette CD, Walsh M, Hoskin DW. Piperine, an alkaloid from black pepper, inhibits growth of human colon cancer cells via G1 arrest and apoptosis triggered by endoplasmic reticulum stress. Molecular Carcinogenesis. 2015;54(10):1070-85.

98. Han MH, Kim GY, Yoo YH, Choi YH. Sanguinarine induces apoptosis in human colorectal cancer HCT-116 cells through ROS-mediated Egr-1 activation and mitochondrial dysfunction. Toxicol Lett. 2013;220(2):157-66.

99. Zeng L, Zhen Y, Chen Y, Zou L, Zhang Y, Hu F, et al. Naringin inhibits growth and induces apoptosis by a mechanism dependent on reduced activation of NF-κB/COX-2-caspase-1 pathway in HeLa cervical cancer cells. Int J Oncol. 2014;45(5):1929-36.

100. Therachiyil L, Haroon J, Sahir F, Siveen KS, Uddin S, Kulinski M, et al. Dysregulated Phosphorylation of p53, Autophagy and Stemness Attributes the Mutant p53 Harboring Colon Cancer Cells Impaired Sensitivity to Oxaliplatin. Front Oncol. 2020;10:1744-.

101. Vaseva AV, Moll UM. The mitochondrial p53 pathway. Biochim Biophys Acta. 2009;1787(5):414-20.

102. Czabotar PE, Lessene G, Strasser A, Adams JM. Control of apoptosis by the BCL-2 protein family: implications for physiology and therapy. Nature Reviews Molecular Cell Biology. 2014;15(1):49-63.

103. Abbas T, Dutta A. p21 in cancer: intricate networks and multiple activities. Nature reviews Cancer. 2009;9(6):400-14.

104. Liou G-Y, Storz P. Reactive oxygen species in cancer. Free radical research.

2010;44(5):479-96.

105. Agarwal A, Kasinathan A, Ganesan R, Balasubramanian A, Bhaskaran J, Suresh S, et al. Curcumin induces apoptosis and cell cycle arrest via the activation of reactive oxygen species–independent mitochondrial apoptotic pathway in Smad4 and p53 mutated colon adenocarcinoma HT29 cells. Nutrition Research. 2018;51:67-81.

106. Tonelli C, Chio IIC, Tuveson DA. Transcriptional Regulation by Nrf2. Antioxid Redox Signal. 2018;29(17):1727-45.

107. Faraonio R, Vergara P, Di Marzo D, Pierantoni MG, Napolitano M, Russo T, et al. p53 suppresses the Nrf2-dependent transcription of antioxidant response genes. J Biol Chem. 2006;281(52):39776-84.

108. Tung M-C, Lin P-L, Wang Y-C, He T-Y, Lee M-C, Yeh SD, et al. Mutant p53 confers chemoresistance in non-small cell lung cancer by upregulating Nrf2. Oncotarget. 2015;6(39):41692-705.

109. Gaur S, Chen L, Ann V, Lin W-C, Wang Y, Chang V, et al. Dovitinib synergizes with oxaliplatin in suppressing cell proliferation and inducing apoptosis in colorectal cancer cells regardless of RAS-RAF mutation status. Molecular cancer. 2014;13:21.

110. Santoro V, Jia R, Thompson H, Nijhuis A, Jeffery R, Kiakos K, et al. Role of Reactive Oxygen Species in the Abrogation of Oxaliplatin Activity by Cetuximab in Colorectal Cancer. Journal of the National Cancer Institute. 2015;108:djv394.

111. Su M-Q, Zhou Y-R, Rao X, Yang H, Zhuang XH, Ke X-J, et al. Baicalein induces the apoptosis of HCT116 human colon cancer cells via the upregulation of DEPP/Gadd45a and activation of MAPKs. Int J Oncol. 2018;53(2):750-60.

112. Walczak K, Turski WA, Rajtar G. Kynurenic acid inhibits colon cancer proliferation in vitro: effects on signaling pathways. Amino Acids. 2014;46(10):2393-401.

113. Randhawa H, Kibble K, Zeng H, Moyer MP, Reindl KM. Activation of ERK signaling and induction of colon cancer cell death by piperlongumine. Toxicol In Vitro. 2013;27(6):1626-33.

114. Peng C, Liu X, Liu E, Xu K, Niu W, Chen R, et al. Norcantharidin induces HT-29 colon cancer cell apoptosis through the $\alpha_v\beta_6$–extracellular signal-related kinase signaling pathway. Cancer Science. 2009;100(12):2302-8.

115. Ryu MJ, Chung HS. [10]-Gingerol induces mitochondrial apoptosis through activation of MAPK pathway in HCT116 human colon cancer cells. In Vitro Cellular & Developmental Biology - Animal. 2015;51(1):92-101.

116. Wang H-j, Wei X-F, Jiang Y-Y, Huang H, Yang Y, Fan S-M, et al. Silibinin induces the generation of nitric oxide in human breast cancer MCF-7 cells. Free radical research. 2010;44:577-84.

117. Yuan Z, Liang Z, Yi J, Chen X, Li R, Wu J, et al. Koumine Promotes ROS Production to Suppress Hepatocellular Carcinoma Cell Proliferation Via NF-**K**B and ERK/p38 MAPK Signaling. Biomolecules. 2019;9(10):559.

118. Choi BH, Hur EM, Lee JH, Jun DJ, Kim KT. Protein kinase Cdelta-mediated proteasomal degradation of MAP kinase phosphatase-1 contributes to glutamate-induced neuronal cell death. J Cell Sci. 2006;119(Pt 7):1329-40.

119. Kim GS, Choi YK, Song SS, Kim W-K, Han BH. MKP-1 contributes to oxidative stress-induced apoptosis via inactivation of ERK1/2 in SH-SY5Y cells. Biochemical and Biophysical Research Communications. 2005;338(4):1732-8.

120. Nguyen TTT, Tran E, Nguyen TH, Do PT, Huynh TH, Huynh H. The role of activated MEK-ERK pathway in quercetin-induced growth inhibition and apoptosis in A549 lung cancer cells. Carcinogenesis. 2004;25(5):647-59.

121. Singh S, Upadhyay AK, Ajay AK, Bhat MK. p53 regulates ERK activation in carboplatin induced apoptosis in cervical carcinoma: A novel target of p53 in apoptosis. FEBS Letters. 2007;581(2):289-95.

VITA

NAME	Rattana Saetung
DATE OF BIRTH	7 August 1993
PLACE OF BIRTH	Suratthani
HOME ADDRESS	Suratthani